The Use of Synthetic Zeolites in Catalysis

Submitted in fulfilment of the requirements for the degree of
Master of Science
at the University of Tasmania

July 1995
Department of Chemistry
University of Tasmania

DECLARATION

This thesis contains no material which has been accepted for the award of any other degree or diploma in any other tertiary institution, and to the best of my knowledge contains no copy or paraphrase previously published or written, except where due reference is given.

Zainurlis Zainuddin

''This thesis is not to be made available for loan. Copying of any part of this thesis is prohibited for two years from the date this statement was signed; after that time limited copying is permitted in accordance with the Copyright Act 1968.

Date: 14 AUGUST 1996

Signed: 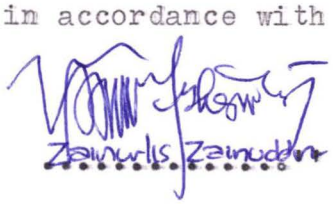

Dedicated to the Memory of My Loving Parents

for their Eternal Loves

Science is always wrong.

It never solves a problem without creating ten more.

George Bernard Shaw

CONTENTS

ACKNOWLEDGEMENTS

I would like to express my sincerest appreciation for the guidance and supervision provided by my supervisors Drs Andrew Seen and Ashley Townsend, Associate Professors John Abbot and Kingsley Cavell throughout the entire course of this degree.

Many thanks are extended to the Central Science Laboratory staff at the University of Tasmania, especially Dr Graham Rowbottom for doing the raman spectroscopy and elemental analyses, Mr Wieslaw Jablonski for doing electron microprobe analyses and electron microscope scanning, and Dr Noel Davies for doing the mass spectroscopy.

I am appreciative of the help provided by Mr Peter Dove (mechanical workshop), Mr John Davis (electronic workshop), Mr Mike Brandon (glass blower), and Mr Marshall Hughes in assembling the cracking experimental apparatus and gas chromatography.

Many thanks also go to the staff and fellow post-graduate students in the Department of Chemistry at the University of Tasmania for creating an extremely enjoyable and rewarding experience during my study.

I would like to specially thank Mrs Margaret Eldridge who has done more than just help me with the English of this thesis but also made my stay in Tasmania a pleasant one.

The financial support jointly provided by the Indonesian Institute of Sciences and the Department of Chemistry, University of Tasmania is greatfully acknowledged.

Last but not least, I would like to express my deepest gratitude to my family for their continuous support and encouragement, my wife Melly for her constant patience, care, and understanding throughout my academic years, and my son Isna for providing a supporting delight since his arrival.

ABBREVIATIONS AND NOTATIONS

Abbreviations (in alphabetical order):-

2,2'-bipy	=	2,2'-bipyridyl
acac	=	acetylacetonate
AA	=	Atomic absorption
AKI	=	Anti knocking index
FCC	=	Fluidised catalytic cracking
GC	=	Gas chromatograph
HSY	=	High Silica Y zeolite
MON	=	Motor octane number
ON	=	Octane number
REY	=	Rare earth Y zeolite
RON	=	Research octane number
SAGE	=	Scientific and glass engineering
T.O.S.	=	Time on stream
USY	=	Ultra stable Y zeolite
UV	=	Ultra violet

Notations (in alphabetical order):-

B#/L#	=	Molar ratio of branched to linear paraffins or olefins (adjusted)
B*/L*	=	Molar ratio of branched to linear paraffins or olefins (predicted)
B/L	=	Molar ratio of branched to linear paraffins or olefins (observed)
C/F	=	Catalyst to feed mass ratio
P	=	Amount of paraffins formed (observed)

P* = Amount of paraffins formed (predicted)

[Y*] = A catalytic cracking system consisting of zeolite HY only (predicted)

[Y-->Z] = A catalytic cracking system consisting of sequential combination of zeolites HY followed by HZSM-5 (observed)

[Y->Z*] = A catalytic cracking system consisting of sequential combination of zeolites HY followed by HZSM-5 (predicted)

[Y<->Z] = A catalytic cracking system consisting of random combination of zeolites HY and HZSM-5 (observed)

[Y] = A catalytic cracking system consisting of zeolite HY only (observed)

[Z*] = A catalytic cracking system consisting of zeolite HZSM-5 only (predicted)

[Z-->Y] = A catalytic cracking system consisting of sequential combination of zeolites HZSM-5 followed by HY (observed)

[Z->Y*] = A catalytic cracking system consisting of sequential combination of zeolites HZSM-5 followed by HY (predicted)

[Z] = A catalytic cracking system consisting of zeolite HZSM-5 only (observed)

X, Y, ZSM-5 = Terminology used for some types of zeolites

HY, NaY = Zeolites Y with H+ and Na+ as the counter balance cations

HZSM-5 = Zeolite ZSM-5 with H+ as the counter balance cation

LC1, LC2, MC1, MC2 = Terminology used for points of intersection between conversion curves of *n*-octane over zeolites HY and HZSM-5

ABSTRACT

This study reports on investigations into the use of synthetic zeolites in catalysis in an attempt to design catalyst systems which have size and shape selectivity. Zeolites have been widely used in petroleum refineries as acid catalysts. This has led to the field of study known as "shape selective catalysis", since the product distribution is limited to those molecules which can pass through the zeolite channel. In this study, zeolites have been used both as an acid catalyst for the cracking of hydrocarbons, and as a catalyst support for a cationic palladium complex.

n-Octane and 2-methylheptane were used in cracking reactions over zeolites HY, HZSM-5, and their combinations. The two hydrocarbons were selected to discern the skeletal effect introduced by the structure of a molecule, while the zeolites were chosen because of their common use in commercial catalytic cracking.

Three ways of mixing the zeolites were employed, by which the influence of each zeolite on a particular feedstock could be isolated:-

i. Placing the bed of zeolite HY prior to that of zeolite HZSM-5.

ii. Placing the bed of zeolite HZSM-5 prior to that of zeolite HY.

iii. Mixing the two zeolites thoroughly.

It was found that overall distributions of cracking products by carbon number from reaction of either paraffin on combinations of HY and HZSM-5, and from reaction of a mixture of the paraffins on either zeolite, can be reasonably described by the addition of product distributions on individual catalysts and from individual paraffins, weighted according to the relative amounts present.

Ratios of branched to linear paraffins are much more strongly influenced by catalyst type and feedstock than the corresponding ratios for olefinic products. For reactions on catalyst mixtures, distributions of the total products by carbon number correspond well to a summation of contributions on the individual catalysts. However, a greater departure from prediction is seen for individual distributions of paraffins, olefins and aromatics, as well as for ratios of branched to linear paraffins, showing that hydrogen transfer processes and isomerisation must occur. The addition of pentasil resulted in enrichment of the linear saturates at lower carbon number which is due to preferential cracking of linear paraffins over the branched isomers.

The use of zeolite as a catalyst support was investigated by immobilising a cationic palladium complex, $[Pd(2,2'\text{-bipy})_2]^{2+}$, in NaY zeolite. Three immobilisation methods were investigated, from which a model for location and distribution of the supported complex was proposed:-

i. Prepared from $[Pd(2,2'\text{-bipy})_2](NO_3)_2$ complex which was exchanged directly with the zeolite (method I).

ii. Synthesised *in-situ* from $Pd(2,2'\text{-bipy})Cl_2$ complex which was exchanged with the zeolite in the presence of 2,2'-bipyridyl (method II).

iii. Synthesised *in-situ* from $[Pd(NH_3)_4]^{2+}$ which was exchanged with the zeolite. Free 2,2'-bipyridyl was then added to the cation-exchanged zeolite in solution to replace the ammine (method III).

UV-visible, atomic absorption, and raman spectroscopies, together with microprobe and elemental analyses, were used to characterise the zeolite supported complexes.

Attempts to directly ion-exchange $[Pd(2,2'\text{-bipy})_2]^{2+}$ into the zeolite resulted in a maximum palladium loading of 0.62 wt% compared with a maximum loading of 8.97 wt% when $[Pd(NH_3)_4]^{2+}$ was ion-exchanged into the zeolite. Efforts to obtain higher loadings of $[Pd(2,2'\text{-bipy})_2]^{2+}$ by *in-situ* synthesis from Pd(2,2'-bipy)Cl_2 and 2,2'-bipyridyl resulted in an increased maximum palladium loading to 1.15 wt%. Although a maximum Pd loading of 8.97 wt% could be obtained by ion-exchanging $[Pd(NH_3)_4]^{2+}$ into the zeolite, it was found that the $[Pd(NH_3)_4]^{2+}$ could only be partially converted to $[Pd(2,2'\text{-bipy})_2]^{2+}$. The inability to achieve 100% conversion using this method is probably due to the steric constraints within the smaller zeolite cages.

The catalytic activity of the zeolite supported complexes was tested for dimerisation of ethene. It was found that the product distribution resulting from the supported complexes was similar to that obtained from the homogeneous system.

Chapter 1

Introduction to Zeolites: An Overview

CHAPTER 1

Introduction to Zeolites: An Overview

1.1 Structure

Zeolites {1} are complex crystalline inorganic polymers based on an infinitely extending framework of XO_4 tetrahedra linked together by the sharing of oxygen ions, where X can be trivalent elements such as Al and Ga, tetravalents elements such as Si or Ge, or even pentavalent elements like P. However, Si and Al are the elements most commonly present in both synthetic and naturally occurring zeolites {2}. The difference in valence electrons of Al and Si gives rise to excess negative charges on the oxides. Cations are required to maintain the electrical neutrality in the crystal lattice.

This zeolite framework {1} contains channels and cages that are occupied by the cations and water molecules. The cations are mobile and replaceable by others via ion-exchange, and the water molecules may be removed by the application of heat and rehydrated by the addition of water {1}. However, dehydration may produce some perturbation of the structure of some zeolites which includes cation movement and some degrees of framework distortion {3}.

Zeolites were first recognised as a new type of mineral in ca. 1756 {1}. These microporous solids with uniform pore sizes that range from 0.3 to 0.8 nm quickly find a way to commercial overstones leading to novel processes for separation of materials based on their molecular sizes, inspiring attempts to prepare the molecular sieves by synthesis. To date, about 40 naturally occurring zeolites and 150 synthetic zeolites are known {1}. Some of the very commonly used are shown in Table 1.1.

Table 1.1 Several commonly used zeolites {1}

Zeolite	Typical Formula
Natural:-	
chabazite	$Ca_2[(AlO_2)_4(SiO_2)_8].13H_2O$
mordenite	$Na_8[(AlO_2)_8(SiO_2)_{40}].24H_2O$
erionite	$(Ca,Mg,Na_2,K_2)_{4.5}[(AlO_2)_9(SiO_2)_{27}].27H_2O$
faujasite	$(Ca,Mg,Na_2,K_2)_{29.5}[(AlO_2)_{59}(SiO_2)_{133}].235H_2O$
clinoptilolite	$Na_6[(AlO_2)_6(SiO_2)_{30}].24H_2O$
Synthetic:-	
zeolite A	$Na_{12}[(AlO_2)_{12}(SiO_2)_{12}].27H_2O$
zeolite X	$Na_{86}[(AlO_2)_{86}(SiO_2)_{106}].264H_2O$
zeolite Y	$Na_{56}[(AlO_2)_{56}(SiO_2)_{136}].250H_2O$
zeolite L	$K_9[(AlO_2)_9(SiO_2)_{27}].22H_2O$
zeolite omega	$Na_{6.8}TMA_{1.6}[(AlO_2)_8(SiO_2)_{28}].21H_2O$ [(a)]
zeolite ZSM-5	$(Na,TPA)_{1.6}[(AlO_2)_3(SiO_2)_{93}].16H_2O$ [(b)]

Key:
(a) TMA = tetramethylammonium
(b) TPA = tetramethylammonium

Of these known zeolites, only 34 different structures have been identified, ten of which are synthetic {1}. However, these structure can be classified into two main types. The first type is the interconnected cagelike voids which form an internal pore system, and the second type is the channel system which could be one, two, or even three dimensional. In most zeolite structures, the primary structural units are the tetrahedra of XO_4 which assemble into secondary building blocks, such as cubes, hexagonal prisms, or octahedra. The final structures of zeolites are the assemblages of these secondary units, and these

determine the pore size and cage volume of the zeolites. An example of these framework formations is shown in Figure 1.1.

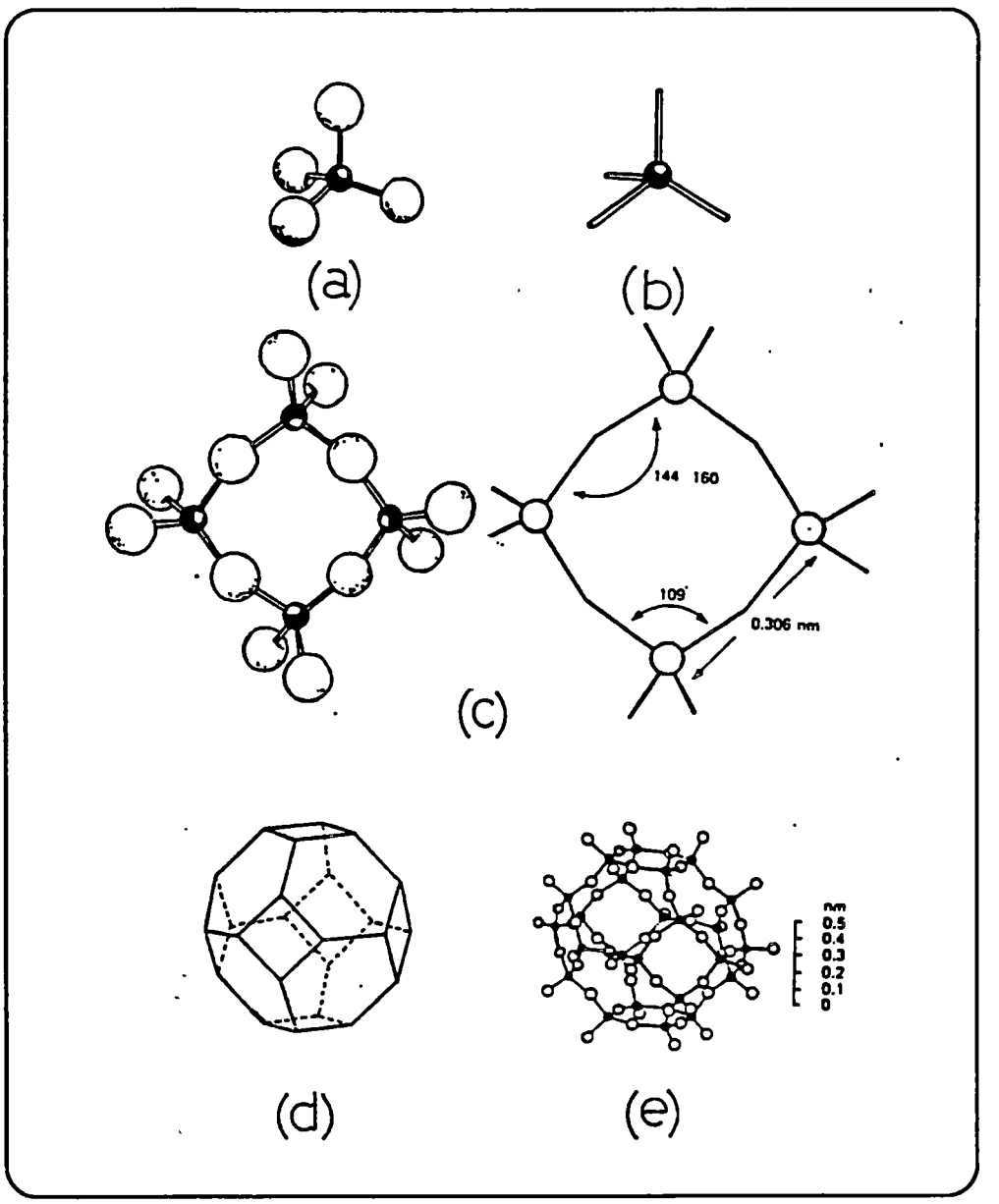

Figure 1.1 Representation of the formation of the framework and building blocks of zeolites {1}: (a) ball-and-stick model and (b) skeletal model of XO_4 tetrahedron, (c) lingking of four tetrahedra in a four-membered ring, (d) secondary building block called the truncated octahedron as a solid model, and (e) as a ball-and-stick model

Of the known naturally occurring zeolites, only a few occur in large quantity and reasonably high purity {1}, namely chabazite, clinoptilolite, erionite, and mordenite, and of the known synthetic zeolites, only a few are important, some of which are shown in Table 1.1. In this study, the use of two widely used synthetic zeolites, Y and ZSM-5 types, in catalysis are investigated.

The basic building blocks of a zeolite Y are the truncated octahedra, called β-cages or sodalite cages. The six membered rings (hexagonal faces) of these sodalite cages have a diameter of around 2.4 Å, at which the octahedra join together through hexagonal prisms, resulting in a tetrahedral stacking structure as shown below {4}. Zeolite Y is sometimes called faujasite (a naturally ocuring zeolite) because of structural similarity.

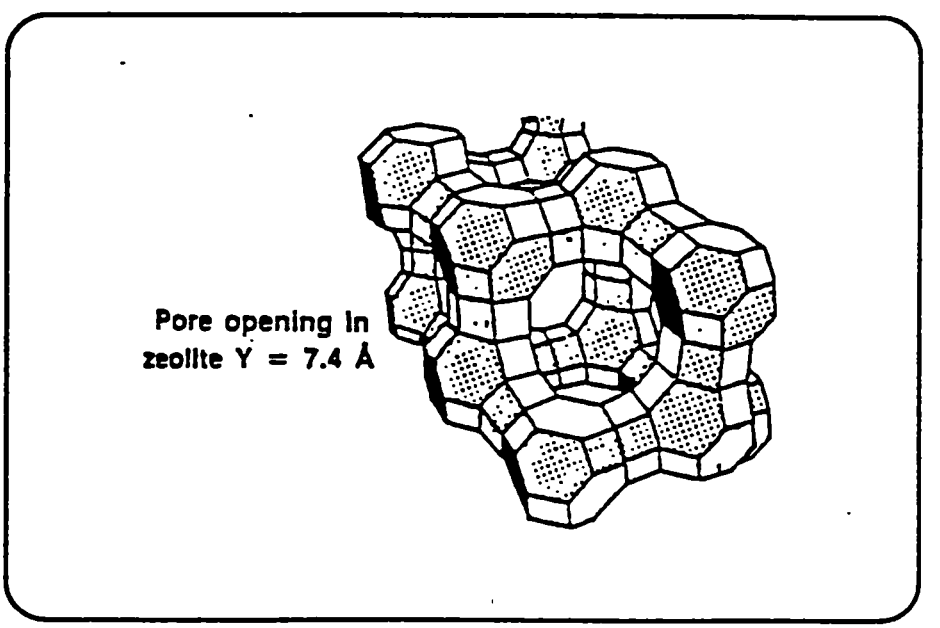

Figure 1.2 Proposed unit cell structure of zeolite Y

This type of stacking creates large cavities called a-cages (supercages) with a diameter around 13 Å, and tetrahedrally distributed 12-membered rings aperture to the cages, each having a diameter of around 7.5 Å.

For zeolite ZSM-5, eight 5-membered rings (pentasil) link together forming the basic framework of ZSM-5 zeolites {5}. These units are connected through edges to form chains, and these chains are joined together forming two types of intersecting channels with 10-membered rings aperture. The first type is sinusoidal and has a near circular aperture with ~5.4 Å diameter. The other type is straight and has an elliptical aperture (5.1 x 5.7 Å). Voids of around 9 Å diameter are formed at the intersection of these channels. Based on the work of Kokotailo {6}, the three dimensional structure of ZSM-5 was determined as shown in Figure 1.3.

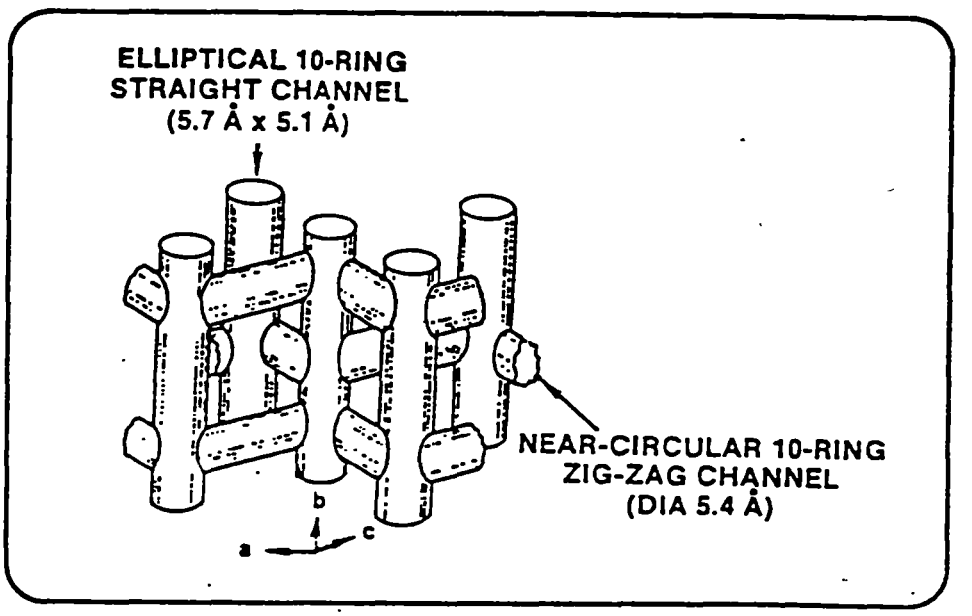

Figure 1.3 Proposed structure of zeolite ZSM-5

1.2 Physical and Chemical Properties

Zeolites are highly porous crystalline structure which possess a network of channels within the molecular lattice {1} which provides a total surface area of several hundred square metre per gram of material and which can be impregnated with various active agents such as oxides of various transition metals {1}.

The stable crystalline structure of zeolite shows a very high selectivity in adsorption. Only molecules smaller than the aperture of the pore can enter, diffuse through, and interact with the active sites inside. This basic characteristic enables highly selective zeolites to be prepared for a specific use. Distribution of pore diameters in zeolites allows separation of compounds based on the molecular size, shape, and other properties, such as polarity, of the materials to be separated {1}. These molecular-sieve effects are influenced by the ratio of SiO_2/Al_2O_3, type of the counter balance cations, their location, size, and charge densities {1}.

The catalytic activity of zeolites is due to the presence of acidic hydroxyl groups. These acidic sites are called called Brønsted sites if they donate protons to reactant molecules during a reaction, and referred to as Lewis sites if they accept hydride ions from similar molecules. Numerous work has been reported concerning the role of these sites in the initiation and the course of a cracking reaction, and all lead to a conclusion that the catalytic activity of zeolites is attributed to these acid sites.

According to Ward {7} and Benesi {8}, the presence of Brønsted sites as hydroxyl groups on the zeolite surface showed a strong correlation with the catalytic activity of the zeolites. Similar correlation was later observed by other workers {9, 10, 11}. Ward {12} discovered that a pair of Brønsted sites was convertable into a Lewis site (as shown in Figure 1.4) through dehydration with a concurrent loss of a water molecule.

The work of Guerzoni and Abbot {13, 14} showed that this conversion was reversible, since the catalytic activity of the dehydrated zeolites was restored by the addition of water (rehydration). It was found that the catalytic activity of the dehydrated zeolite was completely recovered upon rehydration, provided that the dehydration temperature did not exceed 600 °C {14}.

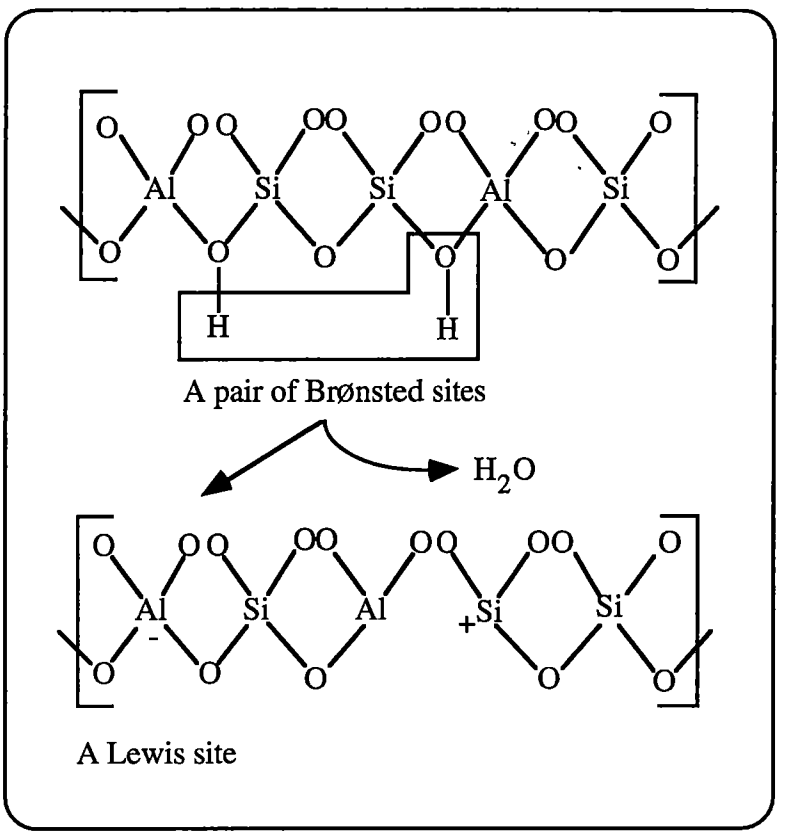

Figure 1.4 Brønsted and Lewis acid sites on zeolites

An earlier observations of Hughes and White {15} showed that dehydration of HY zeolite below 600 °C occurred without appreciable distortion in the zeolite crystal lattice. Once the temperature was raised above 600 °C, the zeolite structure started to show severe physical disruption.

1.3 Applications

Zeolites have enormous applications in many fields of industry, such as food, drugs, petroleum, and petrochemicals {1}. These zeolites are utilised for their excellent molecular-sieve properties. One of the most important uses of zeolites today is as heterogeneous catalysts in petroleum industries. Since their discovery, zeolites Y have continuously been used in hydrocarbon cracking

processes and refineries in the production of gasoline {4}. A more recently discovered zeolite, ZSM-5, is widely used as a commercial catalyst in the production of synthetic gasoline from methanol or syngas, and in the area of petrochemicals {16, 17}.

Both zeolites Y and ZSM-5 quickly found great uses because they have unusual properties due to their distinct silica contents. Zeolite Y is low silica zeolite (SiO_2/Al_2O_3 = 1 - 3), whilst ZSM-5 has a high silica content (SiO_2/Al_2O_3 = 35 - 100). Their properties arise from this ratio difference, as shown in Table 1.2.

Table 1.2 General intrinsic characteristics of zeolites Y and ZSM-5 {6}

Characteristics	Zeolite Y	Zeolite ZSM-5
SiO_2/Al_2O_3 ratio	Low to Medium	High
Unit cell size	Large	Small
Porosity	Large	Medium to small
Active sites density	High	Low
Acid strength	Low	High

Since the last two decades, there has been interest in using zeolites as solid supports for transition metal complexes or transition metal complex ions known active for various reactions, such as oxidation and carbonylation {18, 19}. These reactions have been carried out in homogeneous system, and in some aspects this is disadvantageous, as will be discussed later in Chapter 5. Immobilising these catalysts onto zeolites produce a heterogenised homogeneous system which offers many promissing superiorities over homogeneous system. In this study, the use of synthetic zeolites HY and HZSM-5 as cracking catalysts for reactios of *n*-octane and 2-methylheptane, and

of zeolite NaY as catalyst support for $[Pd(2,2'bipy)_2]^{2+}$ complex were investigated. The immobilised complexes were tested for dimerisation of ethene.

1.4 Summary

Zeolites are complex crystalline inorganic polymers that occur naturally and also sythetically prepared. The unique internal structure of the zeolites which posseses pores and channels makes them an excellent molecular sieve, which has found applications in many industrial fields.

One conventional use of zeolites is as heterogeneous catalysts in the catalytic cracking processes in the petroleum industry. The main task of the zeolites is to facilitate reactions of hydrocarbons under cracking conditions to produce high quality gasoline with optimised yield. Much work has been reported concerning the behaviour of hydrocarbons and the performance of different zeolites under cracking conditions. In spite of this, some of them are still under debate.

During the past two decades, researchers have also been trying to use zeolites as solid supports for various homogeneous catalysts known active for important reactions in the production of petrochemicals. These efforts are directed to create a heterogenised homogeneous catalysts with combined advantages of both homogeneous and heterogeneous catalysts, and at the same time minimising their disadvantages. This heterogenised homogeneous catalysis is expected to broaden and develop the scope of applications of each of its parent catalysis systems.

References

1. Encyclopedia of Chemical Technology, **15** (1981) 638.
2. Sand, L.B. and Mumpton, F.A., "Natural Zeolites, Occurrence, Properties and Use", Pergamon Press, London, 1978.
3. Breck, D.W., "Zeolite Molecular Sieves: Structure, Chemistry and Use", John Wiley and Sons Inc., (New York) 1974.
4. Scherzer, J., Bass, J.L., and Hunter, F.D., "Structural Characterisation of Hydrothermally Treated Lanthanum Y Zeolites", *J. Phys. Chem.*, **79** (1975) 1194-1200.
5. Scherzer, J., "Octane Enhancing, Zeolitic FCC Catalysts: Scientific and Technical Aspects", *Catal. Rev. -Sci. Eng.*, **31(3)** (1989) 215-354.
6. Kokotailo, G.T., Lawton, S.L., Olson, D.H. and Meier, W.M., "Structure of Synthetic Zeolite ZSM-5", *Nature*, **272** (1978) 437-438.
7. Ward, J.W., "The Nature of Active Site on Zeolites: IV. The Influence of Water on the Acidity of X and Y Type Zeolite", *J. Catal.*, **11** (1968) 238-250.
8. Benesi, H.A., "Relationship between Catalytic Activity and Nature of Acidity of the Crystalline Zeolites, Mordenite and Y Faujasite", *J. Catal.*, **8** (1967) 368-378.
9. Olson, D.H., Haag, W.O., and Lago, R.M., "Chemical and Physical Properties of the ZSM-5 Substitutional Series", *J. Catal.*, **61** (1980) 390-396.
10. Jacobs, P.A. and Ballmos, R., "Framework Hydroxyl Groups of HZSM-5 Zeolites", *J. Phys. Chem.*, **86** (1982) 3050-3052.
11. Pine, L.A., Maher, P.J., and Wachter, W.A., "Prediction of Cracking Catalyst Behaviour by a Zeolite Unit Cell Size Model", *J. Catal.*, **85** (1984) 466-476.

12. Ward, J.W., "The Nature of Active Site on Zeolites: VI. The Influence of Calcination Temperature on the Structural Hydroxyl Groups and Acidity of Stabilized Hydrogfen Y Zeolite", *J. Catal.*, **11** (1968) 251-260.
13. Abbot, J., "Active Sites and Intermediates for Isomerization and Cracking of Cyclohexane on HY", *J. Catal.*, **123** (1990) 383-395.
14. Abbot J., and Guerzoni, F.N., "Roles of Bronsted and Lewis Sites During Cracking of *n*-Octane on H-Mordenite", *Appl. Catal.*, **85** (1992) 173-188.
15. Hughes, T.R. and White, H.H., "A Study of the Surface Structure of Decationized Y Zeolite by Quantitative Infrared Spectroscopy", *J. Phys. Chem.*, **71** (1967) 2192-2201.
16. Anunziala, O.A. and Pierella, L.B., "Zn-ZSM-5 Zeolite Catalyst for LPG Aromatization", *Catalysis Letters*, **16** (1992) 437-441.
17. Dejaivfe, P., Vérdine, J.C., Bolis, V., and Derouane, E.G., "Reaction Pathways for the Conversion of Methanol and Olefins on HZSM-5 Zeolites", *J. Catal.*, **63** (1980) 331-345.
19. Primet, M., Vedrine, J.C., and Naccache, C., "Formation of Rhodium Carbonyl Complexes in Zeolites", *J. Molec Catal.*, 4 (1978) 411-421.
20. Knop-Gerrits, P-P., De Vos, D., Thibault-Starzyk, F., and Jacobs, P.A., "Zeolite-encapsulated Mn(II) Complexes as Catalysts for Selective Alkene Oxidation", *Letters to Nature*, **369** (1994) 543-546.

Chapter 2

Zeolites as Cracking Catalysts: An Overview

CHAPTER 2

Zeolites as Cracking Catalysts: An Overview

2.1 Introduction

There are vast quantities of petroleum concealed underneath the earth's surface. Most theories concerning the origin of petroleum agree that it originated from marine organic materials that were buried in the earth's crust for millions of years. The process of transformation from marine deposits to petroleum is assumed to be partly chemical in nature, and partly due to anaerobic bacteria {1}.

Petroleum differs in overall composition with location. However, major chemical components remain the same in most samples. Petroleum comprises thousands of compounds including gases, liquids, and solids. Most of these are hydrocarbons, but there are significant amounts of compounds containing nitrogen, sulfur, and oxygen {2}. Generally, the hydrocarbon constituents of petroleum are classified into three classes based on their chemical structures, namely, paraffins, olefins, naphthenes, and aromatics {2}. Distillation of petroleum results in fractions (or distillates) of different boiling point ranges. One of the most important fractions is called gasoline whose boiling point range spans from about 40 °C to 190 °C {3}.

Since the invention of the internal combustion engine in the mid 19th century {3}, the demand for gasoline has continually increased until gasoline obtained from the distillation of petroleum (straight run gasoline) was no longer sufficient to meet world demand. Since this time gasoline has also been produced from gas oil, a heavier distillate from petroleum, via catalytic cracking. This is a process by which high molecular weight hydrocarbons from the heavy gas oil distillate are cracked at elevated temperatures in the presence of a catalyst to produce hydrocarbons of lower molecular weight. Initially the feedstock used for catalytic cracking was

merely gas oil, however, as the technology has improved, even heavier distillates can now be catalytically cracked to form gasoline {2, 4, 5}.

For gasoline to be commercially acceptable as a fuel, it needs to satisfy the requirement of high quality demand. Many parameters are used as standards to grade gasoline quality, such as volatility, oxidation stability, and octane number {3}. However, the grade of gasoline is more commonly expressed in its *octane number* (ON). This is a measure of a fuel's resistance towards knocking, a situation when the fuel in the cylinder of an internal combustion engine detonates and causes noise (knock) due to poor combustion. Since the internal combustion engine was invented, knocking has been a major problem. Studies have been carried out to investigate the properties of different types of hydrocarbons used as fuels in an attempt to cure the problem {6, 7, 8}.

An arbitrary scale for octane number has been assigned with *n*-heptane and *iso*-octane having values of 0 and 100 respectively. On this basis, a fuel with ON 90, for instance, will resist knocking to the same degree as a blend of 90% *iso*-octane in *n*-heptane when tested in the same test engine. In the 1920's, the octane number of various hydrocarbons was measured in test engines in the laboratory, and as a result was called RON (Research Octane Number). However, when the gasoline was actually tested in a real engine of a motor vehicle on the road, it became evident that the engine conditions employed in the laboratory were not severe enough to simulate the real-life situation. A new method for measuring the octane number was then established, called the Motor method, and the resulting number was suitably called MON (Motor Octane Number). Today in the USA, a more general specification for determining the grade of gasoline has been defined as AKI (Anti Knocking Index), which is the mean value of RON and MON {3}.

In general, hydrocarbons of different types have different octane numbers. Thus, the octane number of a gasoline is essentially dependent on the relative proportion of assorted hydrocarbons present in the blend. Paraffins were found to

have the lowest octane number, while aromatics have the highest. The following sequence shows relative octane numbers in increasing order {9}.

paraffins < naphthenes < olefins < aromatics

Therefore a high grade fuel should contain a sufficient amount of hydrocarbon components which have high octane number, i.e. more olefins and aromatics. On an industrial scale, however, such hydrocarbons are difficult to produce except at very high temperatures {2}, and this is generally not economical. Scientists involved with catalytic cracking have been investigating how to boost the octane number of gasoline by controlling the reactions occurring during the conversion of gas oil into gasoline {10-13}, so that it can be readily used as fuel without having to undergo expensive and complicated refining processes. Table 1.1 shows a summary of ways to improve the octane number of different types of hydrocarbons which can be done via catalytic cracking or refining over zeolites.

Table 2.1 Summary of ways of improving octane number of different types of hydrocarbon {9}

Hydrocarbon Type	Way of Increasing Octane Number
Paraffins	Shortening the main chain
	Introducing branching around the centre of the molecule
	Dehydrogenation to olefins
Naphthenes	Decreasing the ring size and number of rings
	Shortening side chains
	Introducing branching to the side chains
	Centralisation of side chains
	Aromatisation
Olefins	Shortening the main chain of the molecule
	Centralisation of double bonds
	Cyclisation and aromatisation

2.2 Zeolites as Cracking Catalysts

The first recorded cracking process that used a catalyst was in 1927 when Houndry {3} used a silica-alumina clay to catalyse the cracking of heavy oils to produce gasoline. Prior to this, cracking was done solely with the application of heat and pressure, thus called thermal cracking. Since then many studies have been undertaken to find catalysts that best perform under the harsh conditions of catalytic cracking, yet still produce a high yield of high octane gasoline. However, thermal cracking is still used in some cracking processes using very high molecular weight feedstocks and high boiling point distillates of petroleum {2}.

The catalyst in the early catalytic cracking process unit was introduced in a fixed bed system where the catalyst was readily poisoned by carbon residues deposited. This unit was found to be inefficient because the catalyst life was short and it had to be regenerated by burning under controlled conditions. It was soon replaced by a moving bed system, and later by a fluidised catalytic cracking (FCC) unit, as is used today. In an FCC unit, the petroleum vapour is passed through the catalyst powder with proper agitation to form a fluid system that behaves like liquid {2}, hence it can flow from reactor vessels to regeneration vessels in a continuous cycle. However, it still maintains the property of a solid, hence temperature control can be precisely maintained {2}.

The task of a catalyst is to provide a large surface area to facilitate the course of the reaction of interest. Performance of a cracking catalyst is determined by three main attributes {14}:-

1. Activity, as a measure of the amount of feedstock converted by a certain amount of catalyst over a period of time.
2. Selectivity, the ability of the catalyst to promote the formation of a desired product at the expense of less favoured ones.
3. Stability, the durability of the catalyst in maintaining its activity and selectivity without experiencing decay.

Attempts have been made to identify the types and distribution of active sites present on various zeolites and to correlate this information with structural units within the solids. Many researchers have described the active centres in terms of the Brønsted and Lewis acid sites. Most studies concerning the reaction of hydrocarbons over individual zeolites have concentrated on the active sites {15, 16}, the general kinetics and mechanisms of reactions taking place during cracking {17-19}, and the underlying chemical behaviour of hydrocarbons under cracking conditions {20-22}. The observed phenomena associated with cracking reactions are commonly rationalised in terms of ionic mechanisms. These mechanisms involve the formation of a carbocation. There are two types of carbocations: one is termed penta-coordinated carbonium ion {16, 23}, and the other one is called tri-coordinated carbenium ion {24}. Depending on the type of feedstock and catalyst used for study, the product distribution from cracking processes can be explained using these carbocation intermediates. In addition to these two possible intermediates, there is also a possibility of formation of radical species {25}.

The basic characteristic of zeolites which allows only molecules smaller than the aperture of the pore to enter the channel and interact with the active sites inside is advantageous for the purpose of controlling the catalytic cracking of a feedstock such as a gas oil. A number of studies have concentrated on the cracking characteristics of different hydrocarbons over the catalyst {26-28}.

In the last two decades there has been interest in using combinations of catalysts in order to combine unique properties of different zeolite catalysts. This will be reviewed further in the next section.

2.3 Previous Studies

2.3.1 Catalyst Development

The major requirements of a catalyst used for commercial hydrocarbon cracking are its activity, selectivity, and stability, which converge to a capacity to produce a high yield of gasoline with high octane number. Extensive studies have been carried out in order to achieve this goal. These have involved modifying the characteristics of the zeolites (SiO_2/Al_2O_3 ratios, counter-balance cation, etc.), searching for better catalyst formulations, and utilising combinations of catalysts {9}.

The first generation of commercial zeolites was zeolite X, which was used in catalytic cracking for only a short period before being replaced by its homologue, zeolite Y. Zeolite Y was found to have better thermal and hydrothermal stabilities as a result of the higher Si to Al ratio of the zeolite Y (1.5 - 3), compared to that in zeolite X (1 - 1.5). This has offered a concept of modifying the existing zeolite by increasing its silica content, in order to improve its stability. The modified Y zeolite so obtained was simply called HSY (High Silica Y) zeolite. The HSY zeolite can be obtained by either enriching the silica content in the framework by adding silicon containing reagents {9}, or eliminating some of the aluminium from the crystal lattice by dealumination {29}. Combinations of the two can also be employed simultaneously {9}.

The first notable feature from this type of zeolite modification is that the Si to Al ratio in the framework increases quite markedly. Unit cell size decreases upon dealumination. Any variations in the properties of HSY zeolite are basically as a consequence of this increase in Si to Al ratio. HSY zeolites with improved stability are also known as USY (Ultra Stable Y) zeolite. This zeolite can withstand temperatures up to 1000°C without showing any chemical change in their crystalline structure {9}.

Apart from changing the intrinsic properties of the Y zeolite by altering the proportion of Si and Al in the framework, there is another common method of modification, that is by intoducing RE (Rare Earth) elements, such as La, into the crystal lattice giving REY (Rare Earth Y) zeolite {9}. This rare earth element is present as its oxides, e.g. La_2O_3. They are introduced into the zeolite crystal lattice mainly to increase the yield of gasoline produced, rather than to enhance the ON appreciably. It is thought that these RE elements can improve the gasoline yield by retarding the formation of gaseous hydrocarbons and the accumulation of coke during cracking {9}. As for the case with USY, zeolite REY also show gains in stability as well as catalytic activity. Some investigators have reported that the introduction of RE elements into the crystal lattice improves the stability but decreases unit cell size and active site density. Other workers {30} also report that the acid strength of the active sites increases upon dealumination.

From the study of Edwards *et al.* {31}, it was observed that the Si to Al ratio has a significant effect on the quality of the gasoline produced. They showed that USY zeolites are beneficial in terms of producing less paraffins and more olefins, with some loss in aromatics. Generally the gasoline produced was found to have high RON and MON. However, at the same time the yield of the gasoline drops quite appreciably as the quality increases. Leuenberger *et al.* {32} showed that there is a limit in the Si to Al ratio beyond which the fall of gasoline yield cannot be compensated for by the increased quality. In contrast, REY zeolite shows better catalytic activity under normal operating conditions compared to USY zeolite. However, this activity is not maintained with increased reaction temperature.

RE-USY zeolite is another type of modified Y zeolite which results from combining the intrinsic and cracking properties of REY- and USY- zeolites. RE-USY zeolite was found to have stronger acid sites when compared to USY zeolite {9}. It also produces more coke compared to REY zeolite {9}. Scherzer *et al.* {9} showed that the unit cell size increases as more RE element is introduced

into the USY zeolite. In general the catalyst properties lie between those of the parent zeolites.

Pine and co-workers {33} also observed that there is a close relation between the Si to Al ratio in the crystal lattice and its unit cell size, and this unit cell size correlates well with the activity, selectivity, and stability of the catalyst. At elevated temperatures employed in industrial operations, it has been found that the unit cell size actually shrinks {9} resulting in expulsion of some Al from the framework. Generally, a smaller unit cell size limits the types of reaction that can take place at the active sites. However, a smaller unit cell size favours the formation of hydrocarbons with high octane number. A study by Corma *et al.* {34} shows that, apart from reducing the total acidity, an increased Si to Al ratio also reduces the adsorption capacity of the zeolites towards olefins. Brunner *et al.* {35} discovered a simple relationship between the porosity (i.e. unit cell size) of a zeolite and its molecular structure. This discovery is opening a new way of controlling the catalytic activity of zeolite Y by carefully structuring its basic building blocks.

2.3.2 Variation in Hydrocarbon Feedstocks

Because gas oil comprises of thousands of components, it is virtually impossible to fully comprehend the behaviour of a gas oil mixture during cracking process. However, the behaviour of hydrocarbons over zeolites under cracking conditions can be simplified by considering them as groups (paraffin, olefin, naphthene, and aromatic).

A wide and diverse range of hydrocarbon feeds has been used in cracking studies, either as single feedstocks, or mixtures of two or even more components that resemble a gas oil composition. Most of these studies were performed on commercial catalysts used in the petroleum industry, Y zeolites {17, 23}, and to a lesser extent, on ZSM-5 zeolites {20}.

Studies on the reaction of various hydrocarbons on a particular zeolite are usually performed as follows:-

1. A single hydrocarbon component of high purity

Hydrocarbons used for this type of study have ranged from C_4 to C_{16} of paraffins {17, 36}, olefins {36}, aromatics {37}, or even naphtheno-aromatic compounds {38}. Studies to date have primarily concentrated on examining the product distributions obtained from cracking reactions. One important agreement from these studies is that having a large porosity, zeolite Y favours bimolecular reaction mechanisms taking place in the pores. In contrast, zeolite ZSM-5 has moderately small pores that only allow monomolecular reaction processes to occur. A detailed study by Pine *et al.* {33} concluded that the variation in porosity of zeolites can facilitate different routes for cracking reactions of the same hydrocarbon species. Haag and Dessau {24} found that the monomolecular cracking process is more favourable with medium pore zeolites, such as ZSM-5. It was also shown that this observation became more obvious with increased reaction temperature and reactant concentration. Later work by others {39-42} agreed that the monomolecular cracking route is more noticeable with silicon rich zeolites, such as ZSM-5. Close examination of the total product distributions obtained from cracking reactions of hydrocarbons showed that ZSM-5 tends to shift the overall product distributions towards lower carbon number compared to Y zeolite. It has been reported {41, 43} that HY zeolite produces more aromatics and branched paraffins, whereas more olefins and linear paraffins were formed on ZSM-5 {41, 43}. These observations are thought to be partly attributable to differences in the strength of the active sites, and the cracking reaction mechanism taking place on different active sites on the zeolite surface.

2. Two hydrocarbons of the same type.

This type of study has usually used two paraffin isomers, either individually or in a mixture, in order to discern the effect of skeletal arrangement of the molecule on its susceptibility towards cracking, as well as the shape selectivity from zeolites of different porosity {44}. The work of Chen and Garwood {45} reported that the molecular dimension and skeletal arrangement of the paraffin feed are crucial when considering shape selectivity. Later observation by Choudhary and Akolekar {46} reached the same conclusion. Extensive studies by Abbot and Head {47} showed that the instrinsic reactivity of a hydrocarbon species can be significantly influenced by the presence of a hydrogen atom bonded to a tertiary carbon atom.

3. Two hydrocarbons of different type.

This type of study has normally been carried out using mixtures of paraffins and olefins in various relative proportions. When a mixture of the same type of hydrocarbons was used as the reaction feedstock, shape selectivity and isomerisation were the major concerns. In the case of different hydrocarbon types, attention has been focused on the influence of one species on the other during cracking reaction. Anufriev *et al.* {48} reported that the presence of olefins amplified the cracking rate for reactions of linear paraffins, whereas other workers {49, 50} reported little or no effect at all. More recent studies by Abbot {51} concluded that there was a significant inhibiting effect on reactions of linear paraffins when olefinic products were formed. According to Engelhardt and Hall {22}, certain olefins can inhibit the reaction of paraffin, while some others actually enhance the rate of the reaction.

4. A feedstock which represents the diverse mixture of hydrocarbon components in a typical gas oil {49, 52}.

With this type of feedstock, results can be more easily related to those found industrially. However, this approach is also disadvantageous due to the inherent complexity of the products obtained. It is often difficult to trace down the concurrent changes occurring on each individual hydrocarbon. Studies involving complex mixtures that closely resemble the components and physical properties of gas oil, including its non-hydrocarbon impurities and boiling point range, have not been done extensively as this introduces complexity such as cracking the gas oil itself.

2.3.3 Catalyst Combination

As discussed in the preceding section, zeolites Y and ZSM-5 have distinct characteristics and properties. These differences give rise to different behaviour during catalytic cracking. The large porosity of Y zeolites is beneficial in terms of a wide range of molecular species of complex hydrocarbons in a gas oil mixture that can enter the pores, interact with the active sites and undergo cracking reactions. Having much smaller porosity, ZSM-5 zeolite is more size and shape selective. Typically only those molecules with non-bulky structures, such as simple paraffins or olefins, can enter the pores. Regardless of their different physical properties both zeolites have the same types of active sites, the Brønsted and Lewis acid sites.

The behaviour of hydrocarbons over individual catalysts under cracking conditions has been widely investigated. In contrast, there have been relatively few reported fundamental studies on the behaviour of hydrocarbons when combinations of cracking catalysts are employed. Industrially, zeolites of type Y are normally used in combination with a matrix material, which usually contains amorphous silica-alumina and other inorganic oxides which may be catalytically active under cracking conditions {53}. There has also been development of catalysts containing

more active matrices {4}. This active matrix is aimed to provide sites for initial cracking of large molecules, hence subsequent cracking of intermediates in the zeolite becomes feasible. Alumina is a material commonly used for this purpose. In most studies using combinations of zeolites, the two catalysts were blended together thoroughly as a powder {39-41}, as in commercial FCC units. In some studies they were made into a composite {54}.

The cracking activity of a typical commercial catalyst combination, such as Y zeolite dispersed in amorphous silica-alumina or other inorganic oxides, would normally be dominated by the zeolite component. However, once a combination of two zeolite components is introduced, the relative contributions to activity and selectivity will depend upon the relative proportions of each zeolite present and the intrinsic properties of each zeolite. The observed effects may not be simply additive, especially when combinations of zeolites with different activity, selectivity, and stability are employed. During the past decade, there has been increased interest in adding a small amount of zeolite HZSM-5 to the zeolite Y commonly used in commercial cracking units {39-41}. Addition of as little as 1% by weight of HZSM-5 to LaY, one of the most common commercial catalysts, has been tested in Europe and the United States, and found to produce a significant increase in octane number of the gasoline produced {39}. It is thought that more extensive studies in this area may prove advantageous in the future as catalytic cracking processes become more highly efficient and optimised, i.e. producing optimum yield of gasoline products with high octane number.

Anderson *et al.* {20} reported that an increase in gasoline ON was observed when ZSM-5 was used as an additive to USY zeolite. Biswas and Maxwell {55} also found that the addition of ZSM-5 to USY zeolite decreased the gasoline yield quite significantly. They showed that the gasoline produced also underwent selective cracking producing light olefins. Researchers from Chevron {56} have reported that gasoline loss can be minimised by employing ZSM-5 with fairly high

Si to Al ratio. From work carried out for Mobil {57, 58}, two routes by which ZSM-5 can boost the ON were proposed :

1. ZSM-5 cracks out low ON straight chain paraffins and olefins in the gasoline into lighter products.
2. ZSM-5 provides good sites for isomerisation of olefins into those of higher ON.

In another study, Rajagopalan and Young {59} proposed that ZSM-5 actually prevented the formation of paraffins by cracking out carbonium ions or olefin intermediates into smaller fragments. They also observed decreases in the gasoline yield, with consistent gains in C_3 and C_4 olefins. The same observation was made by Pappal and Schipper {58} who reported that ZSM-5 can accomplish this by upgrading the low ON components in the gasoline into light olefins, associated with the observed increase in branched C_3 and C_4 olefins. According to Biswas and Maxwell {55}, the ON enhancement resulting from the addition of a small amount of ZSM-5 may be partly attributed to an increase in yield of the aromatic range of hydrocarbons in the gasoline. This was an effect emerging from preferential cracking of aliphatic components. A more recent study by Madon {60}, however, showed that the increase in the aromatic concentration is attributable to the action of ZSM-5 that catalyses both normal and branched olefins, producing lighter olefins as major products. It was proposed that in the presence of highly reactive olefins, paraffin cracking on ZSM-5 is minimal. This is in agreement with the earlier observation of Haag *et al.* {24}, who reported that both linear and monomethyl branched olefins crack appreciably faster than their corresponding saturated species, and the cracking rates increase with chain length. Model compound studies by Madon {60} showed that ZSM-5 addition catalyses both normal and branched olefin cracking to give mainly propene, and butenes. Elia *et al.* {61} reported similar reasons explaining the ways by which the ZSM-5 boosts the ON. This was generalised by Buchanan {62}, who concluded that with

ZSM-5 additive, the reaction rates of reactions of C_6 - C_{10} hydrocarbons had the following order:

olefin isomerisation >> olefin cracking >> paraffin cracking > aromatisation

It is now apparent that greater understanding and optimisation of the application of ZSM-5 as an additive into commercial cracking catalysts should be met in order to produce a bifunctional catalyst system in FCC units that can achieve the prime goal of producing high octane gasoline with high yield.

2.4 Summary

Catalytic cracking is one of the most important and widely used methods employed to produce gasoline from high boiling point, heavy petroleum distillates obtained from crude oils. Many types of catalysts have been used and investigated since the first introduction of catalytic cracking. Currently the most widely used catalysts are synthetic Y zeolites with a little addition of ZSM-5.

With the continually increasing demand for high quality gasoline, refiners are searching for novel catalyst formulation and suitable catalyst combinations to increase gasoline yield and quality at the same time. The influence of catalysts (ZSM-5 and Y zeolites) and feedstock components on product distributions obtained from catalytic cracking are still under debate. The aim of the first part of this study is to investigate the use of zeolites HY and HZSM-5, and their combination, as catalysts for reactions of *n*-octane and 2-methylheptane under simulated cracking conditions.

References

1. Goodger, E.M., "Hydrocarbon Fuels: Production, Properties and Performance of Liquid and Gases", John Wiley & Sons, N.Y., 1975.
2. Austin, G.T., "Shreve's Chemical Process Industries", 6th Ed., McGraw-Hill Book Co., N.Y., 1988.
3. Hancock, E.G., "Technology of Gasoline", Critical Reports on Applied Chemistry, Vol 10, Blackwell Scientific Publication, London, 1985.
4. Otterstedt, J.E., Yan-Ming, Z., and Sterte, J., Catalytic Cracking of Heavy Oil over Catalysts Containing Different Types of Zeolite Y in Active and Inactive Matrices, *Appl. Catal.*, **38** (1988) 143-145.
5. Anders, G., Burkhardt, I., Illigen, U., Schulz, I.W., and Scheve, J., "The Influence of HZSM-5 on the Product Composition after Cracking of High Boiling Hydrocarbon Fractions", *Appl. Catal.*, **62** (1990) 271-280.
6. Kettering, C.F., "More Efficient Use of Fuel", *S.A.E. Trans.*, **4** (1919) 263.
7. Edgar, G., "Measurement of Knock Characteristics of Gasoline in terms of Standard Fuel", *Ind. Eng. Chem.*, **19** (1945) 145.
8. Ricardo, H.R. and Hempson, J.G., "The High Speed Internal Combustion Engine", 5th Ed., Blackie, Glasgow, 1968.
9. Scherzer, J., "Octane Enhancing, Zeolitic FCC Catalysts: Scientific and Technical Aspects", *Catal. Rev. -Sci. Eng.*, **31(3)** (1989) 215-354.
10. Keyworth, D., Yatsu, C.A., and Reid, T.A., "Gasoline Octane Controlled by Catalyst Selection", *Oil & Gas Journal*, **August 22** (1988) 51-56.
11. Letzsch, W.S., Magee, J.S., Upson, L.L., and Valeri, F., "Advanced Zeolites used in FCC Catalysts Boost Motor Octane Number", *Oil & Gas Journal*, **October 31** (1988) 57-63.
12. Desai, P.H. and Haseltine, R.P., "Advanved FCC Catalyst Formulations can be used to Boost Motor Octane Number of Gasoline", *Oil & Gas Journal*, **October 23** (1989) 68-76.

13. Avidan, A.A., Krambeck, F.J., Owen, H., and Schipper, P.H., "FCC Closed-Cyclone System Eliminate Post Riser Cracking", *Oil & Gas Journal*, **March 26** (1990) 56-62.
14. Article: "Increasing Demands for High Quality Fuels has Spawned a Scientific Multi Million Dollar Industry in Catalytic Research", *Petroleum Gazette*, **3** (1994) 14-18.
15. Abbot, J., "Role of Brønsted and Lewis Acid Sites During Cracking Reactions of Alkanes", *Appl. Catal.*, **47** (1989) 33-44.
16. Corma, A., Planelles, J., Sánchez-Marin, J., and Tómas, F., "The Role of Different Types of Acids in the Cracking of Alkanes on Zeolite Catalysts", *J. Catal.*, **93** (1985) 30-37.
17. Shertukde, P.V., Marcelin, G., and Sill, G.A., "Study of the Mechanism of the Cracking of Small Alkane Molecules on HY Zeolite", *J. Catal.*, **136** (1992) 446-462.
18. Corma, A., Miguel, P.J., and Orchilles, A.V., "Kinetics of the Catalytic Cracking of Paraffins at Very Short Time on Stream", *J. Catal.*, **145** (1994) 58-64.
19. Lombardo, E.A., Pierantozzi, R., and Hall, W.K., "The Mechanism of Neopentane Cracking over Solid Acids", *J. Catal.*, **110** (1988) 171-183.
20. Anderson, J.R., Foger, K., Mole, T., and Rajadhyaksha, R.A., "Reactions on ZSM-5 Type Zeolite Catalysts", *J. Catal.*, **58** (1979) 114-130.
21. Stocker, M., Hemmersbach, P., Raeder, J.H., and Grepstad, J.K., "Isomerisation of *n*-Butane over Zeolite Depending on Catalyst Structure", *Appl. Catal.*, **25** (1985) 223-230.
22. Engelhardt, J. and Hall, W.K., "Contribution to the Understanding of the Reaction Chemistry of *Iso*-butane and Neopentane over Acid Catalysts", *J. Catal.*, **125** (1990) 427-487.

23. Abbot, J. and Wojciechowski, B.W., "The Mechanism of Paraffin Reactions on HY Zeolite", *J. Catal.*, **115** (1989) 1-15.

24. Haag, W.O. and Dessau, R.M., Proceedings the 8th International Congress on Catalysis, Berlin, 1984. Vol II, Dechema, Frankfurt-au-Main, (1984) 305.

25. Abbot, J. and Wojciechowski, B.W., "Reactions of Cyclopentane on HY Zeolite", *Canad. J. Chem. Eng.*, **66** (1988) 637-643.

26. Greensfelder, B.S., Voge, H.H. and Good, G.M., *Ind. Eng. Chem.*, **41** (1949) 2573.

27. Voge, H.H., "Catalysis" (P.H. Emmett Ed.), Vol. 6, Ch. 5, Reinhold, N.Y. (1958).

28. Kissin, Y.V., "Relative Reactivities of Alkanes in Catalytic Cracking Reactions", *J. Catal.* **126** (1990) 600-609.

29. Shertukde, P.V., Hall, W.K., and Marcelin, G., "Effects of Dealumination on the Structure and Acidity of HY Zeolites", *Catalysis Today*, **15** (1992) 491-502.

30. Rabo, J.A. and Gajda, G.J., "Acid Function in Zeolites: Recent Progress", *Catal. Rev. -Sci. Eng.*, **31(4)** (1989-90) 385-430.

31. Edwards, G.C., Rajagopalan, K., Peters, A.W., Young, G.W., and Creighton, J.E., *A.C.S. Symposium Series*, **375** (1988) 101.

32. Leuenberger, E.L., Bradway, R.A., Leskowicz, M.A., and Stegar, J.J., *NPRA Annual Meeting*, **March** 1989, San Fransisco, CA, AM-89-50.

33. Pine, L.A., Maher, P.J., and Wachter, W.A., "Prediction of Cracking Catalyst Behaviour by a Zeolite Unit Cell Size Model", *J. Catal.*, **85** (1984) 466-476.

34. Corma, A., Fornios, V., Martinez, A., and Sanchez, J., *A.C.S. Symposium Series*, **375** (1988) 117.

35. Bunner, G.O. and Meier, W.M., "Framework Density Distribution of Zeolite-Type Tetrahedral Nets", Nature, **337** (1989) 146-147.

36. Abbot, J., "Catalytic Cracking of Long Chain Paraffins and Olefins on HY Zeolite", *J. Catal.*, **124** (1990) 548-552.

37. Corma, A., Miguel, P.J., Orchilles, A.V., and Koermer, G.S., "Cracking of Long Chain Alkyl Aromatics on USY Zeolite Catalysts", *J. Catal.*, **135** (1992) 45-50.

38. Townsend, A.T. and Abbot, J., "Catalytic Cracking of Tetralin on HY Zeolite", *Appl. Catal.*, **90** (1992) 97-115.

39. Rajagopalan, K. and Young, G.W., "Hydrocarbons Cracking: Selectivity with a Dual Zeolite Fluid Cracking Catalyst Containing REY and ZSM-5", *Prepr. Div. Petr. Chem. A.C.S.*, **32(3,4)** (1987) 627-631.

40. Schipper, P.H., Dwyer, F.G., Sparrel, P.T., Mizrahi, S., and Herbst, J.A., "Zeolite ZSM-5 Fluid Catalytic Cracking Performance, Benefits, and Applications", *A.C.S. Symposium Series*, **375** (1988) 64-86.

41. Habib Jr, E.T., and Grace, W.R. & Co.-Conn, "The Effect of Catalyst, Feedstock, and Operating Conditions on the Composition and Octane Number of FCC Gasoline", *Prepr. A.C.S., Div. Petr. Chem*, **34(4)** (1989) 674-680.

42. Mirodatos, C. and Barthomeuf, D., "Cracking of *n*-Decane on Zeolite Catalysts: Enhancement of Light Hydrocarbon Formation by the Zeolite Field Gradient", *J. Catal.*, **14** (1989) 121-135.

43. Abbot, J. and Wojciechowski, B.W., "Catalytic Cracking of *n*-Dodecane on Aluminosilicate Catalysts", *J. Catal.*, **115** (1990) 521-531.

44. Abbot, J., "Reactions of 3-Methylpentane and 2,3 Dimethylbutane on Aluminosilicate Catalysts", *J. Catal.*, **126** (1990) 628-642.

45. Chen, N.Y. and Garwood, W.E., "Some Catalytic Properties of ZSM-5: A New Shape Selective Zeolite", *J. Catal.*, **52** (1978) 453-458.

46. Choudhary, V.R. and Akolekar, D.B., "Shuttlecock-Shuttlebox Model for Shape Selectivity of Medium Pore Zeolites in Sorption and Diffusion", *J. Catal.*, **117** (1989) 542-557.

47. Abbot, J. and Head, J.D., "Hydrogen Formation, Chain Reaction, and Inhibition during Cracking Reactions of Hydrocarbons", *J. Catal.*, **125** (1990) 187-196.

48. Anufriev, D.M., Kuznetsov, P.N., and Ione, K.G., "Transformation of Hydrocarbons on Zeolites of Type Y", *J. Catal.*, **65** (1980) 221-226.

49. Corma, A., Monton, J.B. and Orchilles, A.V., *Appl. Catal.*, **46** (1977) 266.

50. Magnota, V.L. and Gates, B.C., "Superacid Polymers: Paraffin Isomerization and Cracking in the Presence of $AlCl_3$-Sulfonic Acid Resin Complex", *J. Catal.*, **46** (1977) 266-274.

51. Abbot, J., "The Influence of Olefins on Cracking Reactions of Saturated Hydrocarbons", *J. Catal.*, **126** (1990) 684-688.

52. Guerzoni, F.N. and Abbot, J., "Catalytic Cracking of a Binary Mixture on Zeolite Catalysts", *Appl. Catal.*, **103** (1993) 243-258.

53. Venuto, P.B. and Habib, E.T., *Catal. Rev. -Sci. Eng.*, **18(1)** (1978) 1.

54. Dadyburjor, D.B. and Liu, Z., "Selectivity and Yield of Components of a Composite Cracking Catalyst: Effect of Interaction between Composite Components", *J. Catal.*, **141** (1993) 148-160.

55. Biswas, J. and Maxwell, L.E., "Octane Enhancement in Fluid Catalytic Cracking: I. Role of ZSM-5 Addition and Reactor Temperature", *Appl. Catal.*, **58** (1990) 1-18.

56. Miller, S.J. and Hsieh, C.R., "Octane Enhancement in Catalytic Cracking Using High Silica Zeolites", *Prepr. A.C.S., Div. Petr. Chem.*, **35(4)** (1990) 685-693.

57. Dwyer, F.G., Schipper, P.H. and Gorra, F., National Petroleum Refiners Association Annual Meeting, San Francisco, TX, March, 1987.

58. Pappal, D.A. and Schipper, P.H., "ZSM-5 in Catalytic Cracking: RISER Pilot Plant Gasoline Composition Analyses", *Prepr. A.C.S., Div. Petr. Chem.*, **35(4)** (1990) 678-683.

59. Rajagopalan, K. and Young, G.W., "Hydrocarbon Cracking Selectivities with Dual Function Zeolite Catalysts", *A.C.S. Symp. Ser.*, **375** (1988) 34-48.

60. Madon, R.J., "Role of ZSM-5 and Ultrastable Y Zeolites for Increasing Gasoline Octane Number", *J. Catal.*, **129** (1991) 275-287.

61. Elia, M.F., Iglesias, E., Martinez, A., and Perez Pascual, M.A., "Effect of Operation Conditions on the Behaviour of ZSM-5 Addition to a RE-USY FCC Catalyst", *Appl. Catal.*, **73** (1991) 195-216.

62. Buchanan, J.S., "Reactions of Model Compounds over Steamed ZSM-5 at Simulated FCC Reaction Conditions", *Appl. Catal.*, **74** (1991) 83-94.

Chapter 3

Cracking and Isomerisation of Hydrocarbons

CHAPTER 3

Cracking and Isomerisation of Hydrocarbons

3.1 Introduction

There have been numerous studies of cracking and isomerisation reactions of pure hydrocarbons on individual zeolite catalysts {1-5}. Kinetic phenomena relating conversions of feedstocks to variables such as catalyst to feed ratios and reaction times have been extensively studied. These studies have taken into account factors such as ageing characteristics of the catalyst as well as competitive adsorption on the available sites, which may give rise to product inhibition. Product selectivity has also been examined for many systems, providing details of both initiation processes (at low conversion and/or at very short time on stream) and also at higher conversions revealing secondary reaction phenomena, where primary products participate in further reactions. Such investigations have been extended to include studies of simple mixtures of hydrocarbons {6-8} on individual catalysts, as well as very complex gas oils {9} which contain hundreds of individual components.

Although commercial cracking catalysts are composed of a mixture of solid components which can exhibit catalytic activity {10-12}, there have been few detailed studies which have attempted to relate the resultant effect of the composite catalyst to that of the individual components. For the past two decades cracking catalysts have contained a form of zeolite Y. More recently there has been interest in addition of a small proportion of a second zeolite component, in particular the ZSM-5 {13-22}. However, there have been very few reported studies of reactions of individual hydrocarbons on binary zeolite mixtures. For example, in a study by Buchanan {22}, the cracking of C_6-C_{10} normal paraffins and olefins on combinations of zeolites was investigated. It was reported that the ZSM-5 additive

plays an active role in the isomerisation and cracking reactions of olefin species, while the reactivity towards paraffin is limited.

In the first part of this study, the behaviour of *n*-octane (Chapter 3), and a mixture of *n*-octane and 2-methylheptane (Chapter 4) under cracking conditions in the presence of combinations of HY and HZSM-5 zeolites at 400 °C were examined. Previous studies on cracking with zeolite combinations have generally focussed on the effect of the presence of a second zeolite on the product distribution obtained on a single zeolite. The aims of these studies include:- i) to investigate the general behaviour of hydrocarbons under cracking conditions over combinations of HY and HZSM-5 zeolites, ii) to study the catalytic effect of physical mixtures of zeolite on these behaviours, and iii) to develop a methodology for predicting the product distributions resulting from reactions of hydrocarbons over combinations of HY and HZSM-5 zeolites based on adding together product distributions from individual catalysts. This should allow additional effects in which the products from recation on one zeolite interact with the other to be identified. The use of *n*-octane as a feedstock is well suited for this purpose, as the cracking obtained is simple enough to be analysed in detail.

3.2 Experimental

The experimental procedures outlined here are for the investigation of zeolites as cracking catalysts (Chapters 3 and 4).

Cracking Procedures:-

The basic approach employed in this study was to bring the hydrocarbon feed into contact with the catalyst at atmospheric pressure under controlled temperature in a quartz reactor of 60 cm long and 2 cm i.d. The reactor was enclosed in an aluminium alloy furnace with three thermocouple probes (Type K, Chromel-Alumel) attached to it. The reactor consisted of two zones: a preheating zone at the top of the reactor and a catalyst bed at the bottom. The preheating zone was filled

with inert quartz beads. The catalyst used for a particular run was placed in the catalyst zone diluted with an inert sand matrix. Glass wool was used to separate the zones and to hold the catalyst-sand matrix in place. The feedstock was injected at a set flow rate from a syringe pump into the top of the reactor at atmospheric pressure. Liquid products were collected in a flask immersed in an ice bath at the bottom end of the reactor. Gaseous products were collected in a gas burette by displacement of water. Residual carbonaceous material left on the catalyst after each catalyst run was regarded as coke. The schematic experimental apparatus is shown in Figure 3.1.

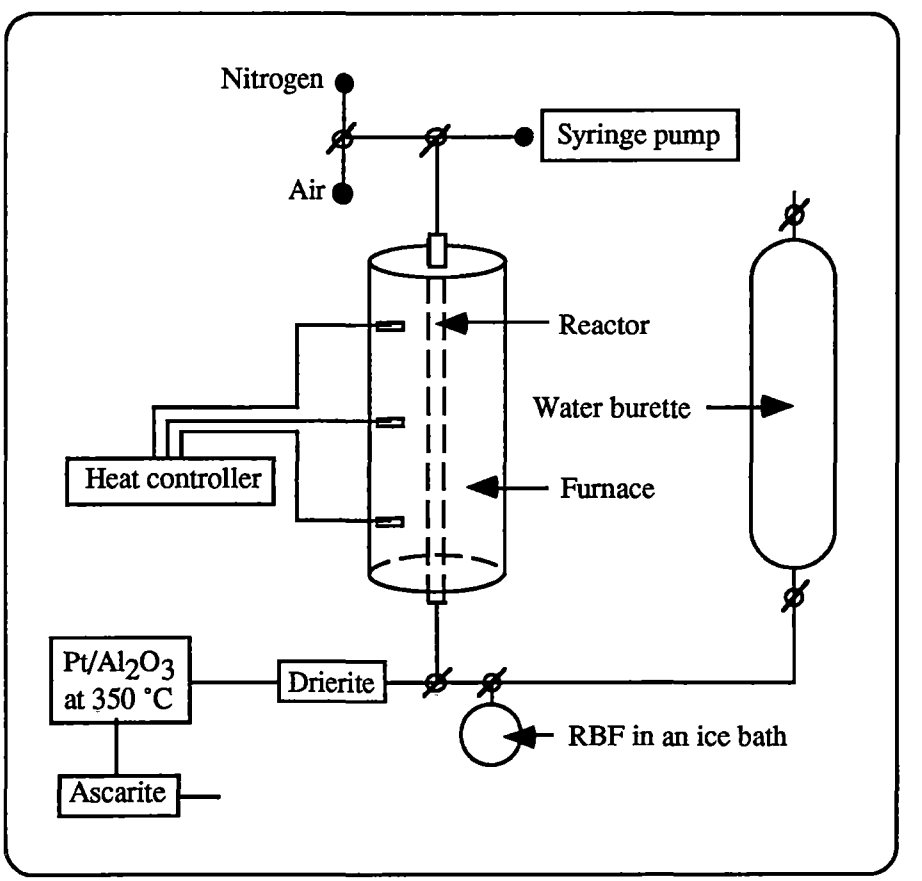

Figure 3.1 Schematic experimental apparatus for cracking experiment

The liquid and gaseous products were analysed by gas chromatography using flame ionisation detectors. From these analyses, the total conversion of feed and yields of each product were calculated. All experiments were carried out at 400 °C. Over this temperature range thermal cracking was found to be negligible.

All reaction feedstocks were obtained from Aldrich® and used without further purification. HY zeolites used were obtained from Linde catalyst (Lot No 45912, SK40; Si/Al = 2.4) and PQ Zeolites, the Netherlands (CBV 400; Si/Al = 5.2). HZSM-5 zeolites used were obtained from SNAM Progretti S.P.A., Milan, Italy (Si/Al = 105) and PQ Zeolites, the Netherlands (CBV 1502, Si/Al = 174). Catalysts were calcined at 400 °C before use. The zeolites' particle sizes of around 1 micron were determined by electron microscope scanning.

The sand matrix that was used for diluting the zeolite powder was washed thoroughly. This consisted of washing the sand with a copious amount of water before it was soaked in concentrated HCl for 72 hrs. After soaking, the sand was rinsed with a copious amount of water and neutralised with concentrated ammonia. The washing was continued until the pH of the mother liquor was about 7.

For a series of experiments, a known mass of catalyst was diluted and placed in the catalyst zone, and a known mass of feed was fed to the reactor, so that there would be a defined catalyst to feed mass ratio (C/F). The amount of feed was kept constant at 5 g, whilst that of catalyst was varied, depending on the C/F ratio employed. The feed was fed to the reactor by a motor driven syringe (Orion SAGE Pumps, Model 355, Serial U 013D) that could be set at different flow rates, resulting in different times required to deliver the feed down the reactor. This time is termed as time on stream (T.O.S.). The terms catalyst to feed ratio and time on stream used throughout the text refer to the above definitions.

Prior to a catalytic run, the catalyst was conditioned by purging the reactor with dry, CO_2-free nitrogen at 0.5 L/min for 5 minutes. The feed was injected into the top end of the reactor, and the liquid products exiting the bottom end of the

reactor were collected in a round bottom flask immersed in an ice bath, while the gaseous products were trapped in a gas burette by water displacement. After the run, the reactor was once again purged with nitrogen (at the same flow rate for the same period of time as prior to the run) which flushed out all remaining liquid and gases left in the reactor.

After a run, the catalyst became poisoned with carbonaceous material, or coke. This was observed by the catalyst turning black in the reactor. The catalyst was regenerated by burning off the coke deposit in an air stream of 0.5 L/min at 500 °C for 24 hrs. At this temperature {5} the coke was combusted to form water vapour, carbon monoxide and carbon dioxide, which were then flushed out along with the air stream exiting the reactor. This air stream was then passed through a drierite absorbant, in which the water vapour was removed, then an alumina supported platinum catalyst (Pt/Al_2O_3) held at 350 °C in a glass reactor, in which the carbon monoxide was converted to carbon dioxide. The air stream was finally passed through an ascarite absorbant, where all the carbon dioxide was absorbed. The weight increases of these absorbants were found to provide a reliable quantitative measure of the coke produced, as the overall mass balance from the liquid, gaseous products, and coke produced was near 100%, as was observed in an earlier work by Abbot {6}. With this procedure, it was possible to perform repetitive experiments with reproducible results.

Data Acquisition and Analysis:-

The liquid products were analysed using a Hewlett Packard 5890 II gas chromatograph (GC) with a Petrocol DH fused silica capillary column (100 m x 0.25 mm i.d.) with a flame ionisation detector. Gaseous products were also analysed using the same type of Hewlett Packard gas chromatograph with a Chrompak capillary column (25 m x 0.32 mm i.d.). Data handling was facilitated using a DAPA software package (Chromatography System V1.30). Identification

of hydrocarbon products was done by using a Hewlett Packard 5890 gas chromatograph coupled to a Kratos Concept S Series mass spectrometer.

The GC temperature program for analysing the gaseous products was isothermal at 30 °C for 3 minutes, followed by rampings at 6 °C/min to 60 °C then at 30 °C/min to 200 °C. This temperature was maintained for 10 minutes before cooling down to 30 °C. The column flow was maintained at 12 cm/sec with nitrogen carrier gas set at 4 psi initial head pressure and helium as the make-up gas. The GC program used for analysing the liquid products was isothermal at 35 °C for 15 minutes, followed by ramping at 2 °C/min to 270 °C at which it was held for 20 minutes before cooling to the initial temperature. Nitrogen was also used as the carrier gas, set for constant flow of 12 cm/sec with 35 psi intial head pressure. Make-up gas used was also helium.

3.3 Reaction of *n*-Octane over Individual Zeolites HY and HZSM-5

In this study the cracking and isomerisation processes which occur during reaction of *n*-octane on the zeolites HY and HZSM-5 at 400 °C both individually and in combinations, have been examined. At this temperature, the contribution from thermal cracking processes was found to be negligible, comfirming previous studies by Abbot and Wojciechowski {23, 24}. The effect of ZSM-5 addition has been envisaged by relating the observed effects of particular combinations of these zeolites to the predicted combined contributions from the individual catalysts under the same conditions. In theory, any discrepancy between the observed and predicted effects of a combination should be explainable in terms of the influence of the presence of the second zeolite on the products from the first, or vice versa.

The general conclusions regarding combination effects which are independent of process conditions such as time on stream or the level of conversion examined have been proposed. For catalysts of different type such as a Y and ZSM-5,

intrinsic activity and decay characteristics can differ very significantly {25-27}. This is illustrated in Figure 3.2 which shows plots of conversion of *n*-octane at 400 °C against time on stream for five catalyst to feed ratios for each zeolite. The conversion is defined as the percentage of feed reacted.

Typical conversion curves from reaction on zeolite HY (Figure 3.2.a) show a rapid increase followed by a plateau. Whereas for HZSM-5 (Figure 3.2.b) there is a steady increase with almost constant curvature. These observations result from the distinct properties of the zeolites, especially their unit cell sizes. The large porosity of HY zeolite allows a larger amount of feed to penetrate and interact with the active sites in the pores. However, because of the abundance of the feed in its pores, carbonaceous deposit (coke) builds up very quickly, blocking further access to the pores, thereby preventing further cracking. In contrast, the medium porosity of HZSM-5 permits a much smaller amount of the feed to penetrate through, while minimising the amount of coke deposited.

In this work comparisons between product distributions obtained from reactions on HY and HZSM-5 zeolites were made under conditions where the activity of the individual catalyst (as measured by cumulative conversion of *n*-octane) was equivalent. This condition can be taken as points of intersection of curves in Figure 3.2, corresponding to a specific time on stream. Four such points were established from these curves and are shown in Figure 3.3. These points are labelled LC1 and LC2 (corresponding to low conversion at two distinct values of time on stream) and MC1 and MC2 (corresponding to medium conversion levels). Thus taking conditions at each of these four points in turn, the behaviour of individual zeolites (HY and HZSM-5) with various combinations of the zeolites were compared, always using the same time on stream, conversion level, the amount of *n*-octane feedstock and the amounts of catalyst introduced. At low conversions of *n*-octane, it is also valid to state that the individual catalyst to reactant values is approximately equal to those presented to the isolated catalysts. This assumption of course becomes less valid as levels of conversion are increased.

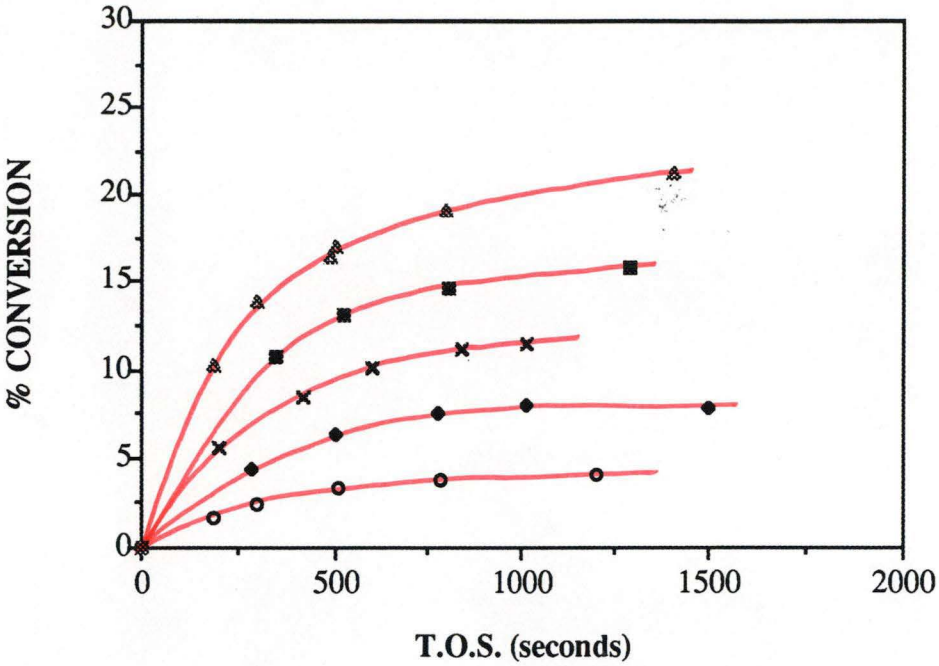

Figure 3.2.a Plots of *n*-octane conversion over zeolite HY at 400 °C
Catalyst to feed ratio : ○ = 0.0033, ● = 0.0101, × = 0.0310
■ = 0.0338, ▲ = 0.0900

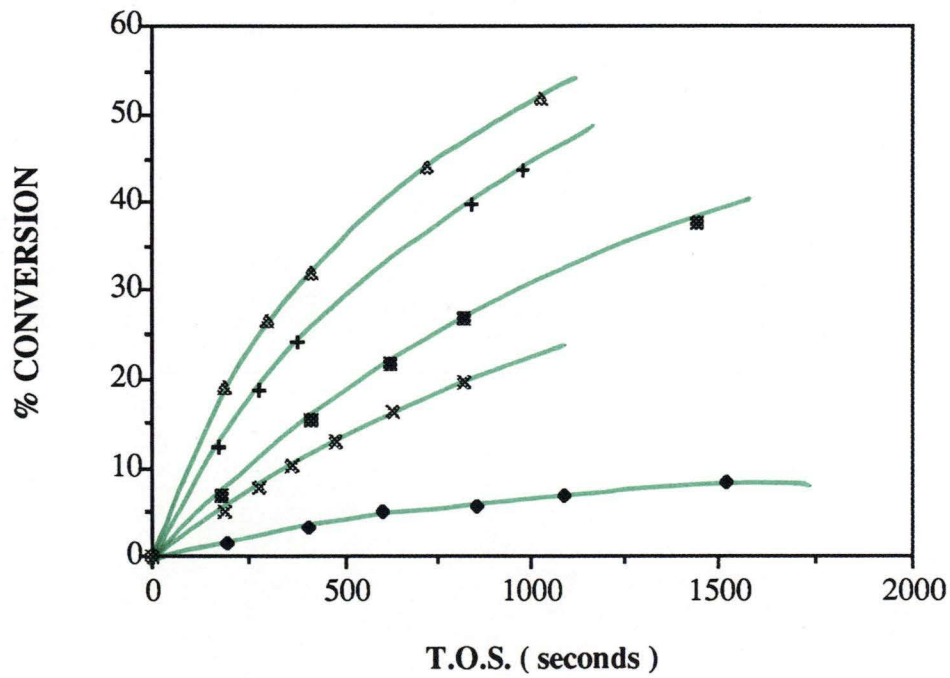

Figure 3.2.b Plots of *n*-octane conversion over zeolite HZSM-5 at 400 °C
Catalyst to feed ratio : ◆ = 0.0101, ✕ = 0.0301, ■ = 0.0338
+ = 0.0642, ▲ = 0.0900

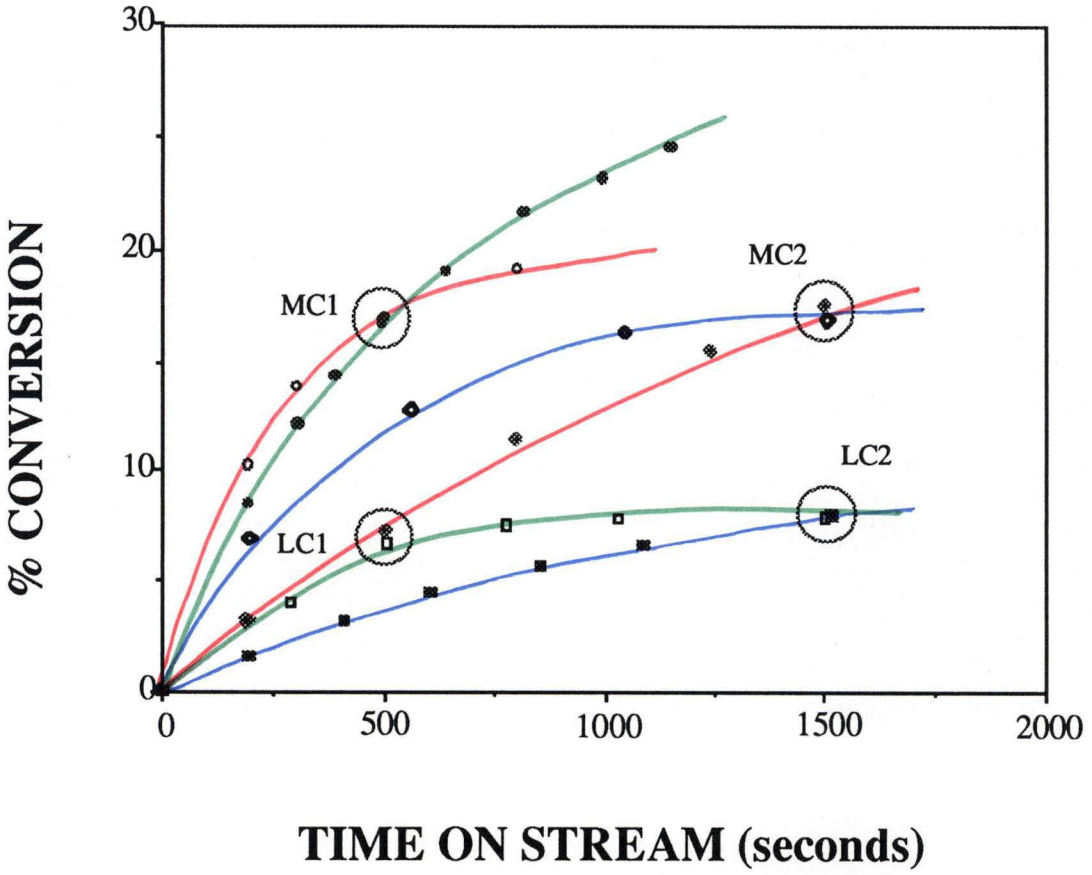

Figure 3.3 Effect of time on stream and catalyst to feed ratio for conversion of *n*-octane over zeolites HY and HZSM-5 at 400 °C
Catalyst to feed ratio : (HY ; ◻ = 0.0101, ◆ = 0.0579, ○ = 0.0900, HZSM-5 ; ■ = 0.0101, ◈ = 0.0179, ● = 0.0310)

For this reason, the system studied was restricted to medium conversion (less than 20%).

Table 3.1 shows the total conversion of *n*-octane corresponding to each of the four points LC1, LC2, MC1 and MC2. In each case, as expected, the conversion of *n*-octane with a catalyst combination is greater than that on an individual zeolite, but the total conversion is always less than the sum of the individual conversions. The difference observed lies in the fact that for second order reactions as in the case for catalytic cracking, the crackability (defined as conversion/(100-conversion)) is additive but not the conversion {28}. This may be expected by considering that doubling the catalyst to feed ratios for any given catalyst generally produces less than twice the conversion {29}. Alternatively, for a sequential mixture of zeolites, it could be inferred that the products from reactions on the first component may cause more rapid ageing than the reactant itself.

Since the patterns are similar at each point (LC1, LC2, MC1, and MC2), representative product distributions at LC1 from reactions of *n*-octane on HY and HZSM-5 at equivalent levels of conversion are shown in Figure 3.4. Distributions from cracking of linear paraffins on individual HY and HZSM-5 catalysts have been previously reported {6, 29}. It is apparent that acyclic olefins and paraffins are the dominant products. The maximum in the distribution of total hydrocarbons was shifted to lower molecular size on HZSM-5 relative to that on HY in each case examined {6, 30} as illustrated for LC1 in Figure 3.4.a. A similar trend was observed when considering the distributions of saturated products according to carbon number (Figure 3.4.b). In particular, it can be seen that at the same level of *n*-octane conversion, C_1, C_2 and C_3 paraffins are formed in greater abundance on HZSM-5 compared to HY. Figure 3.4.c shows that the abundance of olefinic products on HY is lower than on HZSM-5. This can be explained in terms of the increased tendency toward hydrogen transfer processes on the Y zeolite compared to the medium pore of ZSM-5 {19}. This is also revealed by the much higher tendency to produce aromatic products on HY, as illustrated in Figure 3.4.d.

Table 3.1 Percentage conversion of *n*-octane over zeolites HY, HZSM-5, and their combinations at 400 °C

Point	[Y]	[Z]	[Y-->Z]	[Z*]	[Z-->Y]	[Y*]	[Y<->Z]
LC1	6.5	7.0	11.8	5.3	10.2	3.2	13.4
LC2	7.9	8.0	10.6	2.7	9.7	1.7	11.2
MC1	17.1	17.0	30.6	13.5	22.4	5.4	33.5
MC2	16.9	18.0	29.1	12.2	21.6	3.6	32.1

Key:

[Y] = Conversion obtained from reaction over zeolite HY

[Z] = Conversion obtained from reaction over zeolite HZSM-5

[Y-->Z] = Conversion obtained from reaction over a sequential combination of zeolites (HY followed by HZSM-5)

[Z*] = Calculated conversion due to HZSM-5 from reaction over a sequential combination of zeolites (HY followed by HZSM-5)

[Z-->Y] = Conversion obtained from reaction over a sequential combination of zeolites (HZSM-5 followed by HY)

[Y*] = Calculated conversion due to HY from reaction over a sequential combination of zeolites (HZSM-5 followed by HY)

[Y<->Z] = Conversion obtained from reaction over a random combination of zeolites HY and HZSM-5

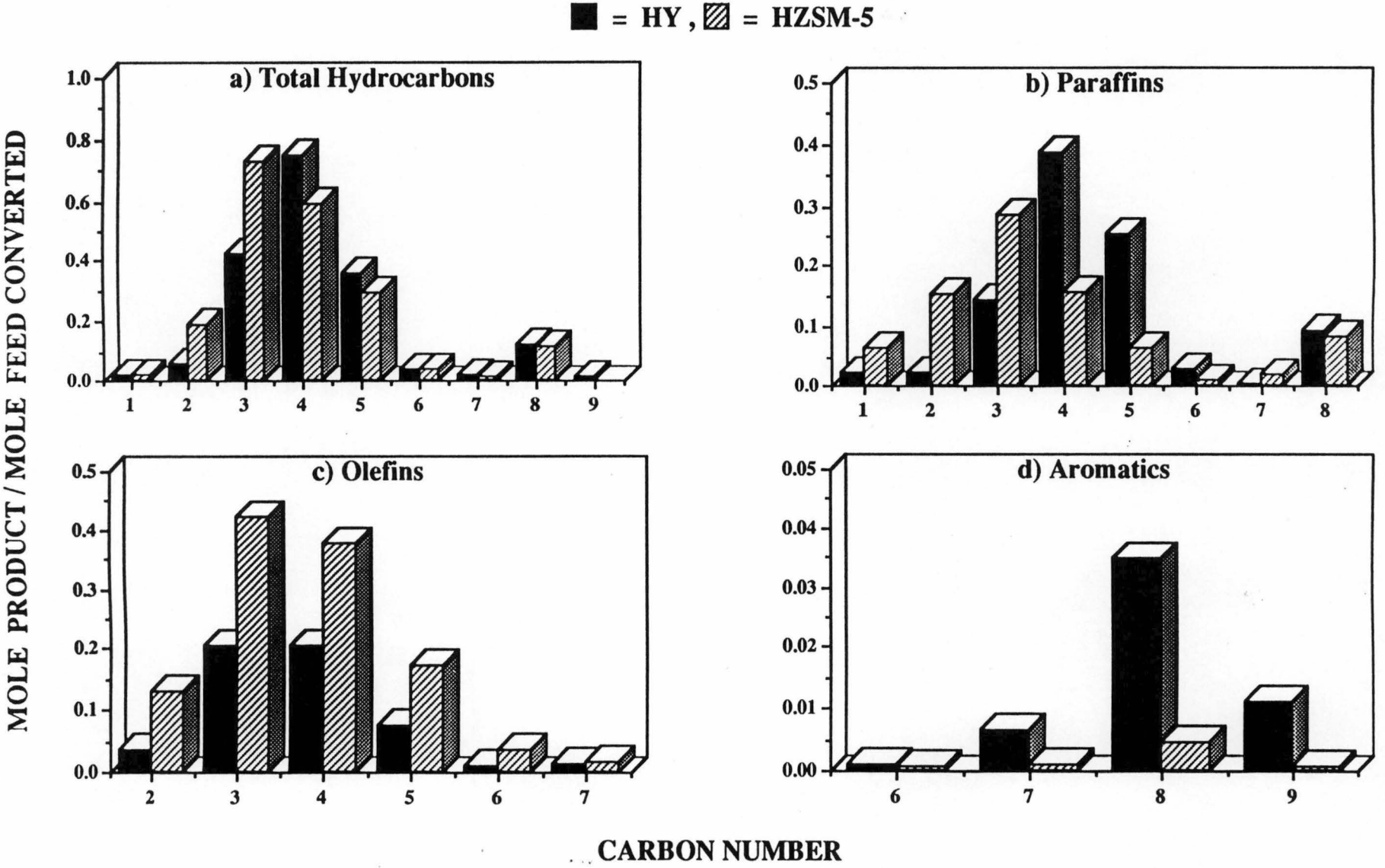

Figure 3.4 Product distributions from reaction of *n*-octane over zeolites HY and HZSM-5 at LC1 at 400 °C

Tables 3.2 and 3.3 show the ratios of branched to linear (B/L) isomers for product C_4 - C_6 paraffins and C_4 and C_5 olefins respectively. It is apparent that for reaction of *n*-octane on the individual zeolites there are significant differences in the branched to linear ratios of paraffin products. Branched paraffins are dominant on HY while the linear isomers are preferentially formed on HZSM-5, confirming earlier studies by Abbot and Wojciechowski {6}.

Table 3.2 Branched to linear ratios of paraffins from reaction of *n*-octane over zeolites HY and HZSM-5 at 400 °C

Point	C_4		C_5		C_6	
	HY	HZSM-5	HY	HZSM-5	HY	HZSM-5
LC1	1.39	0.17	3.01	0.16	2.22	0.47
LC2	1.32	0.11	2.30	0.14	2.83	0.27
MC1	2.03	0.23	5.60	0.22	3.87	0.23
MC2	2.13	0.27	5.84	0.24	5.69	0.66

Table 3.3 Branched to linear ratios of olefins from reaction of *n*-octane over zeolites HY and HZSM-5 at 400 °C

Point	C_4		C_5	
	HY	HZSM-5	HY	HZSM-5
LC1	1.02	1.38	1.92	1.93
LC2	0.94	1.46	1.93	1.84
MC1	0.92	1.43	2.30	2.47
MC2	0.96	1.44	2.10	2.56

Table 3.3 shows that for C_4 and C_5 olefins the branched to linear ratios show less variation than for the corresponding saturated products, with values generally in the range 1 to 2.5. It can be seen that there is a higher tendency to form branched C_4 olefins on HZSM-5 (B/L ratios 1.38-1.46) compared to HY (B/L ratios 0.92-1.02). A similar trend was also found for the C_5 olefins.

3.4 Reaction of *n*-Octane over Combinations of Zeolites

In most studies investigating the effect of ZSM-5 addition to the commercially used Y zeolite on catalytic cracking of hydrocarbons {13-21}, the catalysts are mixed intimately and diluted with some inert matrix. However, with this way of mixing, it is not possible to isolate whether the effect of ZSM-5 is on the feed or on the products of the conversion over the Y zeolite.

In this study, combinations of zeolites HY and HZSM-5 were prepared in three different ways. The first combination was by placing the bed of HY zeolite before that of HZSM-5. Throughout the text this type of combination is designated [Y-->Z]. The second type of combination was the reverse order, and designated as [Z-->Y]. The last type of combination was by mixing the catalysts thoroughly as has been done in most studies {13-21}. This type of combination is designated [Y<->Z].

Theoretical product distributions resulting from the reaction of *n*-octane on combinations of the two zeolites were calculated by adding the experimental product distributions on the individual catalysts, taking into account any change in level of conversion.

3.4.1 Reaction of *n*-Octane over a Sequential Combination of Zeolites HY followed by HZSM-5

The total conversions of *n*-octane when passed over HY together with HZSM-5 are given in Table 3.1. In each case (LC1, LC2, MC1 and MC2), knowing the conversion of *n*-octane under the same conditions without the presence of HZSM-5, it is possible to calculate the total conversion of *n*-octane on the ZSM-5 component, designated as [Z*]. In the first instance, it can be assumed that product distributions from reaction of *n*-octane on HZSM-5 on the combination [Y-->Z] are the same as those observed on HZSM-5 alone. Taking into account the calculated conversion of *n*-octane on each zeolite component of the sequence, it is possible to compute predicted distributions of products for reaction on the catalyst sequence [Y-->Z]. These predicted distributions assume that only *n*-octane reacts on the second catalyst component of the sequence (in this case, HZSM-5) and that the catalyst reaction products formed on HY pass through the HZSM-5 unchanged. These predicted product distributions are designated as [Y->Z*]. By comparing these predicted distributions with those actually observed, the extent to which the assumptions made concerning the interactions on the second zeolite can be inferred as correct. Variations between observed and predicted distributions can then be explained in terms of interactions and additional reaction processes. Figures 3.5 - 3.8 show comparison between observed and predicted product distributions fromreaction over sequential combination of HY followed by HZSM-5. Separate comparisons have been made for total hydrocarbons (Figure 3.5), paraffins (Figure 3.6), olefins (Figure 3.7) and aromatics (Figure 3.8).

Inspection of Figure 3.5 clearly shows that the observed distributions for total hydrocarbons produced are generally well represented by the predicted values. Comparison between the observed and predicted values of C_3, C_4 and C_5 paraffins (Figure 3.6) shows, that in every case, extensive hydrogen transfer processes, which would lead to significant additional paraffins in this range, do not occur on

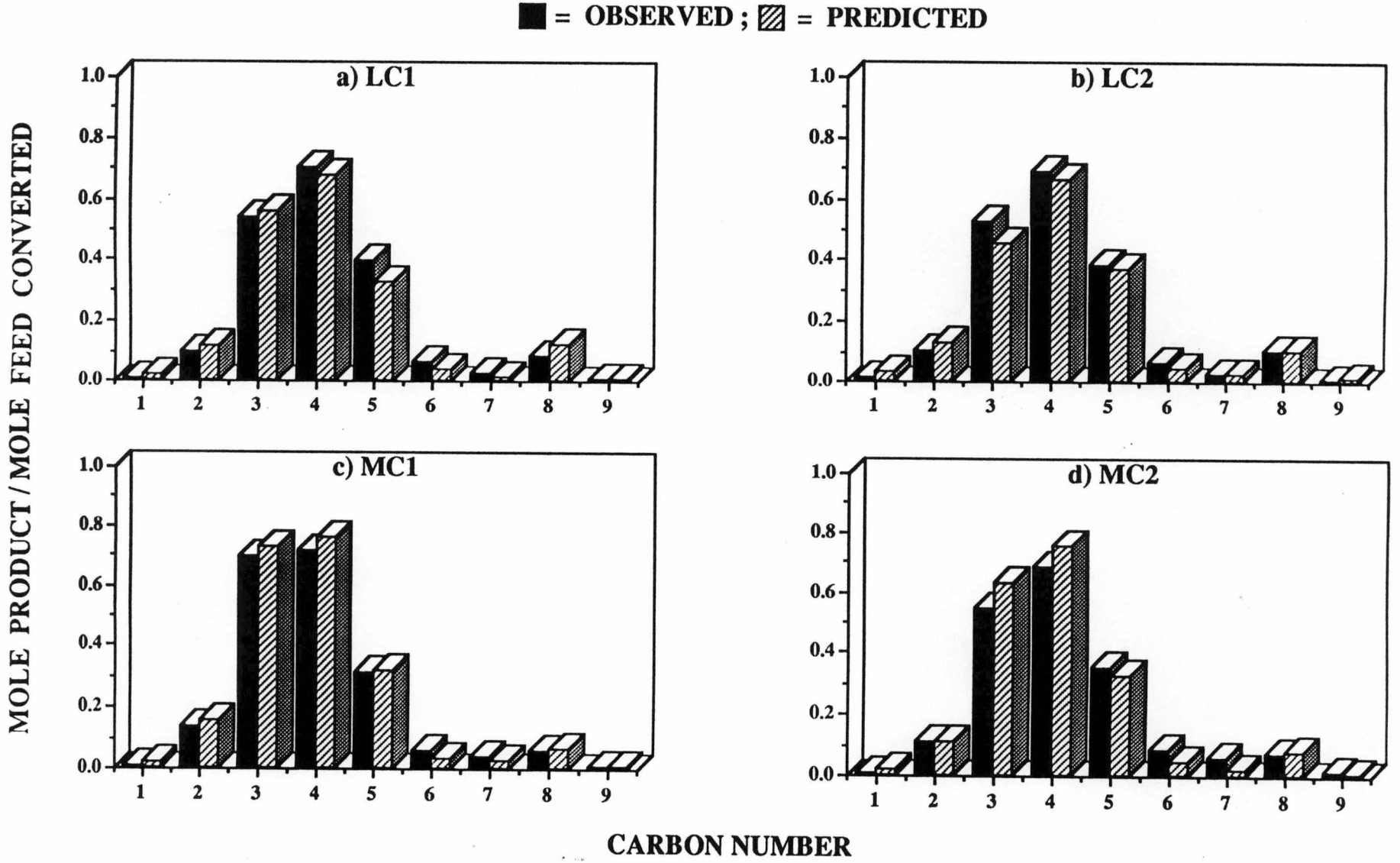

Figure 3.5 Total hydrocarbon distributions from reaction of *n*-octane over a sequential combination of zeolites (HY followed by HZSM-5) at 400 °C

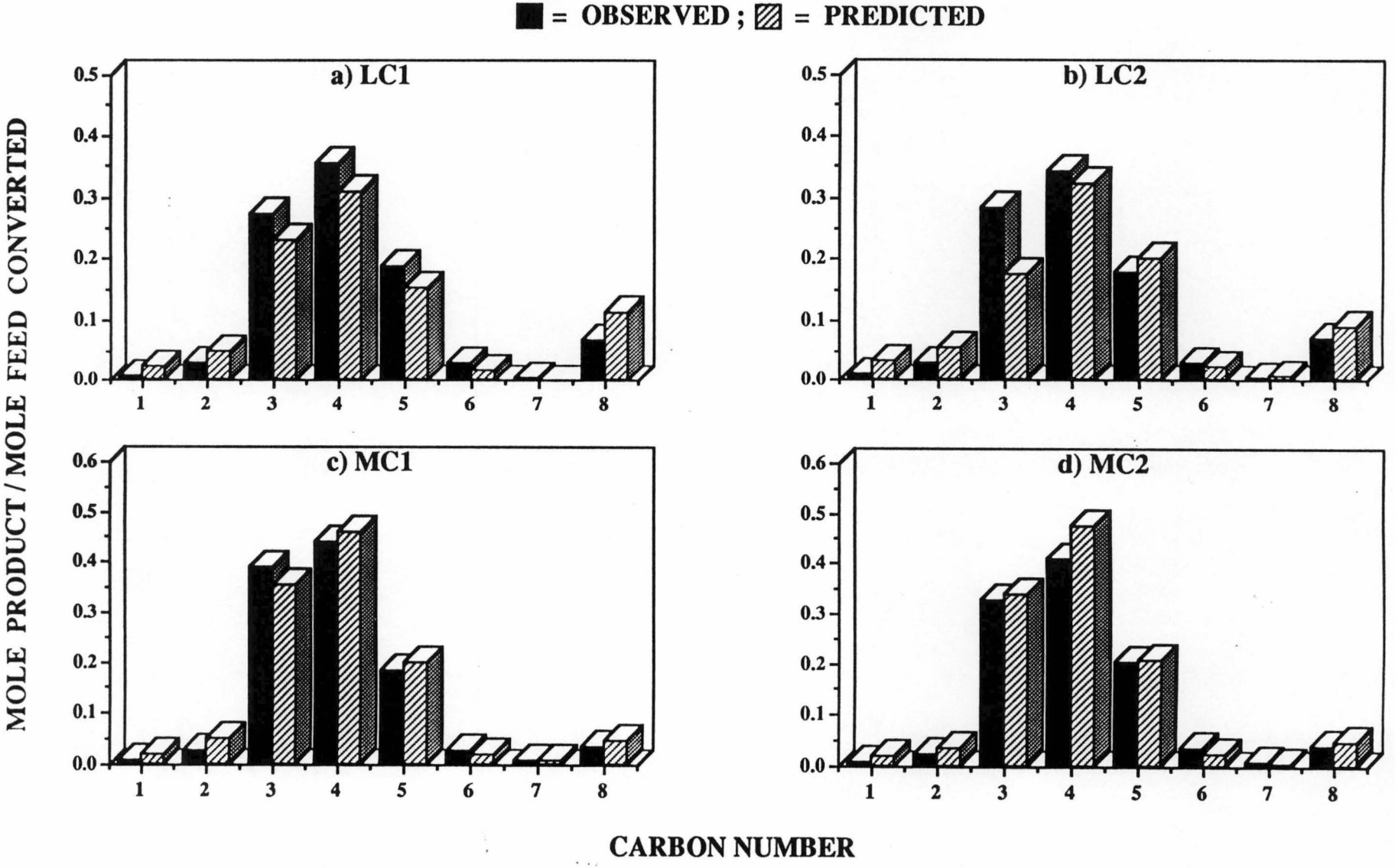

Figure 3.6 Paraffin distributions from reaction of *n*-octane over a sequential combination of zeolites (HY followed by HZSM-5) at 400 °C

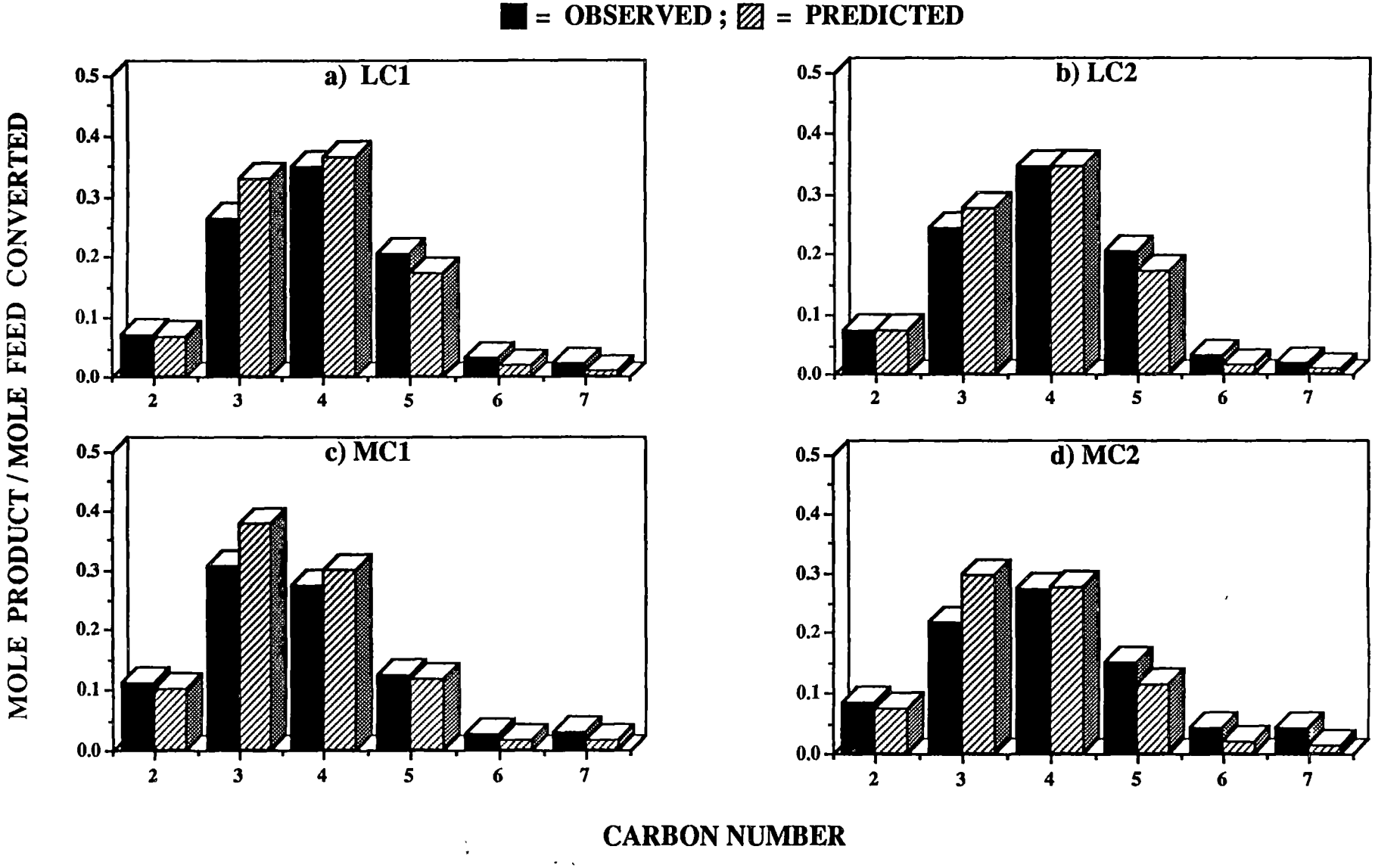

Figure 3.7 Olefin distributions from reaction of *n*-octane over a sequential combination of zeolites (HY followed by HZSM-5) at 400 °C

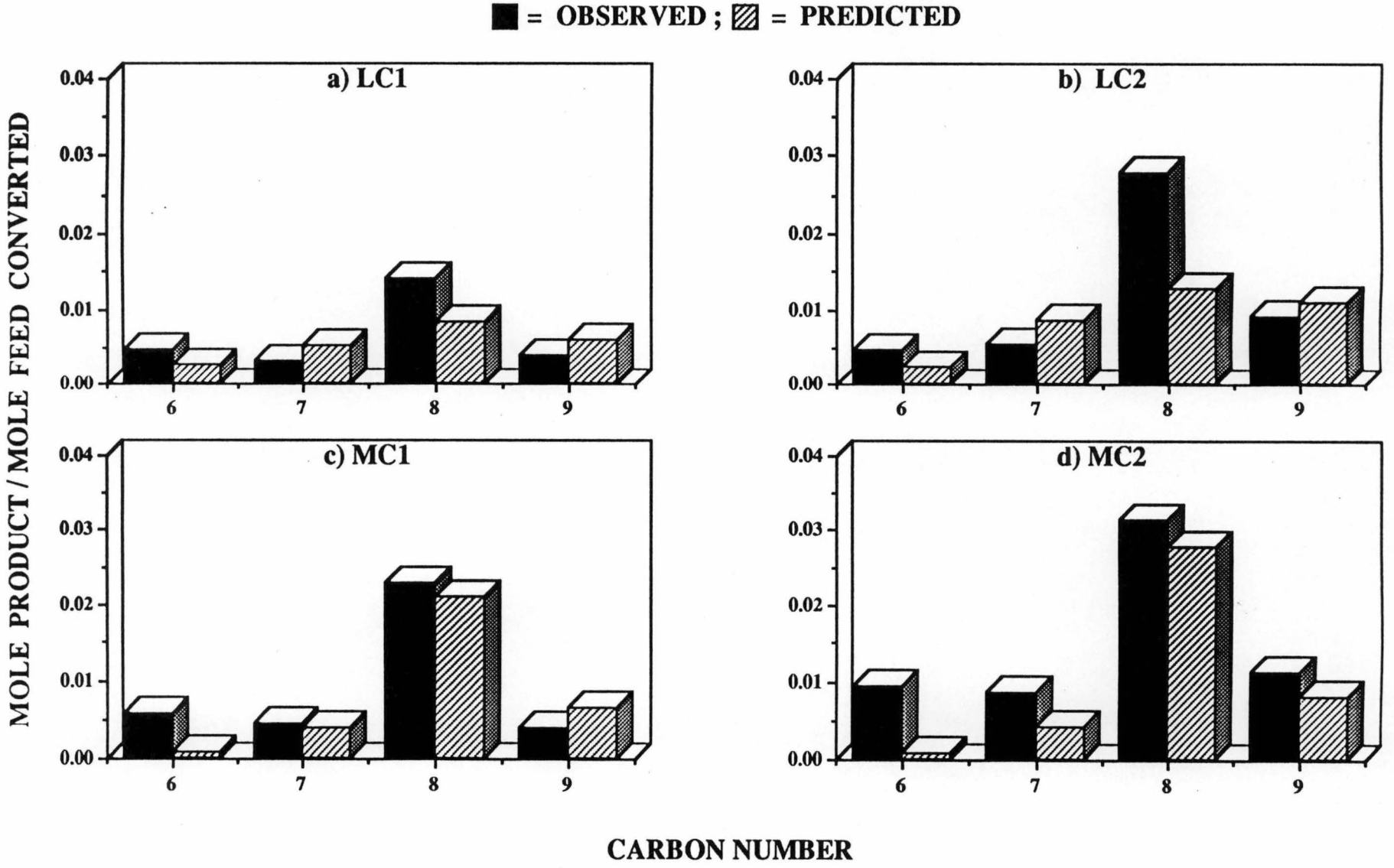

Figure 3.8 Aromatic distributions from reaction of *n*-octane over a sequential combination of zeolites (HY followed by HZSM-5) at 400 °C

ZSM-5. This is confirmed by a similar inspection of the results for the corresponding olefins (Figure 3.7), which does not reveal extensive depletion of olefins present within the distribution. Further inspection of this figure shows that while C_2 and C_4 olefins are very close to predicted values, there are losses in C_3 olefins, with gains in C_5, C_6 and C_7 olefins, while higher olefins were not detected. These observations can be explained by assuming that the olefins produced on ZSM-5 from cracking of *n*-octane, and those entering as products from reactions on HY, can participate in dimerisation-cracking processes {31, 32}, which can result in a redistribution of the olefin species present. These processes eventually result in a net loss in propene, net gains in C_5, C_6 and C_7 olefins and little net change in the butenes.

Closer examination of the branched to linear ratios of paraffins and olefins are presented in Figures 3.9 and 3.10. It is shown in Figure 3.10 that the ratios of branched to linear C_4 and C_5 olefins for [Y-->Z] are close to predicted values, [Y->Z*], with the observed ratios consistently slightly larger than those obtained by calculation. This indicates that while the dimerisation-cracking processes may alter the distribution of molecular size of olefins present, there is little net influence on isomer distribution at each carbon number. The consistent agreement between observed and predicted values for the proportion of ethylene may suggest that the C_2 olefin does not extensively participate in the dimerisation processes, possibly due to instability of the C_2 carbenium ion.

Once formed, a carbenium ion produced from a dimerisation process can crack via ß-scission processes, to give smaller olefins, or desorb directly as a C_6 or C_7 olefin. Alternatively, cyclisation can lead to formation of additional aromatic species. From Figure 3.8, it is evident that, in particular, the amount of benzene produced on this sequential combination is higher than that predicted by simple addition of the distributions. At the same time Figure 3.6 shows consistently higher values for production of C_6 and C_7 paraffins than predicted. Possibly some C_6 and C_7 carbenium ions are available for hydrogenation during concurrent formation of

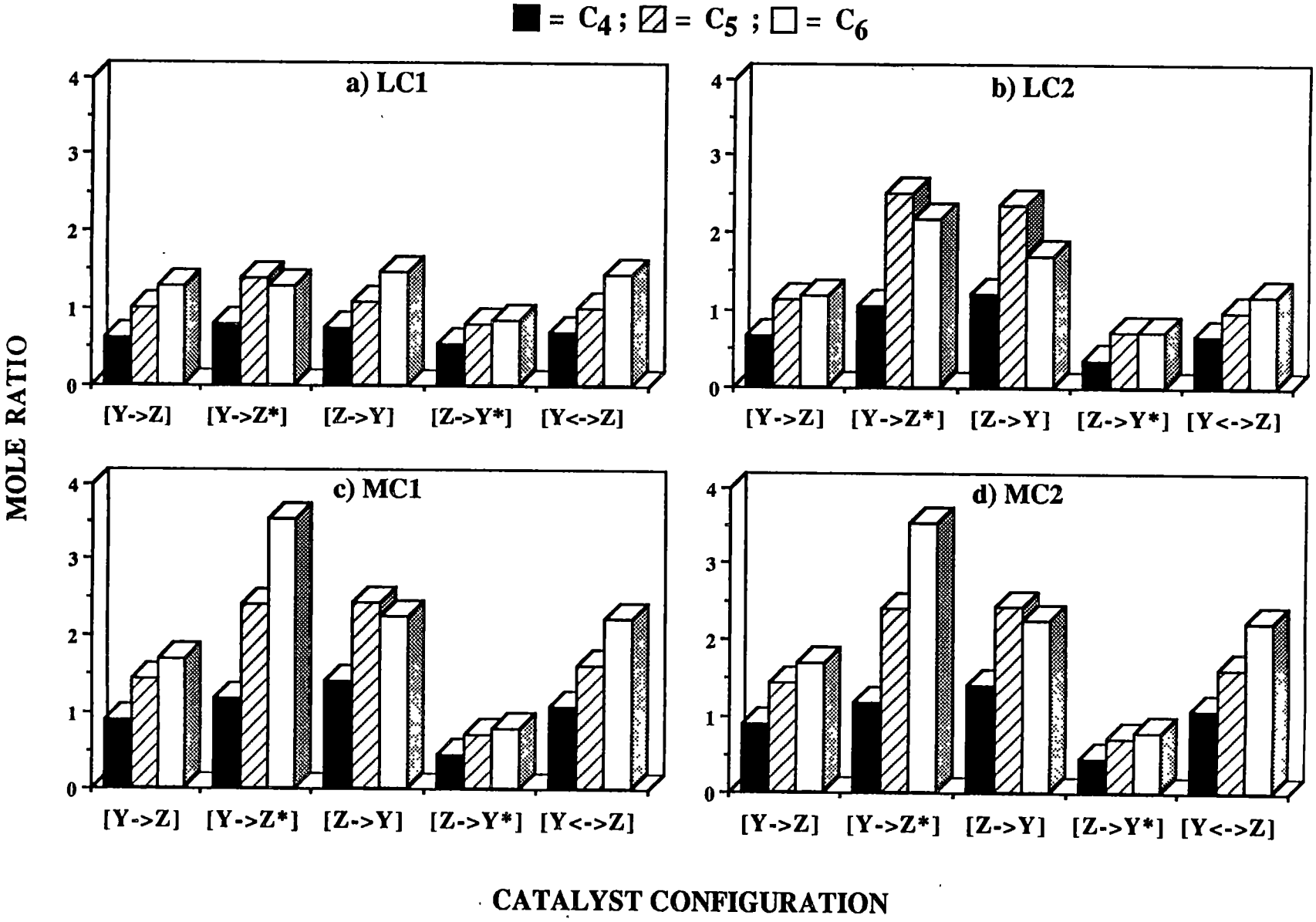

Figure 3.9 Ratios of branched to linear paraffins (C_4, C_5, and C_6) from reaction of *n*-octane over combinations of zeolites HY and HZSM-5 at 400 °C

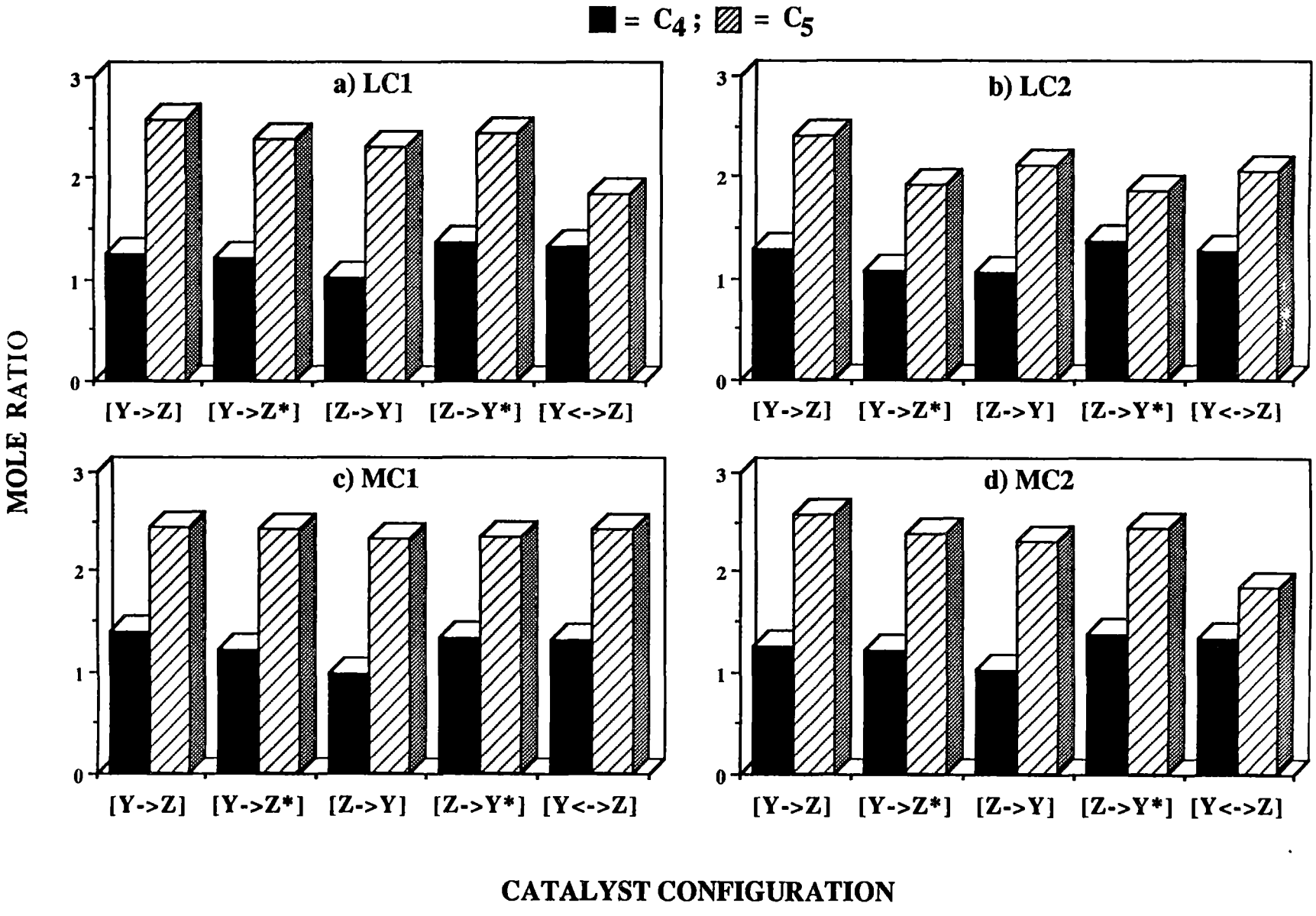

Figure 3.10 Ratios of branched to linear olefins (C_4 and C_5) from reaction of *n*-octane over combinations of zeolites HY and HZSM-5 at 400 °C

aromatics, and these give rise to the saturated products. The depletion in C_8 paraffins as shown in Figure 3.6 can be explained in terms of the instability of the corresponding carbenium ion (i.e. it cracks before it can either desorb as an olefin or participate in hydrogen transfer to produce a C_8 paraffin).

Figure 3.9 shows that the ratios of branched to linear C_6 paraffins for the combination [Y-->Z] are lower than predicted on the basis of simple addition of distributions, [Y->Z*]. However, if it is assumed that additional C_6 paraffins formed on HZSM-5 (Figure 3.5) by hydrogen transfer are predominantly linear, the observed branched to linear ratios can be rationalised. The observed and predicted values of these ratios are given in Table 3.4. Adjusted values represent the predicted values that have been recalculated to meet the observed values, based on the assumption that, any additional paraffins are formed through hydrogen transfer process, and any loss of paraffins can be attributed to selective cracking of branched saturated isomers.

There were three types of deviation in the branched to linear ratios and the amount of paraffins formed which were noted. The following keys are used to illustrate these deviations:-

Keys:

B/L = Observed value of the branched to linear ratio
B*/L* = Predicted value of the branched to linear ratio
B#/L# = Adjusted value of the branched to linear ratio
P = Observed value of the amount of paraffins formed
P* = Predicted value of the amount of paraffins formed

1. If $B/L < B^*/L^*$ and $P > P^*$ such that $\Delta P > 0$, where $\Delta P = P - P^*$, then $B\#/L\# = B^*/(L^* + \Delta P)$. This calculation assumes selective hydrogen transfer takes place giving additional linear paraffins.
2. If $B/L < B^*/L^*$ and $P < P^*$ such that $\Delta P < 0$, where $\Delta P = P - P^*$, then $B\#/L\# = (B^* + \Delta P)/L^*$. This calculation assumes selective cracking of branched paraffins.

Table 3.4 Branched to linear ratios of paraffins from reaction of *n*-octane over a sequential combination of zeolites (HY followed by HZSM-5) at 400 °C

Point	C_4			C_5			C_6		
	Observed	Predicted	Adjusted	Observed	Predicted	Adjusted	Observed	Predicted	Adjusted
LC1	0.59	0.79	0.62[a]	0.98	1.38	0.90[a]	1.26	1.28	0.55[a]
LC2	0.64	1.05	0.92[a]	1.12	2.50	2.13[b]	1.17	2.15	1.21[a]
MC1	0.89	1.17	1.08[a]	1.44	2.39	2.13[b]	1.19	3.53	1.18[a]
MC2	0.75	1.29	0.96[a]	1.30	2.47	2.35[b]	1.72	2.34	0.82[a]

Key:

a = Adjusted values are obtained by recalculating the predicted values assuming that all additional paraffins formed are linear and produced via selective hyrogen transfer on HZSM-5

b = Adjusted values are obtained by recalculating the predicted values assuming that all paraffins lost are due to selective cracking of branched isomers on HZSM-5

3. If B/L > B*/L* and P > P* such that $\Delta P > 0$, where $\Delta P = P - P^*$, then $B\#/L\# = (B^* + \Delta P)/L^*$. This calculation assumes selective hydrogen transfer takes place giving additional branched paraffins.

As an example of this deviation is the production of C_6 paraffin and its branched to linear ratios from the reaction over sequential catalysts [Y-->Z] (*viz.* Figures 3.6 and 3.9). All the observed branched to linear ratios are lower than predicted (i.e. B/L < B*/L*), and at the same time there are more C_6 paraffins than predicted (i.e. P > P*), so this corresponds to the first case above. Thus the deviation in the branched to linear ratios can be rationalised by the hydrogen transfer process alone.

The total amounts of C_3, C_4 and C_5 paraffins do not markedly differ from the predicted values, which assumes products emerging from reaction on the Y zeolite are unchanged on HZSM-5. The absence of extensive hydrogen transfer processes, which could give rise to additional paraffin formation from olefins produced on Y zeolite has already been noted. The lack of additional small cracking fragments (C_1 and C_2) also suggests that these paraffins do not undergo significant cracking on passing through the HZSM-5 (Figure 3.6). It is therefore interesting to note that, in contrast to the corresponding olefins, the ratios of branched to linear paraffins for C_4 and C_5 are significantly lower than predicted in each case, by comparing values obtained for [Y-->Z] and [Y->Z*] in Figure 3.9.

In contrast to the C_6 paraffin isomers previously discussed, the required adjustment in the branched to linear isomer ratio in favour of linear C_4 and C_5 saturated products to coincide with the observed distributions cannot be explained merely in terms of hydrogen transfer with selective production of linear paraffins. In the cases where additional paraffins are observed, (Figure 3.6: LC1 and LC2) the amounts are insufficient to account for the observed branched to linear ratio, as illustrated in Table 3.4. In the other cases (MC1 and MC2), there is in fact, an apparent reduction in the amounts of C_4 and C_5 paraffins formed. Neither can the observed branched to linear ratios for C_4 and C_5 paraffins after contact with

HZSM-5 be explained easily by selective cracking of the branched saturated isomers. Cracking reactions of small branched paraffins such as isobutane and isopentane on HZSM-5 {34-36} give high selectivity towards formation of C_1 and C_2 fragments, whereas Figure 3.6 shows that additional amounts of these products are not observed.

It appears that, in order to explain the observed branched to linear ratios for C_4 and C_5 paraffins, isomerisation of the branched paraffins, must occur on HZSM-5. However, previous studies of reactions of individual branched paraffins on HZSM-5 show that the predominant reaction process is cracking rather than isomerisation, as shown in Table 3.5. For example, reaction of *iso*-butane {33, 35} on HZSM-5 at 400 °C shows a selectivity for formation of *n*-butane of less than 20%. In a series of separate experiments on reaction of 2-methylpentane over HZSM-5 at 400 °C, a selectivity of 0.4% occurs for production of *n*-hexane. These results suggest that isomerisation rather than cracking becomes the preferred reaction mode when the feed contains a high proportion of olefins. The isomerisation of branched paraffins on HZSM-5 represents the first significant difference between predicted and observed behaviour.

Other reported investigations, particularly with *iso*-butane, have shown that a significant selectivity for paraffin isomerisation to produce *n*-butane is observed for reactions on Y zeolites in some cases {36}. High selectivities towards isomerisation have been observed using solid superacid catalysts {37, 38}, in particular for catalysts reported to have an appropiate balance in the amounts of strong Brønsted and Lewis acid sites. It is possible that the change in selectivity in favour of isomerisation of branched paraffins for the system under present consideration may be associated with formation of Lewis sites due to adsorption of product olefins at Brønsted sites in HZSM-5. Lewis acid sites alone do not appear to be active in most hydrocarbon transformations {39-41}. However, coupling of Lewis sites and Brønsted sites can apparently result in significant changes in both acidity {39} and activity.

Table 3.5 Selectivities of cracking and isomerisation from reaction of *n*-octane over zeolite HZSM-5

Feed	Temp(°C)	Cracking	Total Isomerisation	Isomerisation to Linear Isomers	Reference
Iso-butane	400	1.0	0	0	{33}
Iso-butane	500	0.95	0.05	0.05	{33}
Iso-butane	400	0.83	0.17	0.17	{35}
3-methylpentane	500	0.922	0.066	0	{27}
2-methylpentane	500	0.967	0.025	0	{27}
2-methylpentane	400	0.960	0.040	0.004	This study

The second significant difference between observed and predicted distributions for the sequence [Y-->Z] relates to the amounts of methane and ethane formed (Figure 3.6). In each case, it is apparent that there is significantly less of these C_1 and C_2 fragments observed than would be predicted by addition of individual distributions. Again, it can be inferred that reactions of *n*-octane on HZSM-5 are perturbed when the feedstock contains a significant proportion of olefins. The observed reductions in methane and ethane are consistent with the proposal {5} that the cracking pathway via direct protonation of the paraffin becomes less significant in the presence of olefins, in favour of a bimolecular cracking mechanism. This reasoning can explain the reduction in the proportion of ethane formed (Figure 3.6). For methane, however, the absolute amounts present after the product mixtures emerge from reactions on the sequence [Y-->Z] is less than that entering the HZSM-5 stage of the sequence (Figure 3.11). This implies that, not only is there a reduction in cracking processes via protonation yielding methane, but now there is also evidence for reaction of methane itself on this catalyst to form other products. This is unexpected, as methane is generally regarded as a stable product of cracking.

It has been shown that although higher paraffins ($>C_3$) can undergo reaction over HZSM-5, methane and ethane are themselves unreactive when passed through the catalyst as a pure feedstock {42}. The present results show, however, that it is possible for methane to be converted into other products when passed over a zeolite catalyst in the presence of other hydrocarbons. Recent studies {44-46} have shown that methane and ethene can undergo coupling reactions to produce higher hydrocarbons on solid superacid catalysts, and it is possible that our observed losses in methane and ethane are due to coupling reactions involving unsaturated species. Alternatively, it is possible that methane may be involved in a reversible reaction in which interaction with an adsorbed carbenium ion at a Brønsted site produces a penta-coordinated carbonium ion, as proposed by Kanai *et al.* {47}.

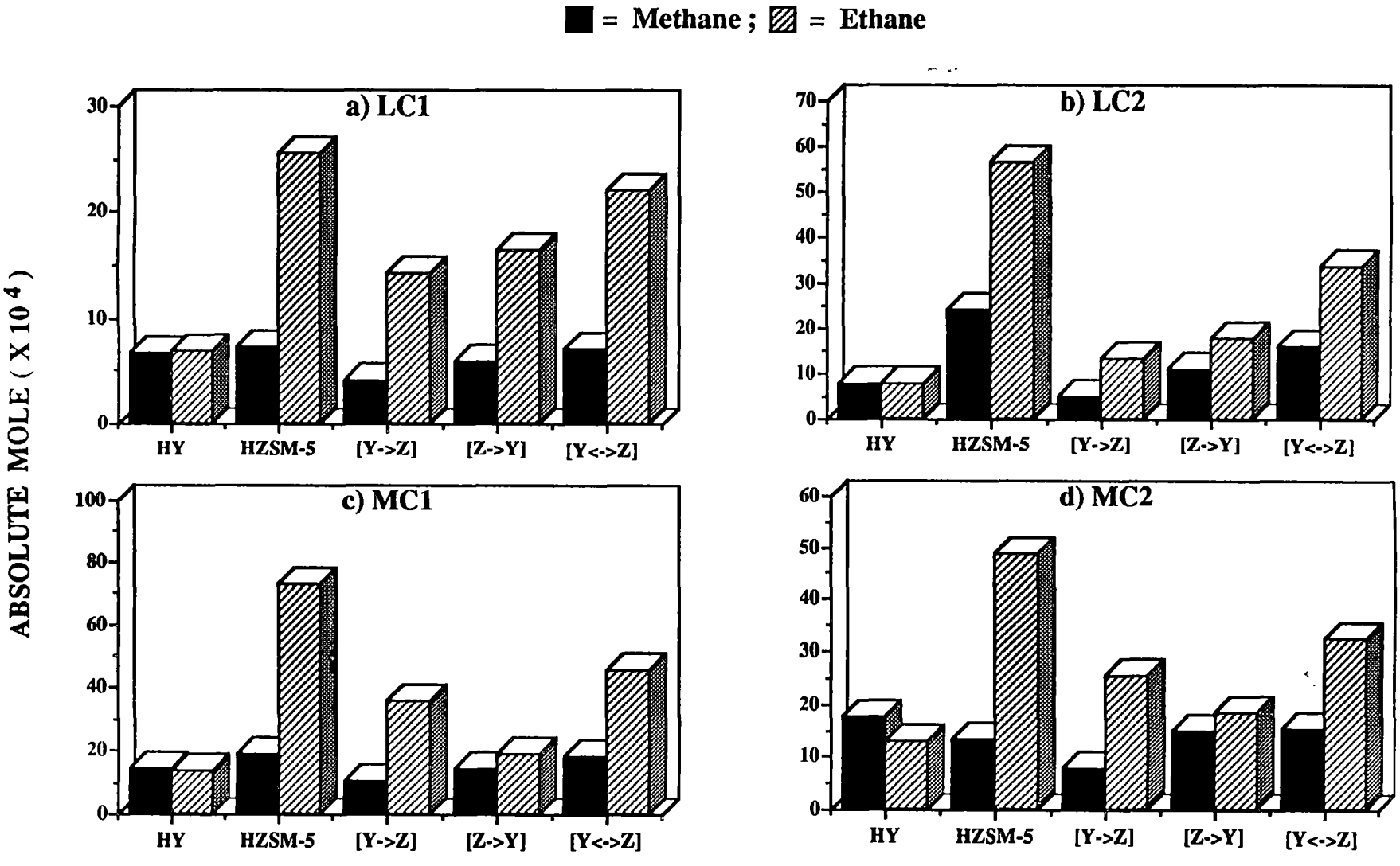

Figure 3.11 Molar amounts of methane and ethane produced from reaction of *n*-octane over zeolites HY, HZSM-5, and their combinations at 400 °C

The results presented for the sequential catalyst [Y-->Z] corresponding to the four conditions show that the general conclusions are independent of time on stream and conversion levels. This was also found to be the case for the combinations discussed in subsequent sections, therefore the results presented are representative.

3.4.2 Reaction of *n*-Octane over a Sequential Combination of Zeolites HZSM-5 followed by HY

Representative examples of observed product distributions for reaction of *n*-octane on the zeolite sequence [Z-->Y] are presented in Figures 3.12 (for MC2) and 3.13 (for LC1 and MC2). As for the previous catalyst sequence, predicted distributions, [Y->Z*], are also presented, using conversions in Table 3.1 and the appropriate distributions of products on individual zeolites as illustrated in Figure 3.4. As for the [Y-->Z] sequence, the predicted distributions of total hydrocarbons, according to carbon number also provide reasonable approximations to the observed values, as shown in Figure 3.12. Again, it is possible to focus on differences in the various observed and predicted product distributions, particularly those for paraffins, olefins and aromatics, to describe any possible additional reactions and interactions as products formed on HZSM-5 pass over the Y zeolite.

A feature which is apparent from inspection of these distributions, is the amounts of C_3 - C_6 paraffins are generally in excess of the predicted values, as illustrated in Figure 3.12.b. In contrast, the observed amounts of olefins in this range are significantly less than those predicted (Figure 3.12.c). This is indicative of significant additional hydrogen transfer processes occurring on the Y zeolite, particularly involving product olefins formed on the HZSM-5. For this catalyst configuration, the extent of these processes is, in fact, sufficient to explain the observed branched to linear ratios for paraffins in the range C_4 - C_6, as shown in Figure 3.9. (*viz.* the results obtained on the sequences [Z-->Y] and [Z->Y*]).

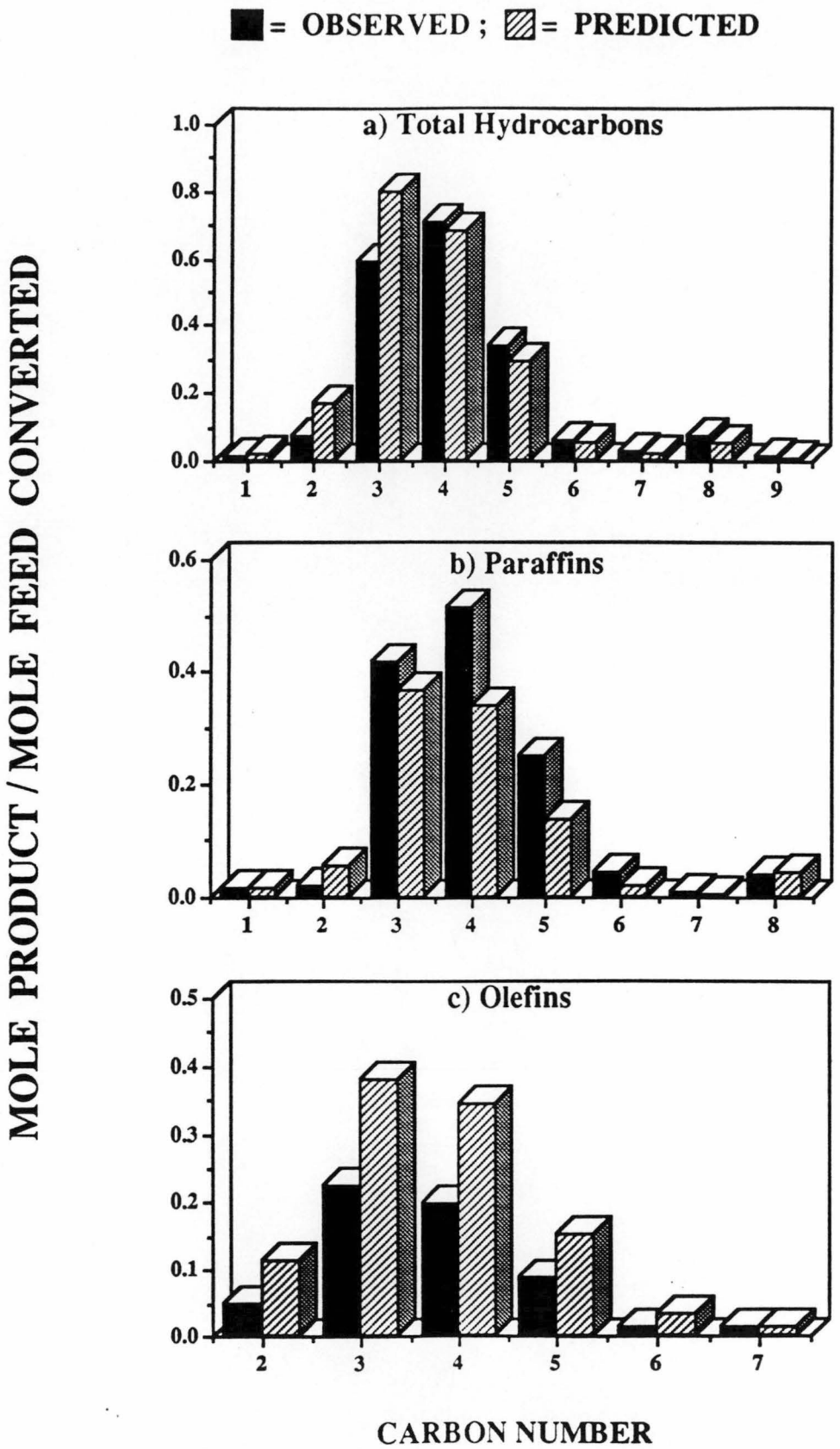

Figure 3.12 Product distributions from reaction of *n*-octane over a sequential combination of zeolites (HZSM-5 followed by HY) at MC2 at 400 °C

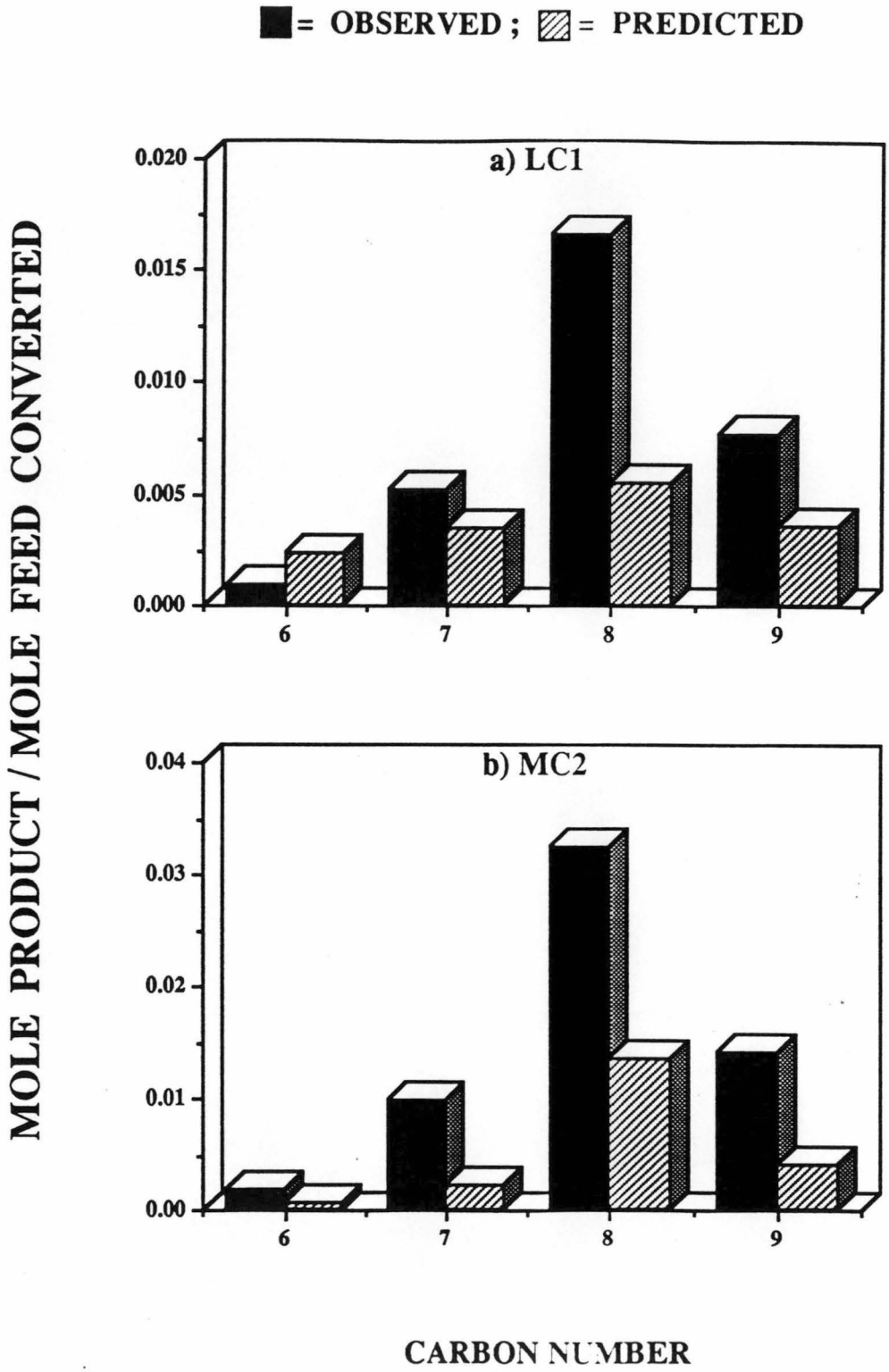

Figure 3.13 Aromatic distributions from reaction of *n*-octane over a sequential combination of zeolites (HZSM-5 followed by HY) at 400 °C

The predicted ratios are lower than those actually observed on the assumption that products formed on the ZSM-5 pass through the Y zeolite unchanged. Table 3.6 shows the limiting adjusted values of these ratios, assuming that all additional C_4, C_5 and C_6 paraffins formed on HY, through hydrogen transfer to olefins result in formation of the corresponding branched saturated isomers. In all cases, the adjusted values are already higher than the corresponding observed value, so that it is not necessary here to invoke a paraffin isomerisation process on the Y zeolite, as proposed for reaction on the ZSM-5 for the [Y-->Z] sequence previously discussed.

Figure 3.13 shows that there is significant additional formation of aromatics using the [Z-->Y] sequence, shown here for LC1 and MC2, comparing calculated values for simple addition of product distributions. This can be rationalised in terms of reactions of olefinic species formed on the HZSM-5 in the first stage of the sequence, through cyclisation and hydrogen transfer processes on HY to produce aromatic species as well as the saturated products already discussed. Figure 3.10 shows that the observed branched to linear ratios for C_5 olefins are very close to the predicted values, while the observed ratios for the C_4 olefins are generally somewhat lower than those predicted. This may be explained by assuming that the hydrogen transfer process occurring on the faujasite was selectively directed towards the branched C_4 olefins yielding branched isomers of the corresponding paraffins. This assumption was fairly well justified by the excess C_4 paraffins observed compared to predicted values (Figure 3.12.b) and the larger observed ratios of branched to linear isomers of C_4, C_5 and C_6 paraffins (Figure 3.9).

As noted previously for reaction on the sequence [Y-->Z], reaction of *n*-octane on the sequence [Z-->Y] also shows an interesting result for the formation of methane and ethane (Figure 3.12.b). There is consistently less of the C_1 and C_2 paraffin fragments observed than predicted by calculation. Figure 3.11 shows that, as for methane on the catalyst sequence [Y-->Z] catalyst, these reductions are not simply due to reduced C_1 and C_2 paraffin formation on the second zeolite of the

Table 3.6 Branched to linear ratios of paraffins from reaction of *n*-octane over a sequential combination of zeolites (HZSM-5 followed by HY) at 400 °C

Point	C_4			C_5			C_6		
	Observed	Predicted	Adjusted	Observed	Predicted	Adjusted	Observed	Predicted	Adjusted
LC1	0.74	0.51	1.09	1.07	0.79	1.59	1.46	0.83	2.24
LC2	1.20	0.35	1.58	2.33	0.69	2.85	1.69	0.69	2.59
MC1	1.41	0.44	2.16	2.42	0.69	3.45	2.44	0.78	3.05
MC2	1.17	0.41	1.14	1.78	0.54	1.82	1.83	0.82	3.22

Key:

All adjusted values are obtained by recalculating the predicted values assuming that all additional paraffins formed are branched and produced via selective hyrogen transfer on HZSM-5

sequence, but an actual reduction in the amounts finally emerging due to reactions on the Y zeolite. Again, it seems that methane and ethane undergo reaction with other hydrocarbons when the mixture comes into contact with the second zeolite component. Therefore it can be concluded that it is not the specific type of zeolite that is responsible for this observed phenomenon, but rather the influence of other hydrocarbons present in the mixture.

3.4.3 Reaction of *n*-Octane over a Random Mixture of Zeolites HY and HZSM-5

The random mixture of HY and HZSM-5 used corresponded to amounts of HY and HZSM-5 which produced equal conversions of *n*-octane under the same conditions. The total conversions of *n*-octane observed for reaction on this random mixture of catalyst are given in Table 3.1. It was found that a simple averaging of distributions for total products on the individual catalysts according to carbon number again provides a very reasonable representation of the observed distribution (Figure 3.14.a). This shows that, as for the sequential combinations previously considered, the overall distribution of total hydrocarbon products by carbon number is well represented by the sum of the individual contributions on the isolated catalysts. It might be thought that a random mixture of particles of HY and HZSM-5 could be regarded as a large number of repeated [Y-->Z] and [Z-->Y] sequences. If that were the case, then we might expect the overall effect to result in a summation of the influences already discussed in the simple binary sequences.

Figure 3.14.b shows that the observed amounts of paraffins in the range of C_3 - C_6 are in excess of predicted values. This can again be correlated with reduced amounts of olefins (Figure 3.14.c) and increased amounts of aromatics (Figure 3.14.d). Seemingly in the random mixture studied, HZSM-5 does not suppress the hydrogen transfer process occurring on HY to a high extent. Rather, the excess formation of small olefins observed by addition of HZSM-5 is due to the direct

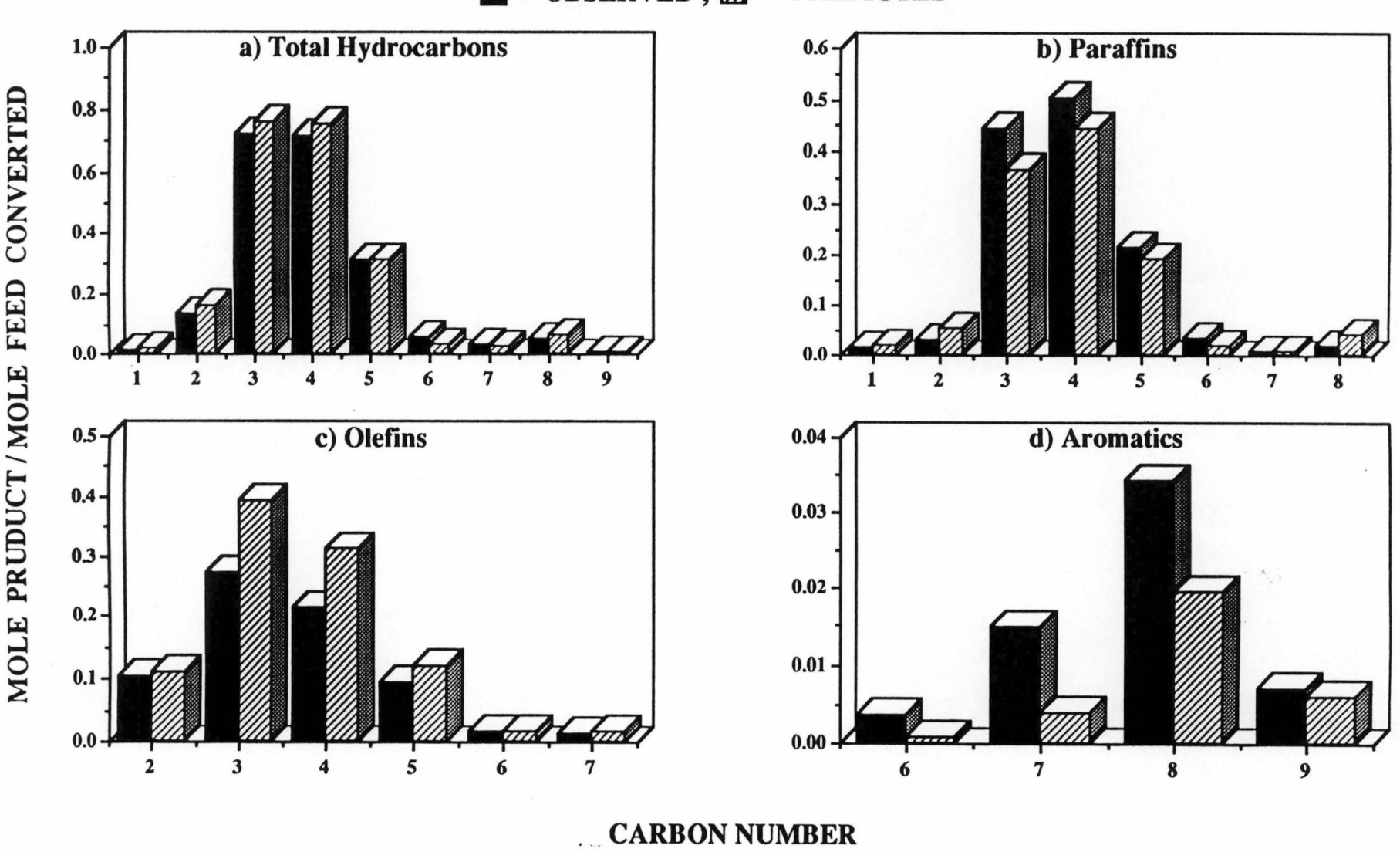

Figure 3.14 Product distributions from reaction of *n*-octane over a random mixture of zeolites HY and HZSM-5 at MC1 at 400 °C

contribution from reaction on the HZSM-5. An indication of the related tendency to undergo hydrogen transfer is provided by paraffin to olefin molar ratios at similar conversion levels. Ratios are presented in Table 3.7 corresponding to C_4, C_5 and C_6 for the three binary catalyst systems. It is apparent that values are highest for the [Z-->Y] sequence, lowest for the [Y-->Z] combination and intermediate for [Y<->Z] mixtures.

Figure 3.14.b also shows that the proportions of C_1 and C_2 paraffins produced on a random mixture of HY and HZSM-5 are less than those predicted. Figure 3.11 shows that the actual amounts of these products lie between those detected from reaction on the individual catalysts. In contrast to the sequential combinations, the amount of methane formed is not reduced below that formed on the first zeolite in the sequence.

Table 3.7 Paraffin to olefin ratios from reaction of *n*-octane over combinations of zeolites HY and HZSM-5 at 400 °C

Point	Carbon Number	[Y-->Z]	[Y<->Z]	[Z-->Y]
	C_4	1.02	1.14	1.18
LC1	C_5	0.91	1.08	1.21
	C_6	0.89	1.39	1.90
	C_4	1.00	0.90	1.14
LC2	C_5	0.88	0.84	1.39
	C_6	0.88	0.80	1.59
	C_4	1.60	2.33	3.03
MC1	C_5	1.48	2.30	4.00
	C_6	0.93	1.96	4.76
	C_4	1.52	1.92	2.60
MC2	C_5	1.34	1.63	2.82
	C_6	0.86	1.34	3.28

A comparison of the B/L ratios of olefins for all systems studied shows that the variations in observed values are not large, with somewhat higher values for the [Y-->Z] sequence compared to either [Z-->Y] or [Y<->Z]. Table 3.8 shows much more overall variation in branched to linear ratios for saturated products, depending on the particular catalyst or catalyst combination. The observed branched to linear ratios for paraffins on the mixture [Y<->Z] are consistently smaller than the predicted values.

Table 3.8 Branched to linear ratios of paraffins from reaction of *n*-octane over a random mixture of zeolites HY and HZSM-5 at 400 °C

Point	C_4			C_5			C_6		
	Observed	Predicted	Adjusted	Observed	Predicted	Adjusted	Observed	Predicted	Adjusted
LC1	0.68	0.78	0.57[a]	0.99	1.59	1.34[a]	1.43	1.35	2.28[c]
LC2	0.65	0.72	0.34[b]	0.96	1.72	0.67[b]	1.18	1.55	1.04[b]
MC1	1.06	1.13	0.88[a]	1.61	2.91	1.93[a]	2.22	2.91	0.63[a]
MC2	0.93	1.20	1.15[b]	1.40	3.04	1.97[b]	2.11	3.18	0.67[a]

Key:

a = Adjusted values are obtained by recalculating the predicted values assuming that all additional paraffins formed are linear and produced via selective hyrogen transfer

b = Adjusted values are obtained by recalculating the predicted values assuming that all paraffins lost are due to selective cracking of branched isomers

c = Adjusted values are obtained by recalculating the predicted values assuming that all additional paraffins formed are branched and produced via selective hyrogen transfer

3.5 Conclusions

Overall distributions of cracking products by carbon number from reaction of a linear paraffin on combinations of zeolites HY and HZSM-5 can be reasonably described by the addition of product distributions on individual catalysts, weighted according to the relative amount of catalysts present. The observed distributions of paraffins, olefins and aromatics comprising a product group at any particular carbon number shows more widespread deviations from calculated product ratios. This arises particularly from hydrogen transfer processes which occur on the faujasite, leading to more extensive formation of paraffins and aromatics at the expense of olefins.

Isomerisation reactions of both olefin and paraffin cracking products are promoted by the presence of HZSM-5. The presence of the HZSM-5 produces higher concentrations of branched olefin isomers. There is also evidence that preferential isomerisation of branched paraffins can occur when high concentrations of product olefins are also present, whereas cracking is favoured at low olefin concentrations.

The latter observation demonstrates that the behaviour of a particular reactant within a complex mixture may not be easily predictable from studies where that reactant is introduced as a pure feedstock. This also applies to the observed disappearance of ethane and methane when contacted with a fresh zeolite sample as a minor component of a complex hydrocarbon mixture.

The effects on product formation found in this study all suggest that the formation of linear paraffins is enhanced by the addition of HZSM-5, whether derived from cracking of the feed, subsequent hydrogen transfer to an olefin, or paraffin isomerisation. It is possible that, for gas oil mixtures, preferential linear paraffin formation in the presence of ZSM-5 additive is balanced by preferential linear paraffin cracking, depending on the relative proportion of the ZSM-5 present. This might explain increased branched to linear ratios in the C_6 - C_9 range in some

cases {18}, and reduced ratios in others {19}. This, however, does not explain why addition of HZSM-5 is consistently reported to enhance ratios of branched to linear C_4 and C_5 paraffins for the cracking of gas oils, whereas results presented in this study show the reverse effect. This observation may reveal a limitation of using a simple *n*-paraffin to represent the behaviour of more complex hydrocarbon mixtures, such as gas oils.

Several investigators {13, 18} have shown that the concentrations of C_3 and C_4 olefins increased upon addition of a small amount of ZSM-5 into zeolite Y during gas oil cracking. This study on cracking of *n*-octane also shows increased formation of these light olefins, mainly arising from the direct contribution of HZSM-5 cracking of the feedstock. Isomerisation of olefins to yield an increased branched to linear isomer ratio is also observed for both gas oil products and for the present study on *n*-octane cracking. It has been concluded that an important function of HZSM-5 additive during gas oil cracking is to reduce bimolecular hydrogen transfer processes {19} which would otherwise easily occur on the faujasite. The competing monomolecular process leading to olefin formation through cracking of the carbenium ion is more favourable on HZSM-5. From this study, it appears that increased proportions of small olefinic products are the direct result of the contribution of feed cracking by the ZSM-5, rather than an interruption of hydrogen transfer process which would otherwise occur on the faujasite.

References

1. Lombardo, E.A., Pierantozzi, R., and Hall, W.K., "The Mechanism of Neopentane Cracking over Solid Acids", *J. Catal.*, **110** (1988) 171-183.
2. Corma, A., Monton, J.B., and Orchilles, A.V., *Appl. Catal.*, **16** (1985) 59.
3. Nace, D.M., *Ind. Eng. Chem. Prod. Res. Dev.*, **8** (1969) 24.
4. Haag, W.O., Lago, R.M., and Weisz, P.B., "Transport and Reactivity of Hydrocarbon Molecules in a Shape Selectivity Zeolite", *Faraday Discuss. Chem. Soc.*, **72** (1981) 317-330.
5. Abbot, J., "Reactions of 3-Methylpentane and 2,3-Dimethylbutane on Aluminosilicate Catalysts", *J. Catal.*, **126** (1990) 628-642.
6. Abbot, J. and Wojciechowski, B.W., *Ind. Eng. Chem. Prod. Res. Dev.*, **24** (1985) 501.
7. Kobolakis, I. and Wojciechowski, B.W., *Can. J. Chem. Eng.*, **63** (1985) 269.
8. Chen, N. Y. and Garwood, W. E., "Some Catalytic Properties of ZSM-5: A New Shape Selective Zeolite", *J. Catal.*, **52** (1978) 453-458.
9. John, T.M. and Wojciechowski, B.W., "On Identifying the Primary and Secondary Products of the Catalytic Cracking of Neutral Distillates", *J. Catal.*, **37** (1975) 240-250.
10. Scherzer, J., "Designing FCC Catalysts with High Silica Zeolites", *Appl. Catal.*, **75** (1991) 1-32.
11. Venuto, P.B. and Habib, E.T., *Catal. Review. -Sci. Eng.*, **18(1)** (1976).
12. Otterstedt, J.E., Yan-Ming, Z., and Sterte, J., "Catalytic Cracking of Heavy Oil over Catalysts Containing Different Types of Zeolite Y in Active and Inactive Matrices", *Appl. Catal.*, **38** (1988) 143-145.
13. Rajagopalan, K. and Young, G.W., "Hydrocarbon Selectivities with Dual Function Zeolite Catalysts", *A.C.S. Symp. Ser.*, **375** (1988) 34-48.

14. Biswas, J. and Maxwell, L.E., "Octane Enhancement in Fluid Catalytic Cracking: I. Role of ZSM-5 Addition and Reactor Temperature", *Appl. Catal.*, **58** (1990) 1-18.

15. Elia, M.F., Iglesias, E., Martinez, A., and Perez Pascual, M.A., "Effect of Operation Conditions on the Behaviour of ZSM-5 Addition to a RE-USY FCC Catalyst", *Appl. Catal.*, **73** (1991) 195-216.

16. Donnelly, S.P., Mizrahi, S., Sparrell, P.T., Huss Jr. A., Schipper, P.H., and Herbst, J.A., *Prepr. A.C.S., Div. Pet. Chem.*, **32(3)** (1987) 621.

17. Anderson, C.D., Dwyer, F.G., Koch, G., and Niiranen, P., "A New Cracking Catalyst for Higher Octane Using ZSM-5", Proc. Ninth Iberoamerican Symp. on Catalysis, Lisbon, (1984) 247-258.

18. Pappal, D.A. and Schipper, P.H., "ZSM-5 in Catalytic Cracking: RISER Pilot Plant Gasoline Composition Analyses", *Prepr. A.C.S., Div. Petr. Chem.*, **35(4)** (1990) 678-683.

19. Miller, S.J. and Hsieh, C.R., "Octane Enhancement in Catalytic Cracking Using High Silica Zeolites", *Prepr. A.C.S., Div. Petr. Chem.*, **35(4)** (1990) 685-693.

20. Madon, R.J., "Role of ZSM-5 and Ultrastable Y Zeolites for Increasing Gasoline Octane Number", *J. Catal.*, **129** (1991) 275-287.

21. Anders, G., Burkhardt, I., Illigen, U., Schulz, I.W., and Scheve, J., "The Influence of HZSM-5 on the Product Composition after Cracking of High Boiling Hydrocarbon Fractions", *Appl. Catal.*, **62** (1990) 271-280.

22. Buchanan, J.S., "Reactions of Model Compounds over Steamed ZSM-5 at Simulated FCC Reaction Conditions", *Appl. Catal.*, **74** (1991) 83-94.

23. Abbot, J. and Wojciechowski, B.W., "Hydrogen Transfer Reaction in the Catalytic Cracking of Paraffins", *J. Catal.*, **107** (1987) 451-462.

24. Abbot, J. and Wojciechowski, B.W., "Catalytic Reactions of *n*-Hexane on HY Zeolite", *Can. J. Chem. Eng.*, **66** (1988) 825-830.

25. Abbot, J. and Wojciechowski, B.W., Catalytic Reactions of *n*-Dodecane on Aluminosilicates", *J. Catal.*, **115** (1989) 521-531.

26. Magnoux, P., Cartraud, P., Mignard, S., and Guisnet, M., "Coking, Aging, and Regeneration of Zeolites", *J. Catal.*, **106**, (1987) 242-250.

27. Abbot, J., "Cracking Reactions of C_6 Paraffins on HZSM-5", *Appl. Catal.*, **57** (1990) 105-125.

28. Mott, R.W., *Oil & Gas Journal*, **January 26** (1987) 73.

29. Abbot, J. and Wojciechowski, B.W., "Kinetics of Catalytic Cracking of *n*-Paraffins on HY Zeolite ", *J. Catal.*, **104** (1987) 80.

30. Abbot, J. and Wojciechowski, B.W., "Role of Bronsted and Lewis Acid Sites During Cracking Reactions of Alkanes", *Appl. Catal.*, **47** (1989) 33-44.

31. Abbot, J. and Wojciechowski, B.W., "Catalytic Cracking and Skeletal Isomerisation of *n*-Hexenes on HY Zeolite", *Canad. J. Chem. Eng.*, **63** (1988) 278-287.

32. Abbot, J. and Wojciechowski, B.W., "Catalytic Cracking and Skeletal Isomerisation of *n*-Hexenes on HZSM-5 Zeolite", *Canad. J. Chem. Eng.*, **63** (1988) 451-461.

33. Lombardo, E. A. and Hall, W. K., "The Mechanism of *Iso*-butane Cracking over Amorphous Crystalline Aluminosilicates", *J. Catal.*, **112** (1988) 565-578.

34. Hall, W. K., Lombardo, E. A., and Englehardt, J., "In Reply to Kramer and McVicker", *J. Catal.*, **115** (1989) 611-615.

35. Shigeishi, R., Garforth, A., Harris, I., and Dwyer, J., "The Conversion of Butanes in HZSM-5", *J. Catal.*, **130** (1991) 423-439.

36. McVicker, G. B., Kramer, G. M., and Riemiak, J. J., "Conversion of *Iso*-butane over Solid Superacids - A Sensitive Mechanistic Probe Reaction", *J. Catal.*, **83** (1983) 286-300.

37. Fuentes, G. A., Boegel, J. V., and Gates, B. C., "*n*-Butane Isomerisation Catalysed by Supported Aluminum Chloride", *J. Catal.*, **78** (1982) 436-444.

38. Dooley, K. M. and Gates, B. G., "Paraffin Isomerisation Catalyzed by Polymer-Supported Superacids", *J. Catal.*, **96** (1985) 347-356.

39. Bourdillon, G., Gueguen, C., and Guisnet, M., *Appl. Catal.*, **61** (1990) 123.

40. Mirodatos, C. and Barthomeuf, D., *J. Chem. Soc. Chem. Commun.*, **39** (1981).

41. Abbot, J., "Active Sites and Intermediates for Isomerization and Cracking of Cyclohexane on HY", *J. Catal.*, **123** (1990) 383-395.

42. Haag, W.O. and Dessau, R.M., Proceedings the 8th International Congress on Catalysis, Berlin, 1984. Vol II, Dechema, Frankfurt-au-Main, (1984) 305.

43. Dass, D. V. and Odell, A. L., "Reactions of *n*-Alkanes over HZSM-5: Detection of Reaction Intermediates", *J. Catal.*, **113** (1988) 259-262.

44. Scurrell, M.S., "Prospects for the Direct Conversion of Light Alkenes to Petrochemical Feedstocks and Liquid Fuels - A Review" *Appl. Catal.*, **32** (1988) 1-22.

45. Scurrell, M.S., "Factors Affecting the Selectivity of the Aromatisation of Light Alkanes on Modified ZSM-5 Catalysts", *Appl. Catal.*, **41** (1988) 89-98.

46. Scurrell, M.S. and Cooks, M., *Sted. Surf. Sci. Catal.*, **36** (1988) 433.

47. Kanai, J., Martens, J.A., and Jacobs, P.A., "On the Nature of the Active Sites for Ethylene Hydrogenation in Metal Free Zeolites", *J. Catal.*, **133** (1992) 527-543.

Chapter 4

Influence of Catalyst and Feedstock

CHAPTER 4

Influence of Catalyst and Feedstock

4.1 Introduction

In the previous chapter, the cracking reactions of *n*-octane over HY, HZSM-5 zeolites, and their combinations were presented. Having distinct intrinsic characteristics, the two zeolites offered different mechanisms for the reactions. The effects of each catalyst on the reactions were able to be isolated by arranging the catalyst beds in the reactor sequentially.

In this chapter, the reactions of a mixture of *n*-octane and 2-methylheptane over zeolites HY, HZSM-5, and a mixture of the catalysts, were studied to investigate how product distributions were affected by catalysts and feedstocks at the same time. This type of feedstock mixture is of the same type, and as was discussed earlier in Section 2.3.2, the susceptibility of each paraffin isomer towards cracking due to their skeletal arrangement can be distinguished. Also the shape selectivity offered by zeolites of different porosity can be studied. The system was approached in a similar manner to that outlined in Chapter 3.

4.2 Reactions of Individual Feedstocks

From the study presented in the previous chapter, it was found that comparison between product distributions from the reactions of a paraffin feedstock over two different zeolites made at similar conversion level resulted in a similar trend to those made at different conversion level, indicating that the phenomena observed are not strongly dependent on catalyst decay.

The levels of conversion of 2-methylheptane and *n*-octane on HY and HZSM-5 were selected so that the conversions of either feedstock over either

zeolite were similar. Table 4.1 shows the conversion of each of the paraffin feedstocks and their binary mixture over each zeolite and their mixture.

Table 4.1 Percentage conversion of 2-methylheptane, *n*-octane, and a mixture of the paraffins over zeolites HY, HZSM-5, and a mixture of the catalysts at 400 °C

Feed	HY	HZSM-5	HY and HZSM-5 (a)
2-methylheptane	17.8	17.2	27.6
n-octane	16.8	16.9	27.1
2-mehylheptane and *n*-octane (b)	18.2 (c)	18.7 (c)	28.2 (c)

Key:
(a) = HY : HZSM-5 - 3 : 1 mass ratio
(b) = 2-methylheptane : n-octane = 1 : 1 molar ratio
(c) = Total conversion of the two components of the feedstock

4.2.1 Reaction over Individual Zeolites

Distribution of Products by Carbon Number

Results in Figures 4.1 and 4.2 compare the total product distributions from cracking of 2-methylheptane and *n*-octane on HY and HZSM-5 respectively, at similar conversion level. Product distributions from reactions on HY show that the tendency to produce C_1 to C_3 fragments is higher for the linear paraffin. In contrast, for reactions on HZSM-5, these fragments are higher for reaction of the *iso*-paraffin.

The overall fragmentation from reaction of the feedstocks over one particular catalyst shows less variation compared to that from reaction of one particular feedstock over the two catalysts. As for the case with reaction of *n*-octane, the major products from reaction of 2-methylheptane on HZSM-5 are shifted towards lower carbon numbers. Similar trends were found when

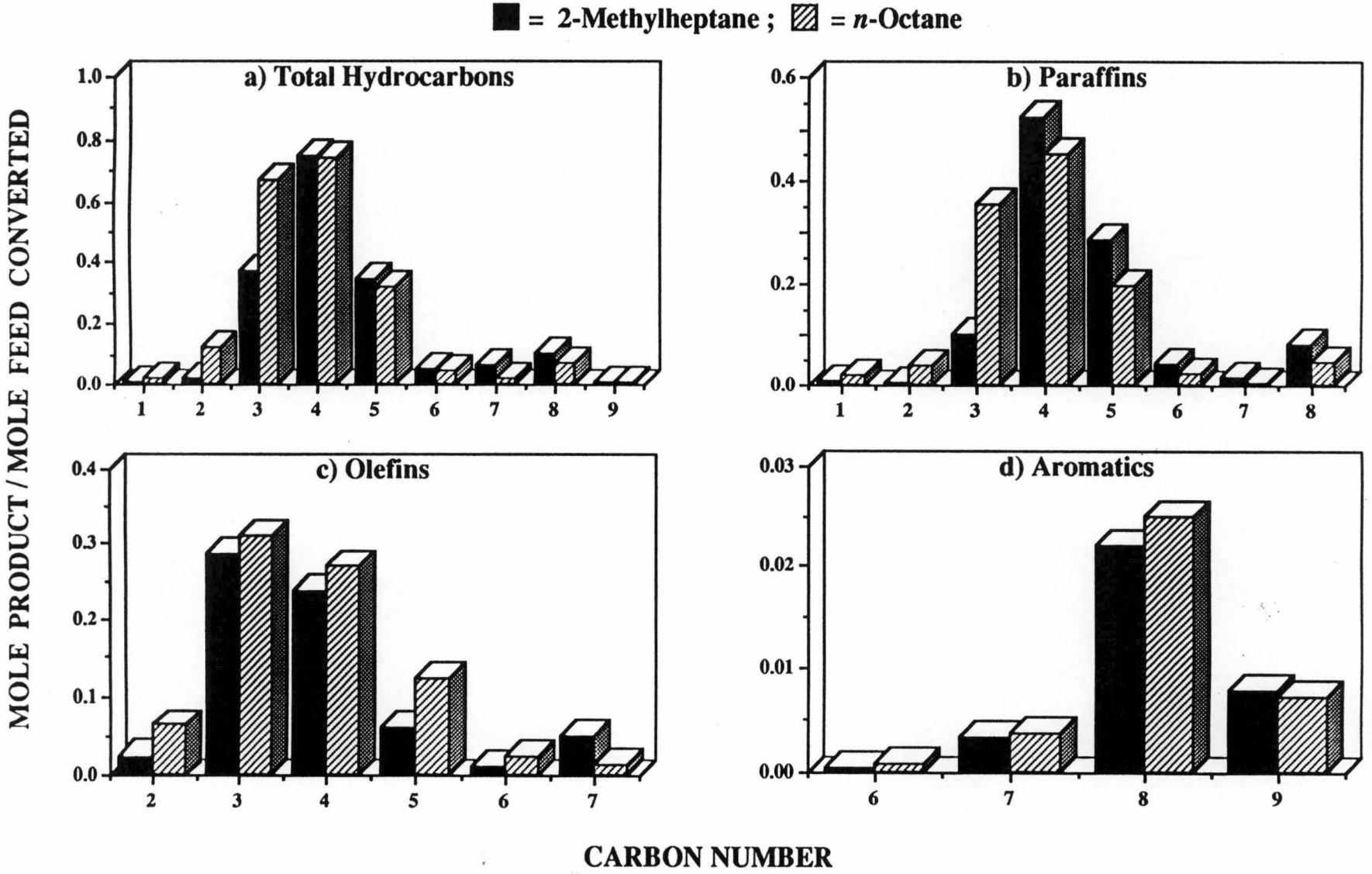

Figure 4.1 Product distributions from reaction of 2-methylheptane and *n*-octane over zeolite HY at 400 °C

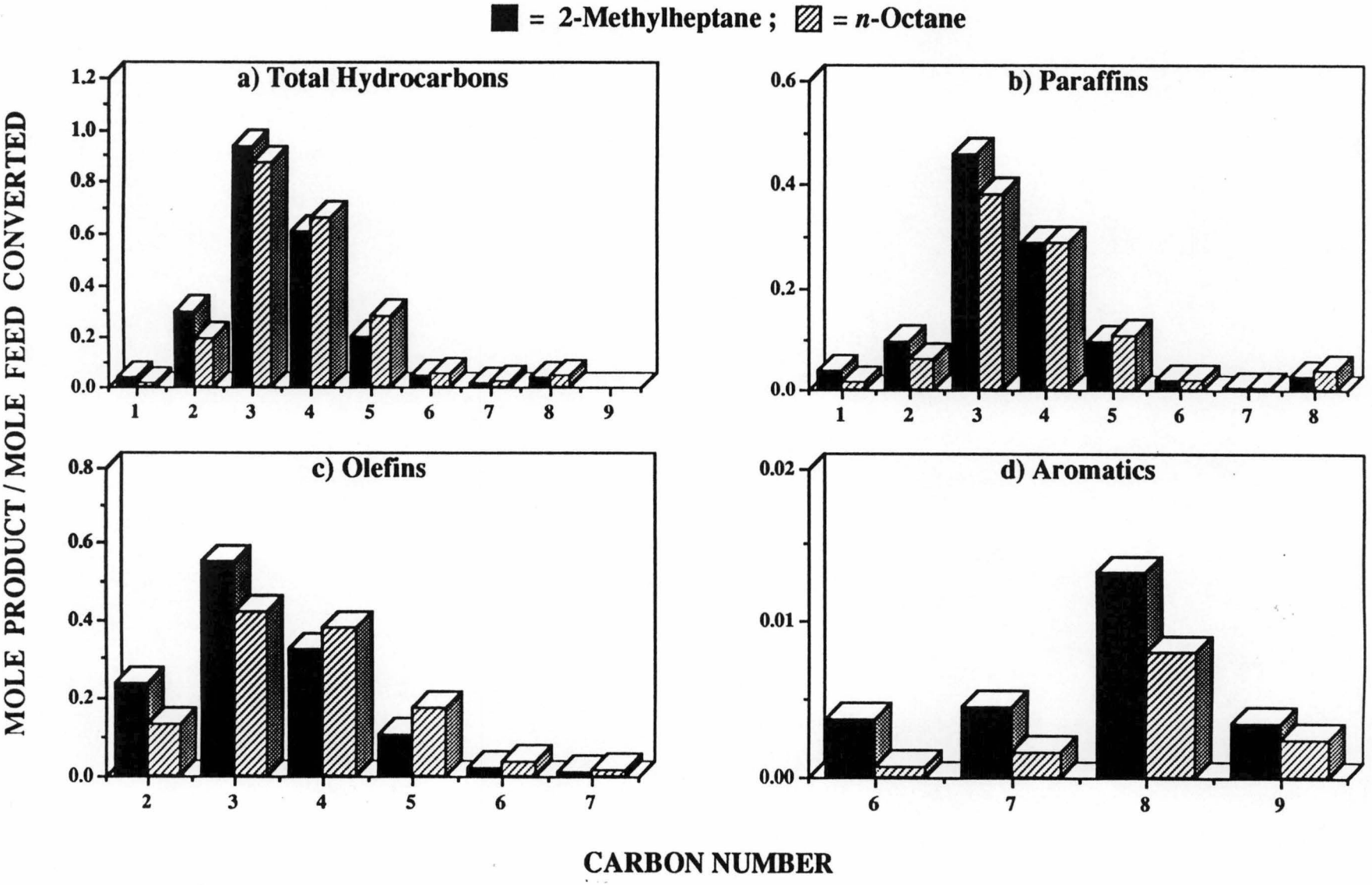

Figure 4.2 Product distributions from reaction of 2-methylheptane and *n*-octane over zeolite HZSM-5 at 400 °C

considering the distributions of saturated products according to carbon number. Examination of Figure 4.1.d shows little difference in the total amount or distribution of aromatics produced from either paraffin on HY. It has been suggested {1} that during cracking of paraffins, aromatics are formed mainly through secondary processes involving olefins. Figure 4.1.c shows that the distribution and amounts of potential olefin precursor are similar for both feedstocks. For reaction on HZSM-5, there is a significantly higher tendency to produce aromatics from reaction of the *iso*-paraffin (Figure 4.2.d). In particular, the amount of benzene produced is about ten times greater for reaction of 2-methylheptane. However, the amounts and distributions of olefins are similar, suggesting that, on HZSM-5 aromatic products are not only formed through secondary processes involving olefins, but also directly from the feedstock as has been proposed in earlier work {2}.

Ratios of Branched to Linear Isomers

The relative amounts of branched and linear isomers of both olefins and paraffins present in a gasoline blend are important factors in determining its octane number. Many workers have reported that HZSM-5 addition to a zeolite HY can influence the ratio of branched to linear (B/L) isomers produced during cracking of gas oils {3, 4, 5}. Table 4.2.a shows ratios of B/L isomers for C_4 and C_5 olefin products, showing the influence of both catalyst and feedstock for reaction of 2-methylheptane and *n*-octane. Higher B/L ratios of C_4 and C_5 olefin are observed for reactions of either feedstock on the ZSM-5, and on either zeolite, reaction of the linear paraffin gives higher branched to linear ratios.

Table 4.2. Branched to linear ratios of olefins and paraffins from reaction of 2-methylheptane and *n*-octane over zeolites HY and HZSM-5 at 400 °C

(a) Olefins

Carbon Number	2-Methylheptane		*n*-Octane	
	HY	HZSM-5	HY	HZSM-5
C_4	0.75	0.93	1.36	1.43
C_5	2.13	2.24	2.41	2.59

(b) Paraffins

Carbon Number	2-Methylheptane		*n*-Octane	
	HY	HZSM-5	HY	HZSM-5
C_4	4.34	1.21	1.96	0.41
C_5	18.3	1.41	2.61	0.40
C_6	24.82	3.78	5.59	0.80

Variations in the ratios of B/L paraffin products (Table 4.2.b) are much more noticable than those for the olefins. Both catalyst and feedstock exert a major influence on the observed degree of branching of the saturated cracking fragments. For both feedstocks, the ratios of B/L paraffin products are significantly higher for reaction on HY compared to HZSM-5, particularly for the C_5 and C_6 paraffins. For either catalyst the B/L ratios are significantly higher for cracking of the branched feedstock. This result shows that the intermediates formed during the reaction are not identical for cracking of the linear and branched C_8 paraffins. The dominant cracking pathway on either catalyst cannot result from equilibrium of the various possible branched and linear C_8 carbonium ions as previously reported by Corma and co-workers {6}.

Branched C_6 paraffins can result from cracking of 2-methylheptane by direct cleavage of a C-C bond which would produce exclusively 2-methylpentane. Alternatively, bimolecular processes leading to a C_6 carbenium ion after ß-scission could give rise to either 2-methylpentane or 3-methylpentane after rearrangement of the residual C_6 carbenium ion. Rearrangement of a C_6 carbenium ion to give branched isomers that occurs on both HY and HZSM-5 to produce similar product distributions was reported by Abbot and Wojciechowski {7, 8}. They claimed that for skeletal isomerisation of linear hexenes, the ratios of 2-methylpentenes to 3-methylpentenes formed were 0.76 and 0.62 on HY and HZSM-5 respectively. Figure 4.3 shows, however, a marked preference for formation of 2-methylpentane rather than 3-methylpentane for cracking of 2-methylheptane on both catalysts, especially on HZSM-5.

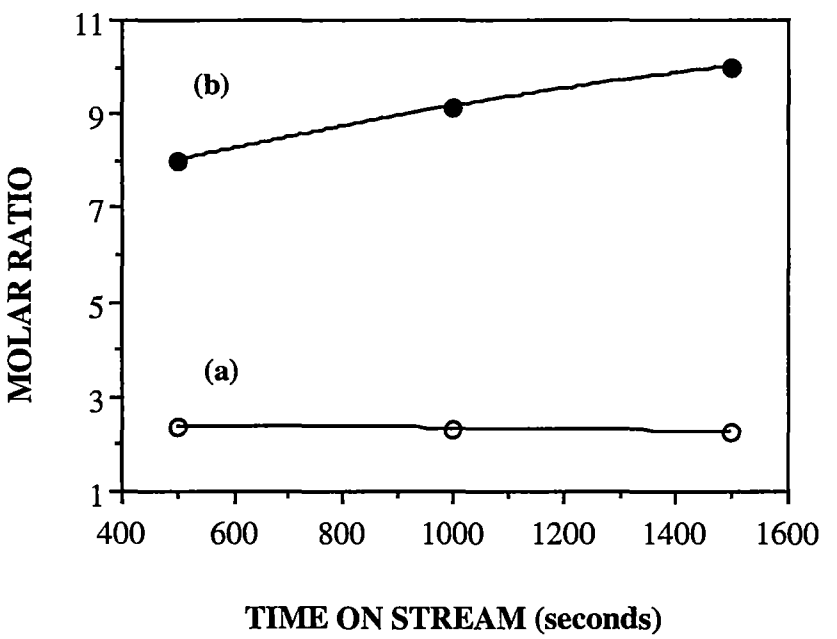

Figure 4.3 Molar ratio of 2-methylpentane to 3-methylpentane from reaction of 2-methylheptane over zeolites HY (a) and HZSM-5 (b) at 400 °C

The ratios of the C_6 isomers formed suggest that on both catalysts, direct cracking via protolysis is favoured over processes involving an intermediate C_6 carbenium ion. Results obtained over a range of times on stream, as illustrated in Figure 4.3, show that the reported phenomena are not strongly influenced by conversion level.

4.2.2 Reaction over a Random Mixture of Zeolites HY and HZSM-5

From the study of reaction of *n*-octane in Chapter 3, the product distributions obtained from reaction over a random mixture of the catalysts are well approximated by taking the average of those resulting from the sequential combinations. For this reason the study of reaction of 2-methylheptane and a mixture of 2-methylheptane and *n*-octane were carried out only on a random mixture of the zeolites.

Product distributions for reactions of 2-methylheptane and *n*-octane on a random mixture of zeolites HY and HZSM-5 are shown in Figures 4.4 and 4.5. Predicted distributions are calculated from the product distributions for reactions on the individual catalysts, assuming that the relative contribution from each catalyst in the mixture is proportional to activities found for the isolated case. Although the overall distributions on the random mixture of zeolites HY and HZSM-5 are well represented by the predicted values (Figures 4.4.a and 4.5.a), greater deviations are seen when considering the observed and predicted distributions for individual product classes. These deviations can be attributed to additional processes where products formed on one catalyst interact with the other catalyst, particularly in secondary processes involving hydrogen transfer and isomerisation as discussed in Chapter 3. As for the reaction of *n*-octane over a random mixture of HY and HZSM-5, the observed amounts of C_3 to C_6 paraffins from the reaction of 2-methylheptane are consistently higher than

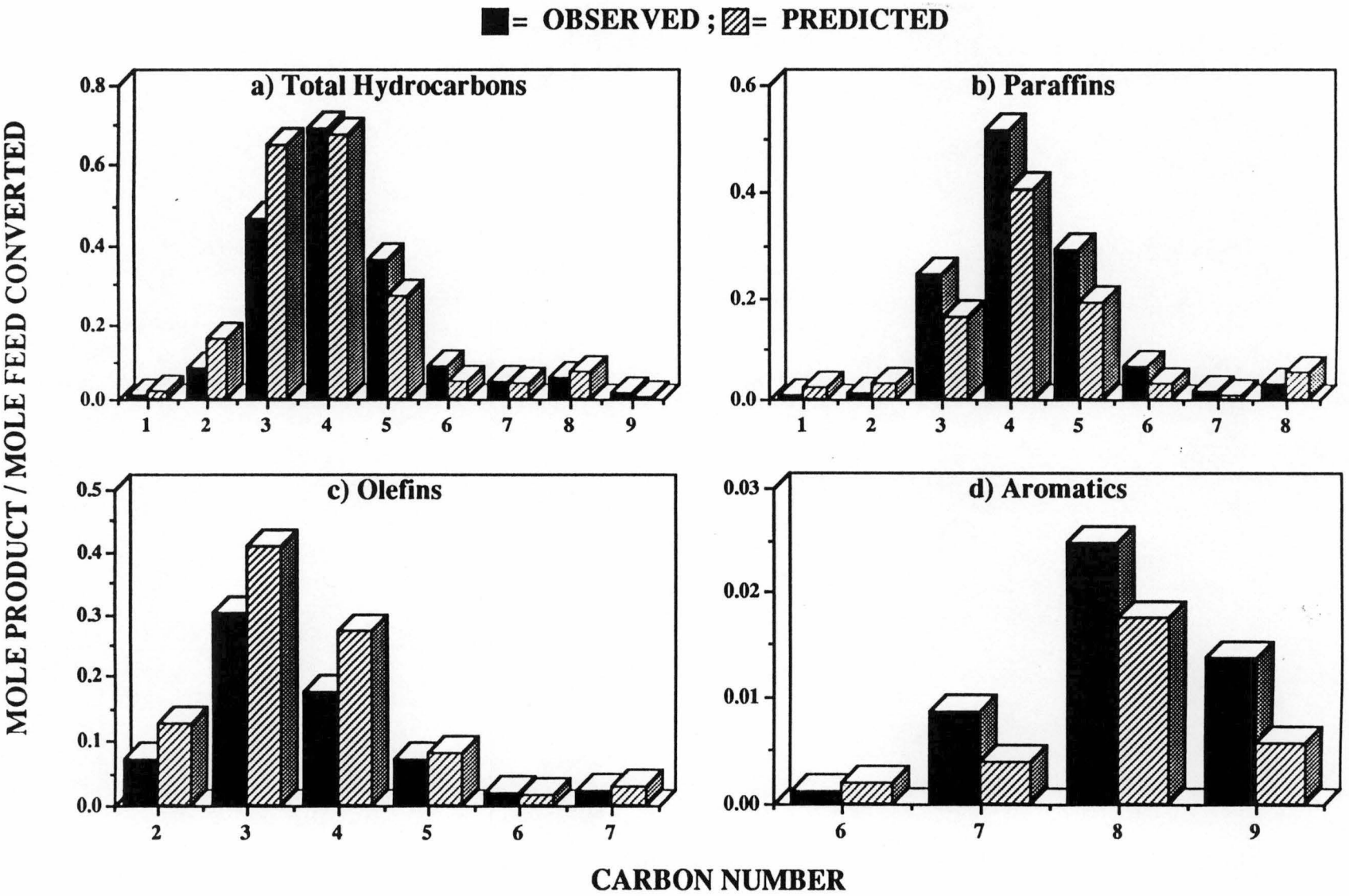

Figure 4.4 Product distributions from reaction of 2-methylheptane over a random mixture of zeolites HY and HZSM-5 at 400°C

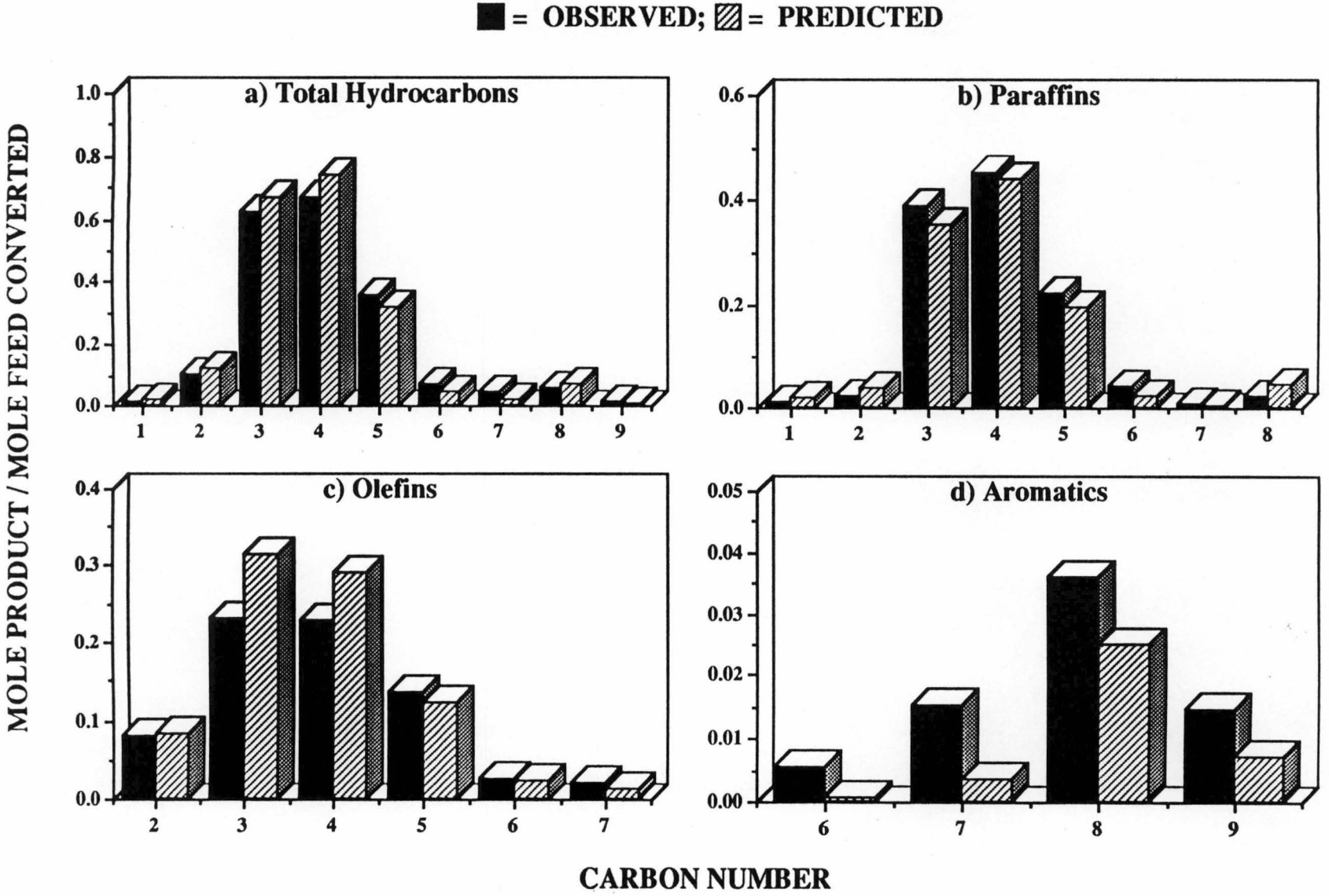

Figure 4.5 Product distributions from reaction of *n*-octane over a random mixture of zeolites HY and HZSM-5 at 400 °C

predicted. This paraffin gain can be related to the loss in olefinic products (Figure 4.4.c) and gain in aromatics (Figure 4.4.d) due to occurrence of hydrogen transfer processes.

Table 4.3 Branched to linear ratios of olefins and paraffins from reaction of 2-methylheptane and *n*-octane over a random mixture of zeolites HY and HZSM-5 at 400 °C

(a) Olefins

Carbon Number	2-Methylheptane		*n*-Octane	
	Observed	Predicted	Observed	Predicted
C_4	1.18	1.09	1.38	1.21
C_5	2.29	2.25	2.59	2.27

(b) Paraffins

Carbon Number	2-Methylheptane		*n*-Octane	
	Observed	Predicted	Observed	Predicted
C_4	4.19	2.88	1.08	1.15
C_5	10.77	9.65	1.54	3.12
C_6	15.75	14.81	2.13	3.27

Key:
Predicted ratios are calculated by taking proportional contributions from each individual catalyst

Table 4.3 shows a comparison between observed and predicted branched to linear ratios for both olefins and paraffins. Although observed ratios for the olefins are close to predicted values, addition of HZSM-5 to the HY zeolite leads to a cracking product distribution with a somewhat higher degree of branching of the product olefins. Predicted ratios for the C_4 - C_6 paraffins show greater deviation from the observed values (Table 4.3.b) with more branching observed

than expected for reaction of the branched C_8 paraffin, while the reverse is true for the reaction of the linear isomer.

Examination of results presented in Tables 4.2 and 4.3 shows that for 2-methylheptane, reaction over the random mixture of the zeolites resulted in higher B/L ratios of olefins compared to that over either catalyst individually, while for the reaction of *n*-octane, B/L ratios of olefins lie between those resulting from reaction over individual catalysts. For both feedstocks, the B/L ratios of paraffins over the random mixtures of the zeolites lie between those resulting from reaction over individual catalysts.

From reaction of 2-methylheptane, the B/L ratios of paraffins are higher than predicted (Table 4.3.b), whilst there are more C_4 - C_6 paraffins produced than predicted (Figure 4.4.b). According to the assumptions discussed in Section 3.4.1, this case corresponds to the situation where B/L > B*/L* and P > P*, where there are selective hydrogen transfer processes taking place producing additional branched paraffins.

For reaction of *n*-octane, the B/L < B*/L (Table 4.3.b) whilst P > P* (Figure 4.5.b), hence in this case hydrogen transfer processes selectively produce additional linear paraffins. This result indicates a selectivity of hydrogen transfer which depends on the structure of the reactant molecule.

4.3 Reaction of a Mixture of *n*-Octane and 2-Methylheptane

A mixture of 2-methylheptane and *n*-octane (1:1 molar ratio) was prepared and used as the reaction feedstock. The conversions of each component in the mixed feedstock over HY, HZSM-5, and a random mixture of the zeolites are presented in Table 4.1.

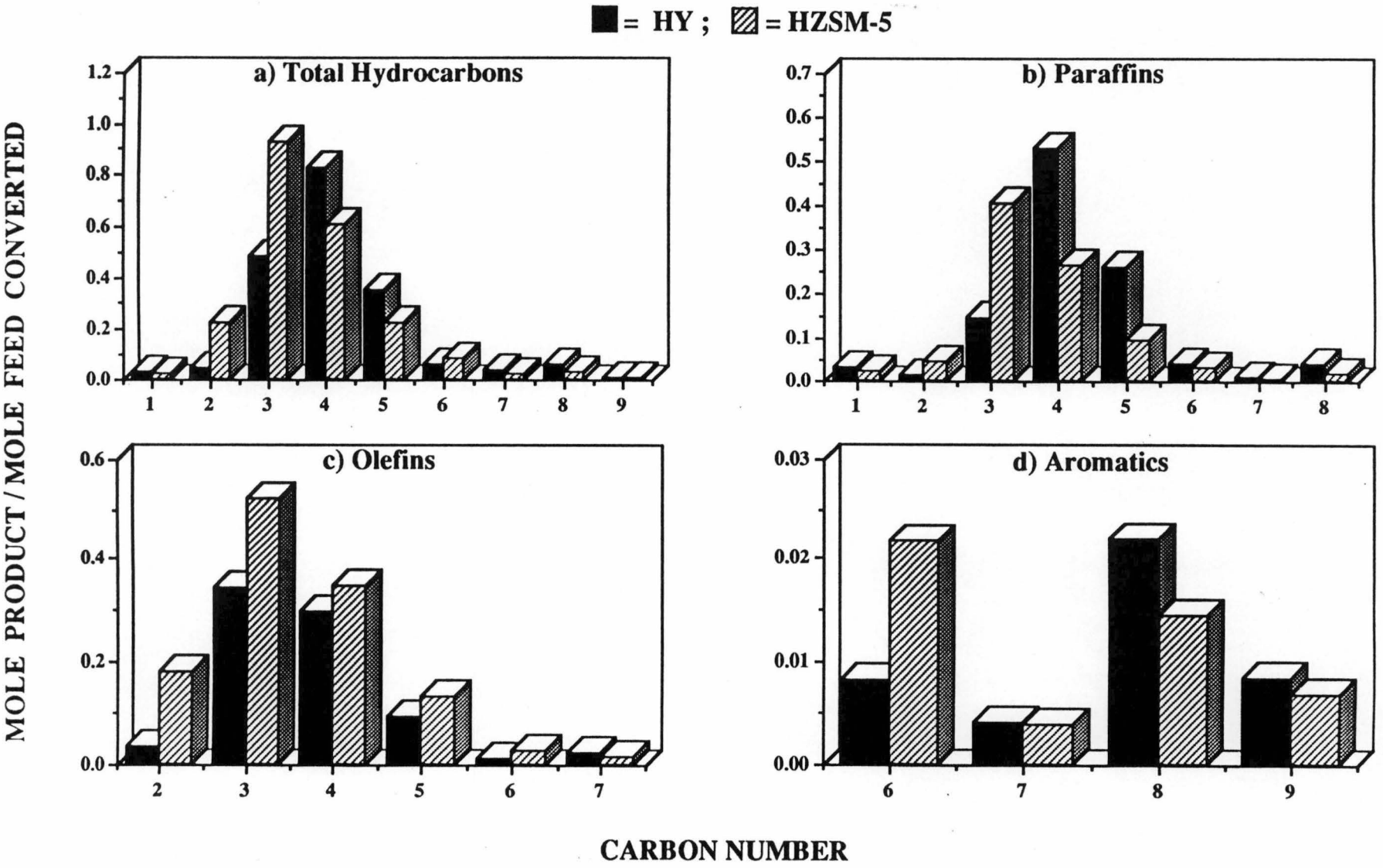

Figure 4.6 Product distributions from reaction of a mixture of 2-methylheptane and *n*-octane over zeolites HY and HZSM-5 at 400 ₀C

4.3.1 Reaction over Individual Zeolites

Figure 4.6 shows a comparison of product distributions from cracking the paraffin mixture over zeolites HY and HZSM-5. The major products were shifted to lower molecular size on the pentasil, just as for the reaction of individual feedstocks. Generally, the overall fragmentation from reaction of the mixed feedstock over one particular catalyst is similar to those from reactions of individual feedstocks.

Table 4.4 Branched to linear ratios of olefins and paraffins from reaction of a mixture of 2-methylheptane and *n*-octane over zeolites HY and HZSM-5 at 400 °C

(a) Olefins

Carbon Number	HY		HZSM-5	
	Observed	Predicted	Observed	Predicted
C_4	0.95	0.88	1.56	1.41
C_5	2.36	2.24	2.68	2.51

(b) Paraffins

Carbon Number	HY		HZSM-5	
	Observed	Predicted	Observed	Predicted
C_4	4.34	2.81	0.74	0.70
C_5	11.48	6.11	0.81	0.72
C_6	16.30	8.89	3.60	1.15

Key:
Predicted ratios are calculated by taking proportional contributions from each individual feedstock

Branched to linear ratios of C_4 and C_5 olefin isomers are lower for reaction on HY compared to HZSM-5 (Table 4.4). In contrast, the corresponding ratios for C_4 to C_6 paraffins are much higher on the faujasite. It was also found that observed ratios for olefinic products correspond closely to those predicted, with ratios for paraffins significantly higher than predicted. These effects were previously observed for reaction of the individual feedstocks.

A series of separate experiments were performed for the reaction of a mixture of 2-methylheptane and *n*-octane over HY, HZSM-5, and a combination of the zeolites where the comparisons were made at similar catalyst to feed ratio.

The relative rates of conversion of C_8 isomers in the mixed feedstock are shown in Figure 4.7. The branched isomer was preferentially cracked over HY zeolite (Figure 4.7.a). This observation agrees with that of Chen and Garwood {9} who reported that in the absence of steric hindrance from the catalyst, 2,3-dimethylbutane is more reactive than *n*-hexane. This selectivity is purely due to the activity of the reactant molecules. In contrast, for the reaction on HZSM-5 (Figure 4.7.b), there is a preferential cracking of the linear paraffin. Biswas and Maxwell {10} observed the same preference from cracking of a complex feedstock.

Examination of results presented in Tables 4.2 and 4.4 shows that over HZSM-5, reaction of the mixed feedstock resulted in higher B/L ratios of olefins compared to that obtained from reaction of either paraffin individually, while for the reaction over HY zeolite, B/L ratios of olefins lie between those resulting from the reaction of individual feedstocks. For both catalysts, the B/L ratios of paraffins from the reaction of the binary mixture of the feedstocks lie between those resulting from reaction of individual feedstocks.

From reaction over HY zeolite, the B/L ratios of paraffin is higher than predicted as there are more C_4 - C_6 paraffins produced than predicted. Again, based on the assumptions discussed in Section 3.4.1, this case corresponds to

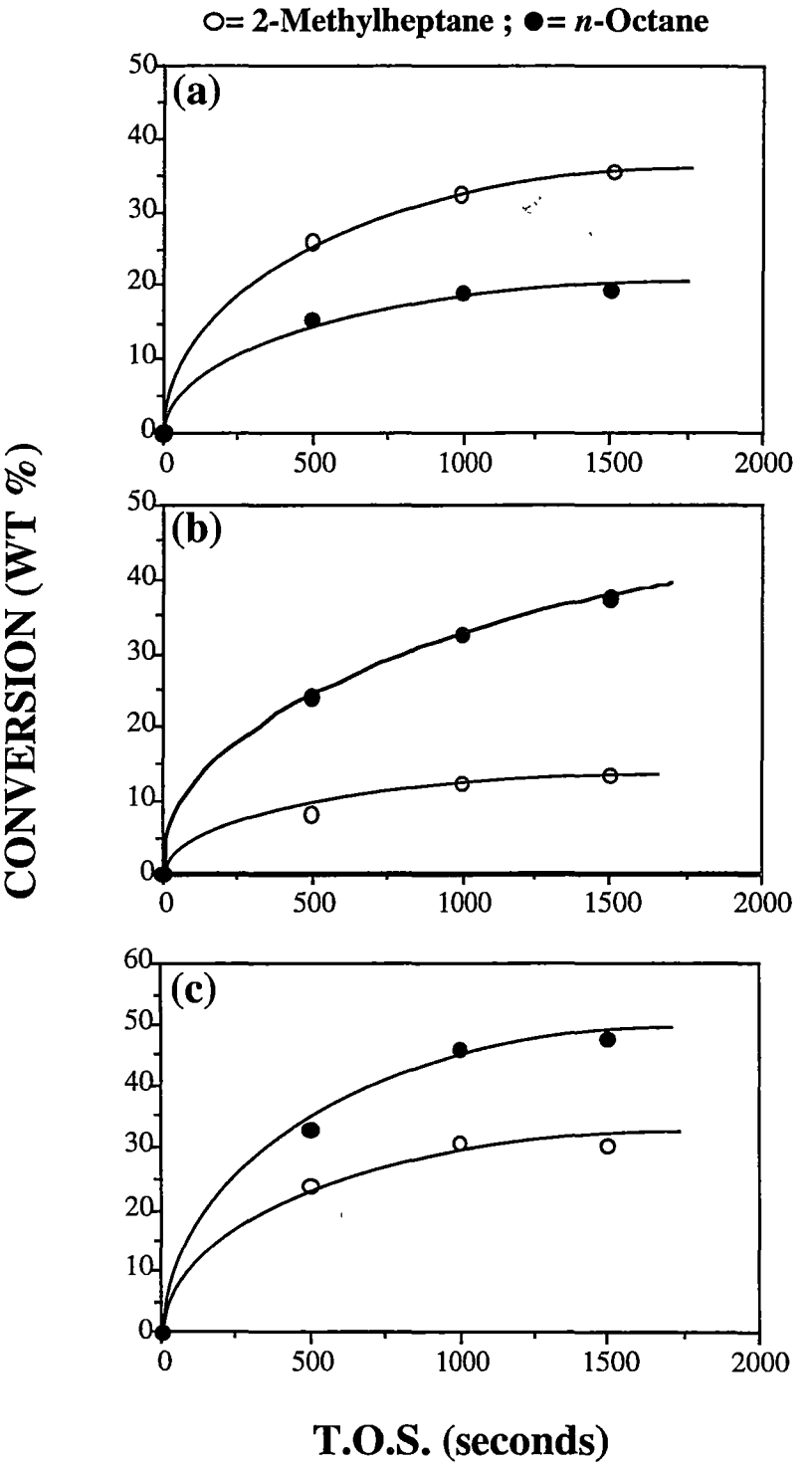

Figure 4.7 Conversions of 2-methylheptane and *n*-octane from reaction of a mixture of the paraffins over zeolites HY (a), HZSM-5 (b), and a random mixture of the zeolites (c) at 400 °C

the situation where B/L > B*/L* and P > P*, where there is selective hydrogen transfer processes taking place producing additional branched paraffins. This effect has been observed for reaction of individual feedstock over HY zeolite.

For reaction over HZSM-5 zeolite, the B/L > B*/L whilst P < P*, this condition was not observed before for reaction of *n*-octane on HZSM-5. The difference between the observed and predicted value of B/L ratios could be rationalised by assuming selective cracking of linear paraffins occurring on HZSM-5 which is in agreement with the findings presented in Figure 4.7.

4.3.2 Reaction over a Random Mixture of Zeolites HY and HZM-5

Product distributions from reaction of the mixed feedstock of the C_8 paraffins on a random mixture of the zeolites are presented in Figure 4.8. As for reactions on the individual catalysts, the distribution of total cracking products is again well represented by the predicted distribution. Greater deviations are observed when considering individual product classes. The observed amounts of C_3 to C_6 paraffins are consistently higher than predicted, and again can be related to the loss in olefinic products (Figure 4.8.c) and gain in aromatics (Figure 4.8.d) due to hydrogen transfer process occurring.

A comparison between observed and predicted B/L ratios of olefinic and paraffins are shown in Table 4.5. The B/L ratios for olefins lie between those for reaction on the individual catalysts (*viz.* Tables 4.4.a and 4.5.a), and also between those for reaction of the individual feedstocks (*viz.* Tables 4.3.a and 4.5.a), while at the same time the production of the branched isomers is higher than predicted.

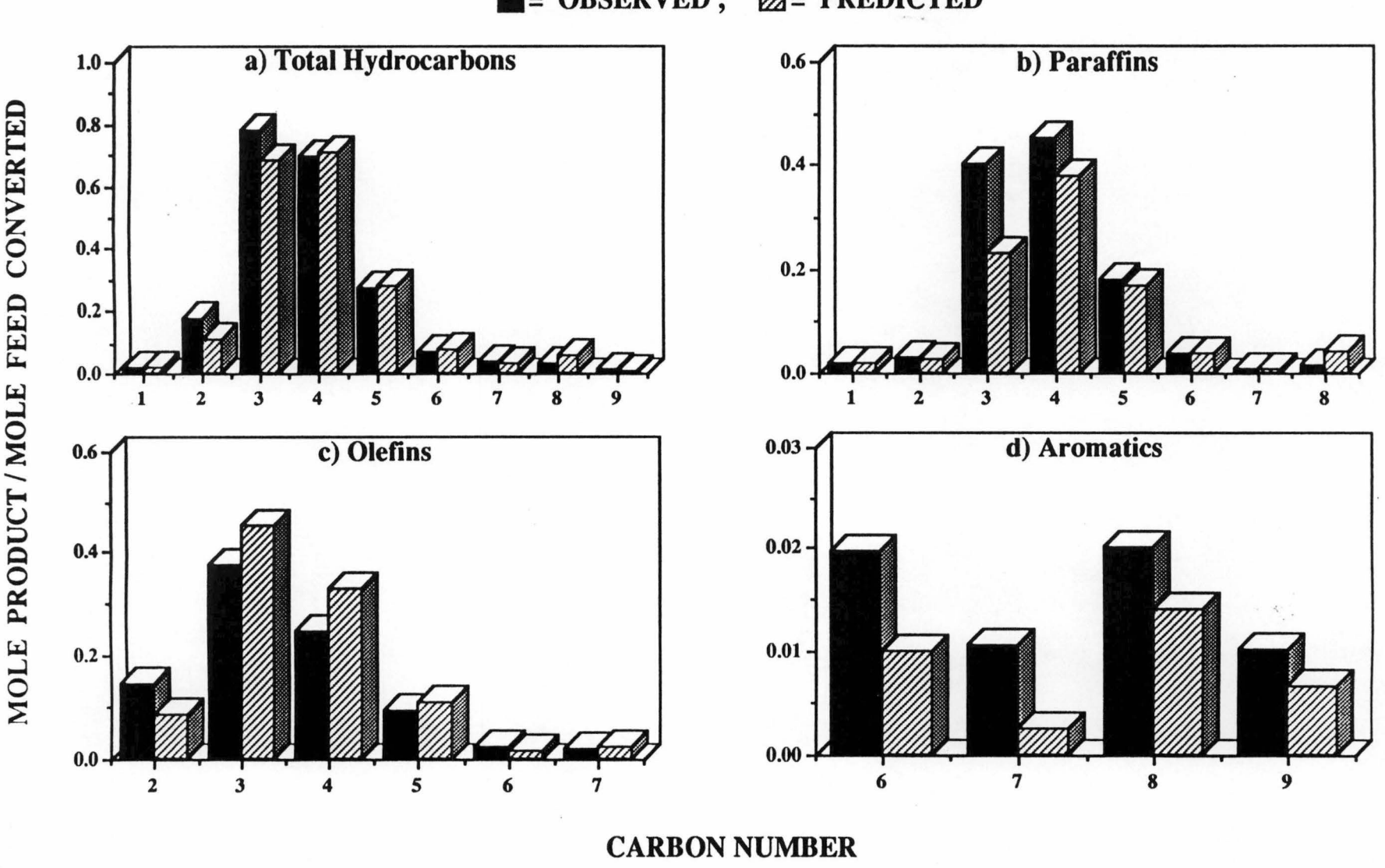

Figure 4.8 Product distributions from reaction of a mixture of 2-methylheptane and *n*-octane over a random mixture of zeolites HY and HZSM-5 at 400 °C

Table 4.5 Branched to linear ratios of olefins and paraffins from reaction of a mixture of 2-methylheptane and *n*-octane over a random mixture of zeolites HY and HZSM-5 at 400 °C

(a) Olefins

Carbon Number	Observed	Predicted
C_4	1.33	1.14
C_5	2.42	2.21

(b) Paraffins

Carbon Number	Observed	Predicted
C_4	1.73	2.18
C_5	2.69	4.58
C_6	4.95	9.27

Key:
Predicted ratios are calculated by taking proportional contributions from each individual feedstock and catalyst

Tables 4.4.b and 4.5.b show that the B/L ratios for paraffins from the reaction of the mixed feedstock on the random mixture of the zeolites lie between those obtained from reaction on the individual catalysts, and also between those for reaction of the individual feedstock (*viz.* Tables 4.3.b and 4.5.b), but are somewhat lower than predicted. Examination on Table 4.5.b and Figure 4.8.b shows that $B/L < B^*/L^*$ while $P > P^*$, which corresponds to a condition where selective hydrogen transfer takes place producing additional linear paraffins.

4.4 Conclusion

Catalytic cracking reactions of *n*-octane and 2-methylheptane, as well as a mixture of these paraffins, have been studied on HY and HZSM-5 zeolites, and also on a random mixture of the catalysts. For cracking on individual catalysts, both feedstock and catalyst type influence the resulting product distributions. For all feedstocks, product distributions are shifted towards smaller fragments for reaction on HZSM-5 compared to HY.

Ratios of branched to linear paraffins are much more strongly influenced by catalyst type and feedstock than the corresponding ratios for olefinic products. For reactions on catalyst mixtures, distributions of the total products by carbon number correspond well to a summation of contributions on the individual catalysts. However, a greater departure from prediction is seen for individual distributions of paraffins, olefins and aromatics, as well as for ratios of branched to linear paraffins, showing that hydrogen transfer processes and isomerisation must occur. The addition of pentasil did not suppress the extent of hydrogen transfer processes, and also resulted in enrichment of the linear saturates at lower carbon number, due to preferential cracking of linear paraffins over the branched isomers.

Cracking of a mixture of paraffins on a random mixture of zeolites can be considered in the context of reported studies for cracking of complex gas oil mixtures concerning the impact of addition of ZSM-5 to a Y zeolite, as well as the influence of one component on the other(s) in the feedstock mixture. This study has shown that both catalyst and feedstock are important factors in determining the product distribution for cracking of paraffins, particularly on ratios of branched to linear paraffins produced.

It has been suggested that pentasil addition produces selective removal of low octane linear paraffins, and can contribute towards enhancement of gasoline quality. However, the present studies consistently show that cracking of either linear or branched paraffins results in a greater proportion of linear paraffin isomers at lower molecular weight. In contrast, reported cracking studies on gas oils indicate higher B/L ratios of C_4 and C_5 paraffins on pentasil addition {3, 5, 11}. This suggests that selective cracking of linear paraffin isomers by HZSM-5 may not be the dominant mechanism for octane number enhancement. Higher ratios for B/L isomers of light olefins have also been reported for studies on gas oils {10, 11, 12}, in agreement with the present studies. The presence of HZSM-5, however, contributes to the isomerisation of olefins, increasing the proportion of branched isomers, thereby enhancing the octane rating of the gasoline produced.

References

1. Scherzer, J., "Octane-Enhancing, Zeolitic FCC Catalysts: Scientific and Technical Aspects", *J. Catal. Rev. -Sci. Eng.*, **31(3)** (1989) 215-354.
2. Anders, G., Burkhardt, L., Illigen, U., Schulz, I.W., and Scheve, J., "The Influence of HZSM-5 Zeolite on the Product Composition after Cracking of High Boiling Hydrocarbon Fractions", *Appl. Catal.*, **62** (1990) 271-280.
3. Elia, M.F., Iglesias, E., Martinez, A., and Perez Pascual, M.A., "Effect of Operation Conditions on the Behaviour of ZSM-5: Addition to a RE-USY FCC Catalyst", *Appl. Catal.*, **73** (1991)195-216.
4. Miller, S.J. and Hsieh, C.R., "Octane Enhancement in Catalytic Cracking Using High-Silica Zeolites", *Prepr. A.C.S., Div. Pet. Chem.*, **3(4)** (1990) 685-693.
5. Madon, R.J., "Role of ZSM-5 and Ultrastable Y Zeolites for Increasing Gasoline Octane Number", *J. Catal.*, **129** (1991) 275-287.
6. Corma, A., Planelles, J., Sanchez-Marin, J., and Tomás, F., "The Role of Different Types of Acid Sites in the Cracking of Alkanes on Zeolite Catalysts", *J. Catal.*, **93** (1985) 30-37.
7. Abbot, J. and Wojciechowski, B.W., "Catalytic Cracking and Skeletal Isomerisation of *n*-Hexenes on HY Zeolite", *Canad. J. Chem. Eng.*, **63** (1985) 278-287.
8. Abbot, J. and Wojciechowski, B.W., "Catalytic Cracking and Skeletal Isomerisation of *n*-Hexenes on HZSM-5 Zeolite", *Canad. J. Chem. Eng.*, **63** (1985) 451-461.
9. Chen, N.Y. and Garwood, W.E., "Some Catalytic Properties of ZSM-5: A New Shape Selective Zeolite", *J. Catal.*, **52** (1978) 453-458 .

10. Biswas, J. and Maxwell, I.E., "Octane Enhancement in Fluid Catalytic Cracking: I. Role of ZSM-5 Addition and Reactor Temperature", *Appl. Catal.*, **58** (1990) 1-18.

11. Pappal, D.A. and Schipper, P.H., "ZSM-5 in Catalytic Cracking: RISER Pilot Plant Gasoline Composition Analyses", *Prepr. A.C.S., Div. Pet. Chem.*, **35(4)** (1990) 678-683.

12. Anderson, C.D., Dwyer, F.G., Koch, G., and Niiranen, P., "A New Cracking Catalyst for Higher Octane Using ZSM-5", Proc. Ninth Iberoamerican Symp. on Catalysis, Lisbon, (1984) 247-258.

Chapter 5

Zeolites as Catalyst Supports: An Overview

CHAPTER 5

Zeolites as Catalyst Supports: An Overview

5.1 Homogeneous and Heterogeneous Catalyses

When first recognised, petrochemicals were defined as relatively pure, identifiable substances derived from petroleum and used in chemical trade {1}. Based on this definition, gas oil and gasoline are two examples of petrochemicals. To date, however, as more conversion and separation processes are built in, most organic chemical substances are classified as petrochemicals {1}.

Traditionally, engineering methods have been used to separate individual species (distillates) from petroleum. Complex chemical processes are then undertaken to convert the materials into more desirable and useable products. These conversion processes involve the use of both homogeneous and heterogeneous catalysts. The conversion of gas oil into gasoline with the use of zeolites in an important example of a heterogeneous catalysis. Several other important processes which involve the use of homogeneous catalysts include oligomerisation of olefins to produce higher grade olefin isomers, oxidation of paraffin or olefins to produce various aldehydes and organic acids, and halogenation of alkanes to produce alkylhalides {1}.

Both homogeneous and heterogeneous catalyses started to be used industrially in *ca.* 1910 {2}. Heterogeneous catalysts have been traditionally used for production of large scale commodity chemicals, such as gaoline, methanol, and ammonia {2}. Homogeneous catalysts on the other hand, are more commonly used in the manufacture of high purity and high value

chemicals, such as reactions of acetylene {2}.

Heterogeneous catalysts are thought to be the first generation of catalysts, while homogeneous catalysts are considered to be the second {3}. The homogeneous catalysts have been developed in which a specific chemical compound is introduced into the reaction as a molecular entity {3}. Such catalysts normally operate in solution and the catalsysts is dissolved in the reaction mixture {3}. Thus, the nature of homegeneous catalysis creates a serious difficulty in separation of the catalysts from the system at the end of the operation, because the reactants, products, and catalysts are all in the same phase {3}. The separation at least requires non-economical ion-exchange or distillation processes {3}. In contrast, with heterogeneous catalysis this can be easily achieved by some kind of filtration {3}.

The thermal stability of heterogeneous catalysts is often much higher than that of homogeneous catalysts {3}. Because some reactions involved in the production of chemicals proceed well at elevated temperature, where the stability and endurance of the catalyst is a significant factor, the thermal stability is another concern which favours the use of heterogeneous catalysts. Another important factor worth considering is the availability of the solvent {3}. The range of suitable solvents for a homogeneous catalyst is often limited by the solubility of the catalyst, whilst in homogeneous catalysis, this problem is not recognised {3}.

On the other hand, homogeneous catalysts also have some advantages over heterogeneous catalysts, which include reproducibilty, controllability, and efficiency {3}. Homogeneous catalysts are said to be reproducible catalysts because they have a definite stoichiometry and structure {3}. In contrast, the structure of heterogenous catalysts is partly governed by the method of preparation and pretreatment {3}. Also because homogeneous catalysts have a

definite structure, they can be easily modified in order to control a reaction {3}. For example, hydroformylation of 1-hexene {4} with a homogeneous complex catalyst [Rh(acac)CO_2] was found to produce a ratio of normal to branched aldehydes of 1.2:1, but when the complex was altered to [Rh(acac)CO(PPh_3)] via ligand manipulation, the ratio changed to 2.9:1.

With these advantages and disadvantages of the two systems of catalysis, it might seem that the balance lies with the homogeneous catalysis {3}. However, the ease of catalyst recovery and product separation after the completion of a chemical process is the most imprtant factor {3}. Over the past two decades there has been recent interest in the development of heterogenised homogeneous catalyts, which combine the advantages of both homogeneous and heterogeneous catalysts. Efforts to create such systems have been carried out by immobilising the homogeneous catalysts onto solid supports, which may or may not be catalytically active. This heterogenised homogeneous catalysis may become the third generation of catalysts {3}.

5.2 Heterogenised Homogeneous Catalysis

The original objective in immobilising homogeneous catalysts (transition metal or transition metal complexes) onto insoluble solid supports was to get over the disadvantages inherited by homogeneous catalysis. Apart from that, immobilisation of a homogeneous catalyst may induce its activity. Bonds *et al.* reported that titanocene complexes readily polymerise to form catalytically inactive materials {5}. However, these catalysts can be siginificantly activated when supported onto polystyrene, because the polymerisation of the catalyst is prevented when it is immobilised. Also, the selectivity of supported catalysts is often greater than their homogeneous counterparts because the solvent channel leading to the active sites has both size restriction and polar properties which

introduce futher selectivity in addition to the electronic and steric hindrance offered by the free complex {3}.

Much work has been done in an attempt to immobilise active homogeneous catalysts on solid supports, such as silica {6}, alumina {3}, clay {7}, and polymers {8-10}. This process usually combines the advantages of both homogeneous and heterogeneous catalysts, while minimising their disadvantages {6}. The heterogenised homogeneous catalyst is believed to have enhanced selectivity, ease of separation and purification of the reactants, products, and catalysts {6}. The higher thermal stability of the heterogenised homogeneous catalysts when compared to homogeneous catalysts offers the ability to perform at elevated temperature, hence promotes reactions with high activation barriers {6}.

Although many materials have been studied as solid supports, silica and polystyrene are two of the most common {3}. The active group of the silica responsible for binding the metal complex is silanol, while polystyrene cross-linked with a proportion of divinylbenzene can have a range of functional groups or none at all, i.e. metal complex interacts directly with the polymer {3}. By far, the most common route for preparing supported complex catalysts is to displace the ligand already coordinated to the metal complex by that from the support. Other routes include direct reaction of a metal halide with support and oxidative addition of support to a metal complex. Seen *et al.* {8, 9} reported that a series of ionic palladium and nickel complexes had been successfully immobilised onto Nafion® polymer via ion-exchange. The ability of the supported complexes as dimerisation catalysts was also tested using ethene as the feedstock. They concluded that both the ligand attached to the metal complex and the type of cations of the polymer have influences in the stability of the resulting supported catalysts. It was found that the method of

immobilisation of the catalysts within the polymer via ion-exchange produced a relatively strong hold as virtually no leaching of catalysts was observed during catalytic testing.

5.3 Zeolite-Supported Catalysts

Zeolites have been extensively used in the petroleum industries as cracking catalysts because of their active acidic sites and unique shape and size selectivity characteristics. More recently there has been interest in using zeolites as supports for various metal complexes which have been widely used in homogeneous catalysis for many important reactions, such as oxidation {11-15}, carbonylation {16, 17}, hydrogenation-dehydrogenation {18}, and oligomerisation {19}.

Immobilisation of transition metal complexes inside the zeolites can be carried out by supporting the complexes onto both the external and internal surfaces {20-22} or simply by encapsulating the complex inside the cages {11-15}. The former is normally used if the complex is cationic, whilst the latter is used if it is neutral.

Supporting cationic metal complexes onto zeolite surfaces is carried out via ion-exchange processes. The already present cation in the zeolite (usually H^+ or Na^+) is exchanged with the ionic metal complex in solution. However, because of the size of the aperture of the zeolite, this method is only suitable for small complexes. Alternatively, a bulky complex can be synthesised *in-situ* by firstly ion-exchanging the zeolite with a smaller metal complex that can enter the aperture and penetrate into the internal structures of the zeolite and exchange the interior cations. Once the cations are exchanged, the ligand of the complex can be replaced *in-situ* via ligand replacement procedures. Lunsford and co-workers {20} reported that a tris(2,2'-bipy)ruthenium(II) complex

could be prepared *in-situ* within the cavities of dehydrated Y zeolites from $[Ru(NH_3)_6]^{3+}$ with similar procedure.

Encapsulating neutral metal complexes inside zeolite cages may be performed using the same procedure, using ion-exchanged complexes as precursors. The process is followed by calcination and reduction of the supported complexes, before synthesising the complex *in-situ*. A wide variety of metal clusters have been successfully encapsulated in a range of different zeolite hosts {18, 23-25}, and to a lesser extent organometallic and coordination compounds {13, 15}. The first *in-situ* synthesis of large metal complex, such as metallophthalocyanines, inside the large cages of zeolite Y was carried out in 1976 by Russian chemists {15} and later reproduced by others {11, 12, 14}. Chemists at Du Pont {11} claimed that they had successfully synthesised the iron phthalocyanine complex inside the supercages of zeolites NaX and NaY and studied the catalytic activity of this complex for oxidation reactions.

Zeolite-supported and -encapsulated catalysts are prepared for specific requirements or reactions based on the combined advantages of the homogeneous and heterogeneous catalysts. Li and Govind {13} reported that transition metal complexes prepared inside zeolites showed a considerable decrease in the rate of irreversible oxidation of the central metal ion. Herron and co-workers {12} reported that competitive oxidation of cyclohexane and cyclododecane or *n*-pentane and *n*-octane using iodosylbenzene as the oxidant by iron phthalocyanine encapsulated inside large pores of zeolites NaX and NaY shows that the zeolite-encapsulated complex favours oxidation of the smaller substrate, probably because smaller molecules can diffuse through the zeolite framework faster {12}. The selectivity introduced by the zeolite is an added bonus to the advantages of immobilising the catalyst onto zeolite.

Summary

The unique intrinsic structure of zeolites have not only found important applications in petroleum industries for many decades, but also more recently have offered a promising use as solid supports for metal complexes that have been extensively used in homogeneous catalysis for various important reactions which are involved in the production of a wide variety of chemicals.

The zeolites may be able to impose their molecular sieve effect (intrinsic shape and size selectivity factor) on otherwise non-selective metal complex catalysts. The zeolite-supported or -encapsulated complexes are also hoped to have several other superiorities to their homogeneous equivalents, such as longer life-time {13}.

In this study, the use of zeolite NaY as a catalyst support for a cationic palladium complex $[Pd(2,2'\text{-bipyridyl})_2]^{2+}$ was investigated. The complex was prepared via three methods which all involve an ion-exchange process. The supported complexes were characterised by various analytical techniques, including ultraviolet-visible, atomic absorption, and raman spectroscopies, together with microprobe and elemental analyses.

References

1. Austin, G.T., "Shreve's Chemical Process Industries", 6th Ed., McGraw-Hill Book Co., N.Y., 1988.
2. Parshall, G.W. and Putscher, R.E., "Organometallic Chemistry and Catalysis in Industry", *J. Chem. Educ.*, **63** (1986) 189-191.
3. Hartley, F.R. and Vezey, P.N., "Supported Transition Metal Complexes as Catalysts", *Adv. Organomet. Chem.*, **15** (1977) 189-234.
4. Alum, K.G., Hancock, R.D., McKenzie, S., and Pitkethly, R.C., *Proc. Int. Cong. Catal.*, 5th (1972) 477.
5. Bonds Jr, W.D., Brubaker Jr., C.H., Chandrasekaran, E.S., "Polystyrene Attached Titanocene Species, Peparation and Reactions", *J.A.C.S.*, **April 16** (1975) 2128-2132.
6. Ozin, G.A. and Gil, C., "Intrazeolite Organometallic and Coordination Complexes: Internal versus External Confinement of Metal Guests", *Chem. Rev.*, **89** (1989) 1749-1764.
7. Crocker, M. and Herold, R.H.M., "Carbomethoxylation of Ethylene Catalysed by Pd(II) Complexes Intercalated in Smectite Clay", *J. Molec. Catal.*, **70** (1991) 209-216.
8. Seen, A.J., Cavell, K.J., Mau, A.W.-H., and Hodges, A.M., "Nafion Supported Cationic Palladium Complexes as Catalysts", *J. Membrane Sci.*, **87** (1994) 149-157.
9. Seen, A.J., Cavell, K.J., Mau, A.W.-H., and Hodges, A.M., "Ethene Dimerisation Using a Nafion® Supported σ-arylnickel(II) Species", *J. Molec. Catal.*, **90** (1994) 245-256.

10. Ciardelli, F., Braca, G., Carlini, C., Sbrana, G., and Valentini, G., "Polymer-Supported Transition Metal Catalysts: Established Results, Limitations, and Potential Developments", *J. Molec. Catal.*, **14** (1982) 1-17.
11. Herron, N., Stucky, G.D., and Tolman, C.A., "Shape Selectivity in Hydrocarbon Oxidations using Zeolite Encapsulated Iron Phthalocyanine Catalysts", J. Chem. Soc., Chem. Commun., 647 (1986) 1521-1527
12. Herron, N., "Selective Partial Oxidation of Alkenes using Zeolite Based Catalysts: Phthalocyanine (PC) "Ship-in-Bottle" Species", *J. Coord. Chem.* **19** (1988) 25-38.
13. Li, G.Q. and Govind, R., "Preparation of Dioxygen Binding property of a New Zeolite Encapsulated Cobalt Tetramethylmorphin Complex", *Inorg. Chimica Acta.*, **217** (1994) 135-140.
14. Meyer, G., Wöhrle, D., Mohl, M., and Schulz-Ekloff, G., "Synthesis of Faujasite Supported Phthalocyanine of Cobalt, Nickel, and Copper", *Zeolites*, **4** (1984) 30-34.
15. Romanovsky, B.V. and Gabrielov, A.G., "Zeolite-Included Phthalocyanines: Synthesis, Characterisation and Catalysis in Ox-Red Reactions", *J. Molec. Catal.*, **74** (1992) 293-303.
16. Primet, M., Vedrine, J.C., and Naccache, C., "Formation of Rhodium Carbonyl Complexes in Zeolites", *J. Molec. Catal.*, **4** (1978) 411-421.
17. Gelin, P., Coudurier, G., Taarit Y.B., Naccache, C., "Formation of Iridium Carbonyl Complex in NaY Zeolite", *J. Catal.*, **79** (1981) 32-40.
18. Komatsu, T., Miyoshi, R., Namba, S., and Yashima, T., "Catalytic Activity of Low Valent Chromium Supported on Y-Zeolites", *J. Molec. Catal.*, **78** (1993) 57-66.

19. Cai, T., Cao, D., Song, Z., and Li, L., "Catalytic Behaviour of $NiSO_4/\gamma$-Al_2O_3 for Ethene Dimerisation", *Appl. Catal., A: General*, **95** (1993) L1-L9.

20. DeWilde, W., Peeters, G., and Lunsford, J.H., "Synthesis and Spectroscopic Properties of Tris(2,2'-bipyridine)ruthenium(II) in Zeolite Y", *J. Phys. Chem.*, **84** (1980) 2306-2310.

21. Quayle, W.H., and Lunsford, J.H., "Tris(2,2'-bipyridine)ruthenium(III) in Zeolite Y: Characterisation and Reduction on Exposure to Water", *Inorg. Chem.*, **21** (1982) 97-103.

22. Knop-Gerrits, P-P., De Vos, D., Thibault-Starzyk, F., and Jacobs, P.A., "Zeolite-encapsulated Mn(II) Complexes as Catalysts for Selective Alkene Oxidation", *Letters to Nature*, **369** (1994) 543-546.

23. Feeley, J.S. and Sachtler, M.H., "Mechanism of the Formation of $PdNi_X$ in the Cages of NaY", *J. Catal.*, **131** (1991) 573-581.

24. Zhang, Z., Yin, Y-G., and Scahtler, W.M.H., " A Novel Preparation Method for Zeolite Encaged Co Clusters", *Catal. Letters*, **18** (1993) 73-79.

25. Moller, K. and Bein, T., "Reduction and Cluster Growth of Palladium in Zeolite Y Containing Transition Metal Ions. X-Ray Absorption Studies", *J. Phys. Chem.*, **94** (1990) 845-853.

Chapter 6

Immobilisation of Cationic Palladium Complexes

CHAPTER 6

Immobilisation of Cationic Palladium Complexes

6.1 Introduction

A study by Drent {1} shows that homogeneous catalysts are developed for a variety of reactions by manipulation of ligand. This method is also used to introduce selectivity in the homogeneous catalysis. However, as it was reviewed in the preceding chapter, there has been interest in supporting homogeneous catalysts onto solid supports in attempts to create a heterogenised homogeneous catalysis system with characteristics superior to those of its parent systems.

Several palladium based complexes have been known as active catalysts for various important reactions in homogeneous catalysis {1}. Although a number of the Pd complex catalysts are observed to show catalytic activities, fewer of them are present in ionic forms, such as $[Pd(2,2'\text{-bipy})_2]^{2+}$ complex. A work by Seen *et al.* {2} investigated the immobilisation of this cationic Pd complex within the framework of a polymer, Nafion®. The activity of the immobilised complex was tested for dimerisation of ethene.

In this study, immobilisation of $[Pd(2,2'\text{-bipy})_2]^{2+}$ complex within the structure of zeolite NaY was attempted via ion-exchange technique. Characterisations of the supported complex were achieved by using various analytical techniques, namely electron microprobe and elemental analyses, ultraviolet-visible, atomic absorption, and raman spectroscopies.

6.2 Experimental

The zeolite used as support was zeolite NaY (Rhenisch-Westfälischen Aachen; HV 92/85, Si/Al = 5).

Three ways of immobilising the $[Pd(2,2'\text{-bipy})_2]^{2+}$ complex were attempted:-

1. Directly impregnating the zeolite with previously prepared $[Pd(2,2'\text{-bipy})_2](NO_3)_2$ complex via ion-exchange in aqueous solution (method I).

From the empirical formula of the zeolite, $Na_{32}[(AlO_2)_{32}(SiO_2)_{160}]\cdot 240H_2O$, there are 32 exchangeable Na^+ per unit cell, which require 16 complex ions to replace them completely. Zeolite (5 g) was exchanged with a series of aqueous solutions of $[Pd(2,2'\text{-bipy})_2](NO_3)_2$ with different concentrations to produce different loadings (0.25 to 16 molecules per unit cell). Each exchange was carried out for 72 hrs at room temperature. The impregnated zeolite was then recovered, washed, and dried at room temperature under vacuum for 72 hrs.

2. Impregnating the zeolite with previously prepared $Pd(2,2'\text{-bipy})Cl_2$ complex in the presence of free 2,2'-bipyridyl (method II).

This procedure is similar to that of method I, but using a series of $Pd(2,2'\text{-bipy})Cl_2$ solutions in the presence of free 2,2'-bipyridyl. There are two possibilities of where the addition of the second 2,2'-bipyridyl could take place:-

a. Outside the zeolite structure:-

$$Pd(2,2'\text{-bipy})Cl_2 + 2,2'\text{-bipyridyl} \Leftrightarrow [Pd(2,2'\text{-bipy})_2]^{2+} + 2Cl^- \quad \text{(Eq. 6.1)}$$

$$[Pd(2,2'\text{-bipy})_2]^{2+} + \text{Zeolite} \Leftrightarrow [Pd(2,2'\text{-bipy})]^{2+}\text{---Zeolite} \quad \text{(Eq. 6.2)}$$

b. Inside the zeolite structure:-

$$Pd(2,2'\text{-bipy})Cl_2 + \text{Zeolite} \Leftrightarrow Pd(2,2'\text{-bipy})Cl_2/\text{Zeolite} \quad \text{(Eq. 6.3)}$$

$$Pd(2,2'\text{-bipy})Cl_2/\text{Zeolite} + 2,2'\text{-bipyridyl} \Leftrightarrow [Pd(2,2'\text{-bipy})_2]\text{---Zeolite} \quad \text{(Eq. 6.4)}$$

The reaction as in Eq. 6.2 is essentially the same as in method I. This method of immobilisation enables the competition between reactions occurring as in case 'a' and case 'b' to be observed.

3. Ion-exchanging the zeolite with aqueous solution of $[Pd(NH_3)_4]^{2+}$ (pH =7.2 - 8.0). Free 2,2'-bipyridyl was then added to the cation-exchanged zeolite in solution (method III).

With this technique, the zeolite was subject to cation exchanges followed by ligand replacement. Once again the procedure of ion-exchange was similar to that in method I, but using a series of $[Pd(NH_3)_4]^{2+}$ solutions. Ligand replacement was then carried out on the cation-exchanged zeolite. Cation-exchanged zeolite (5 g) was made into a suspension in a minimum amount of water, and a stoichiometric amount of 2,2'-bipyridyl was added. The mixture was then stirred for 72 hrs with N_2 purging at 50 mL/min to purge the free ammonia from solution. Modified zeolite was then recovered from the suspension, washed, and dried at room temperature under vacuum for 72 hrs.

Preparation of $Pd(2,2'\text{-bipy})Cl_2$ and $[Pd(2,2'\text{-bipy})_2](NO_3)_2$:-

$PdCl_2$ (Johnson Matthey Loan Scheme) was used as received. Preparation of the complexes was as described previously by Seen *et al.* {2}. $PdCl_2$ (0.177 g, 1.0 mmol) was dissolved in 20 mL of dilute HCl and to this was added 2,2'-bipyridyl (0.156 g, 1.0 mmol) in 10 mL of water.

$Pd(2,2'\text{-bipy})Cl_2$ was filtered from the solution after 3 hrs and then dried at room temperature under vacuum for 72 hrs (Yield = 56%).

$AgNO_3$ (0.339 g, 2.0 mmol) and 2,2'-bipy (0.164 g, 1.05 mmol) were added to a slurry of $Pd(2,2'\text{-bipy})Cl_2$ in 20 mL of water. After stirring in darkness for 2 hrs the AgCl was removed by filtration yielding a bright yellow filtrate. The filtrate was allowed to evaporate before recrystalisation of the complex from ethanol/ether. An orange complex of $[Pd(2,2'bipy)_2](NO_3)_2$ was obtained and dried under vacuum at room temperature (Yield = 42%).

6.3. Characterisation

The exchange solutions were analysed qualitatively for unsupported complexes with a Schimadzu UV 160 spectrometer. Quantitative analyses on atomic palladium were carried out on a Varian SpectrAA-800 spectrometer. The zeolite-supported complexes were also quantitatively analysed for palladium and carbon contents by microprobe (SX-CAMECA 500) and elemental (CARLO ERBA EA-1108) analysers. Raman spectra of the impregnated zeolites were obtained using a BRUKER IFS 66 with BRUKER FRA 106 attachment.

6.3.1 UV-Visible and Atomic Absorption Spectroscopies

The complex $Pd(2,2'\text{-bipy})Cl_2$ is sparingly soluble in water. UV-visible spectrum of an aqueous solution of this complex along with those of $[Pd(NH_3)_4]^{2+}$ and $[Pd(2,2'\text{-bipy})_2]^{2+}$ are shown in Figure 6.1.a. Peaks at *ca.* 295, 309, and 312 nm are due to $[Pd(2,2'\text{-bipy})_2]^{2+}$, $Pd(2,2'\text{-bipy})Cl_2$, and $[Pd(NH_3)_4]^{2+}$ respectively. Free 2,2'-bipyridyl in water shows two distinct peaks at *ca.* 233 and 278 nm as can be seen in Figure 6.1.b. The spectra of these

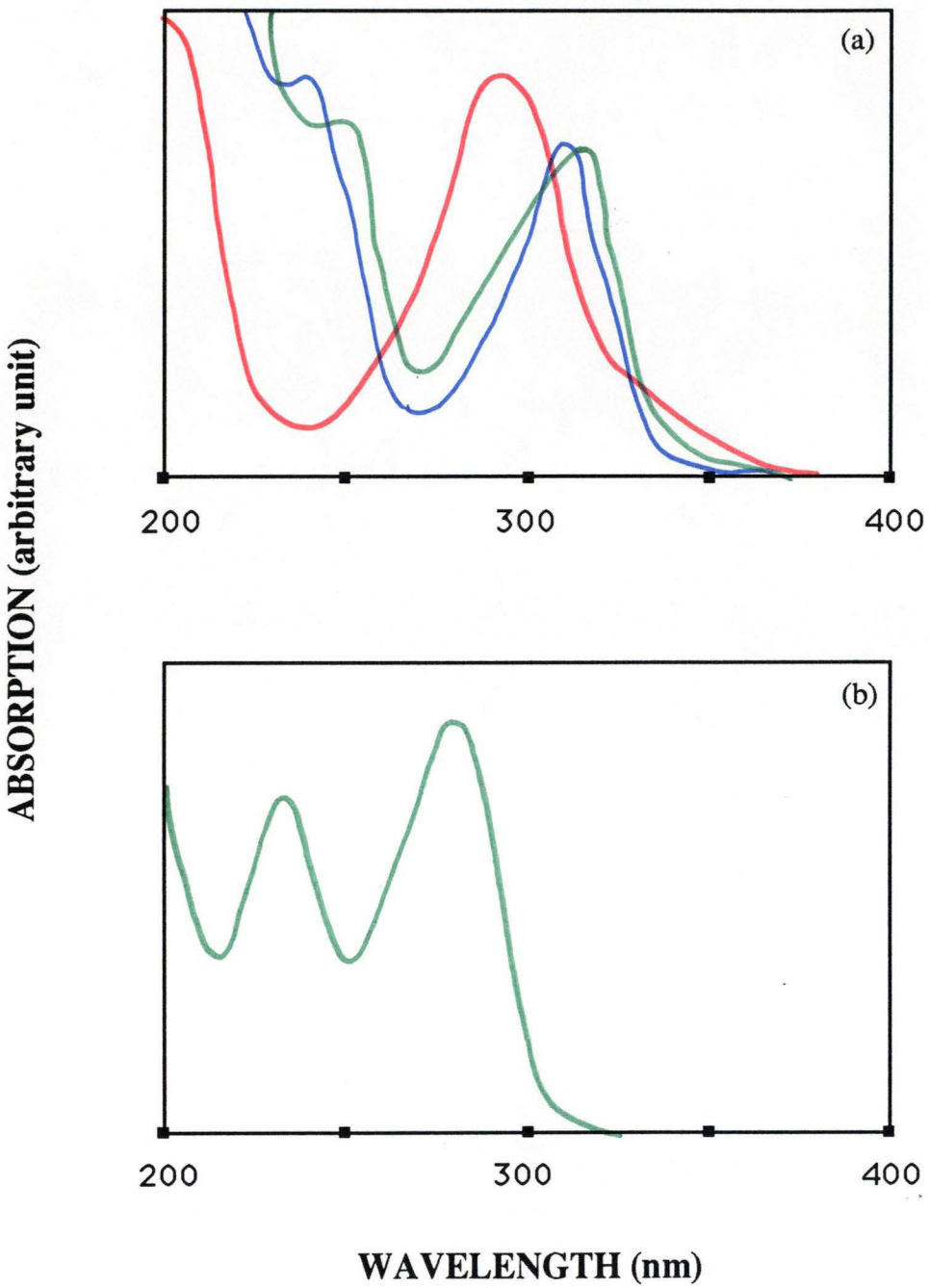

Figure 6.1 UV-visible spectra of aqueous solutions of (a) $[Pd(2,2'\text{-bipy})_2]^{2+}$ ●, $Pd(2,2'\text{-bipy})Cl_2$ ●, and $[Pd(NH_3)_4]^{2+}$ ●, (b) 2,2'-bipyridyl

solutions provided a qualitative determination of the presence of these complexes in solutions.

All solutions analysed by uv-visible spectroscopy for palladium complexes were also analysed quantitatively by atomic absorption spectroscopy for atomic palladium. Thus, combined analyses on the solutions after exchange and ligand replacement were used determine the extent of these processes.

6.3.2 Microprobe and Elemental Analyses

Bulk concentration of atomic palladium in the impregnated zeolites was determined by microprobe analysis based on the silica and aluminium contents of the zeolite. Results from this analysis are given in Table 6.1. It is important to note at this point that this analysis does not distinguish the state of the palladium, whether it is present in atomic state or bonded to the 2,2-bipyridyl or ammine ligand.

It is interesting to note that with sample H, even though $[Pd(NH_3)_4]^{2+}$ present during ion-exchange was sufficient to produce a loading of 32 molecules per unit cell, the result shows that it was not possible. In fact, the loading is comparable to that of sample G which indicates that the maximum exchange capacity of the zeolite is no more than 16 molecules per unit cell, as expected from the empirical formula of the zeolite.

From the work by Carty and Chieh {3}, the molecular dimensions of $[Pd(2,2'\text{-bipy})_2]^{2+}$ and $Pd(2,2'\text{-bipy})Cl_2$ are approximately 7.5 x 8.0 Å and 7.5 x 5.5 Å respectively. (*cf.* Diameter of zeolite aperture is about 7.4 Å, and diameter of the supercages is around 13 Å). Thus, it is apparent that $[Pd(2,2'\text{-bipy})_2]^{2+}$ is too big to enter the aperture. The slightly smaller $Pd(2,2'\text{-bipy})Cl_2$, however, is able to diffuse through the channels of the zeolite and exchange the Na^+ in the internal structure. However, the complex is still too

Table 6.1 Loadings of Pd in the zeolite-supported complexes determined by microprobe analysis

Sample	Expected Number of Complex/Unit Cell	Theoretical Pd loading (wt %)	Experimental Pd Loading (wt %)		
			Method I	Method II	Method III
A	0.25	0.16	0.16	0.16	0.16
B	0.5	0.32	0.32	0.32	0.32
C	1	0.64	0.60	0.60	0.64
D	2	1.28	0.61	1.10	1.24
E	4	2.56	0.61	1.12	2.38
F	8	5.12	0.62	1.14	4.24
G	16	10.24	0.62	1.15	8.97
H	32	20.48			8.96

big to get into the sodalite cages and hexagonal prisms. Thus, the achievement of the maximum exchange capacity of the zeolite on the external surface and in the supercages explains the levelling of Pd concentration for the zeolite-supported complexes prepared via method I and II, even though the loadings were increased. The higher maximum Pd loading attainable via method II compared to method I also suggests that the equilibrium for the addition of the second 2,2'-bipyridyl ligand tends to occur inside the zeolite structure.

Because the zeolite does not have carbon in its structure, any carbon detected from elemental analysis could be directly related to the amount of 2,2'-bipyridyl present. With the elemental analysis, information on whether the 2,2-bipyridyl is attached to the palladium or just trapped inside the zeolite structure is not yet clear. However, from these two analyses, it was found that the mole ratio of palladium to 2,2'-bipyridyl in the zeolite-supported complexes prepared via method I and II were proportional (Pd : 2,2'-bipy = 1 : 2). For those prepared via method III, however, this proportionality was no longer maintained, especially as the loading of $[Pd(NH_3)_4]^{2+}$ increased. These ratios are given in Table 6.2.

Table 6.2 Palladium to 2,2'-bipy ratio [Pd : 2,2'-bipy = 1 : X] of the zeolite-supported complexes determined by microprobe and elemental analyses

Sample	Method I	Method II	Method III
A	2	2	1.93
B	2	2	1.39
C	2	2	1.38
D	2	2	1.24
E	2	2	1.21
F	2	2	1.14
G	2	2	0.51

Since the starting complex in method III was $[Pd(NH_3)_4]^{2+}$, and the palladium to 2,2'-bipy mole ratio is not consistently proportional, then it is reasonable to expect that a mixture of three cationic palladium complexes, $[Pd(NH_3)_4]^{2+}$, $[Pd(2,2'\text{-bipy})(NH_3)_2]^{2+}$, and $[Pd(2,2'\text{-bipy})_2]^{2+}$ could have been present. Unfortunately the exact proportion of each complex was not able to be determined, however, an approximation of the amount of $[Pd(2,2'\text{-bipy})_2]^{2+}$ and $[Pd(2,2'\text{-bipy})(NH_3)_2]^{2+}$ can be calculated if the ligand exchange is stepwise and all $[Pd(NH_3)_4]^{2+}$ reacts with at least one 2,2'bipyridyl (i.e. no $[Pd(NH_3)_4]^{2+}$ is present).

Let the absolute amount of $[Pd(NH_3)_4]^{2+}$, $[Pd(2,2'\text{-bipy})(NH_3)_2]^{2+}$, $[Pd(2,2'\text{-bipy})_2]^{2+}$, palladium, and 2,2'-bipyridyl present in the zeolite be designated as α, β, γ, M, and N respectively. Then the following equations hold when $\alpha = 0$:-

$$\beta + \gamma = M \qquad \text{(Eq. 6.5)}$$

$$\beta + 2\gamma = N \qquad \text{(Eq. 6.6)}$$

such that:-

$$\gamma = N - M \qquad \text{(Eq. 6.7)}$$

$$\beta = 2M - N, \quad \text{where } \beta, \gamma \geq 0 \qquad \text{(Eq. 6.8)}$$

The values of M and N are obtained from microprobe and elemental analysis respectively. By using equations 6.7 and 6.8, the values for β and γ are calculated and given in Table 6.3. Except for sample G, these values are acceptable ($\beta, \gamma \geq 0$). When the Pd : 2,2'-bipy mole ratio becomes too low, as for sample G, the assumption that $\alpha = 0$ is no longer valid and γ becomes negative. The only way to correct this is for $[Pd(2,2'\text{-bipy})(NH_3)_2]^{2+}$ to

Table 6.3 Proportion of palladium complexes in zeolite-supported complexes prepared via method III

Sample	Palladium (mmole) **M**	2,2'bipyridyl (mmole) **N**	[Pd(NH3)4]2+ (mmole) α	[Pd(2,2'-bipy)(NH3)2]2+ (mmole) β	[Pd(2,2'-bipy)2]2+ (mmole) γ
A	0.015	0.029	0	0.001	0.014
B	0.030	0.042	0	0.018	0.012
C	0.060	0.083	0	0.038	0.023
D	0.120	0.145	0	0.095	0.025
E	0.220	0.313	0	0.127	0.093
F	0.400	0.497	0	0.303	0.097
G	0.840	0.450	0	1.230	-0.390

transform into $[Pd(NH_3)_4]^{2+}$ and $[Pd(2,2'\text{-bipy})_2]^{2+}$ by the following equation:-

$$2[Pd(2,2'\text{-bipy})(NH_3)_2]^{2+} \text{ ----> } [Pd(NH_3)_4]^{2+} + [Pd(2,2'\text{-bipy})_2]^{2+} \quad \text{(Eq. 6.9)}$$

And now equations 6.5 and 6.7 respectively become:-

$$\alpha + \beta + \gamma = M \quad \text{(Eq. 6.10)}$$

$$\gamma = N - M - \alpha \quad \text{(Eq. 6.11)}$$

such that for $\gamma \geq 0$ to hold, α has to be bigger than or equal to M - N.

Thus, it could be said that there is at least γ amount of $[Pd(2,2'\text{-bipy})_2]^{2+}$, and at most β amount of $[Pd(2,2'\text{-bipy})(NH_3)_2]^{2+}$ in the zeolite-supported complex prepared via method III.

Earlier work with tris(2,2'-bipy)ruthenium(II) complex supported on a zeolite Y was reported by Lunsford *et al.* {4, 5}. They claimed that they were able to synthesise the complex *in-situ* from $[Ru(NH_3)_6]Br_3$ via ion-exchange technique. However, the potential formation of a mixture of complexes due to incomplete transformation of $[Ru(NH_3)_6]^{3+}$ to $[Ru(2,2'\text{-bipy})_3]^{2+}$ inside the zeolite cages was not clearly recognised.

6.3.3 Raman Spectroscopy

Raman spectra of the zeolite, 2,2'-bipyridyl used in this study and that from a reference {6} are shown in Figure 6.2. It is advantageous that the zeolite does not produce any peaks in the area where the 2,2'-bipyridyl does, hence it does not produce a disturbed background. On comparison between Figures 6.2.b and 6.2.c, it was assured that the 2,2'-bipyridyl used was pure. The 1200-1700 cm^{-1} region is characteristic of the aromatic ring vibrations and

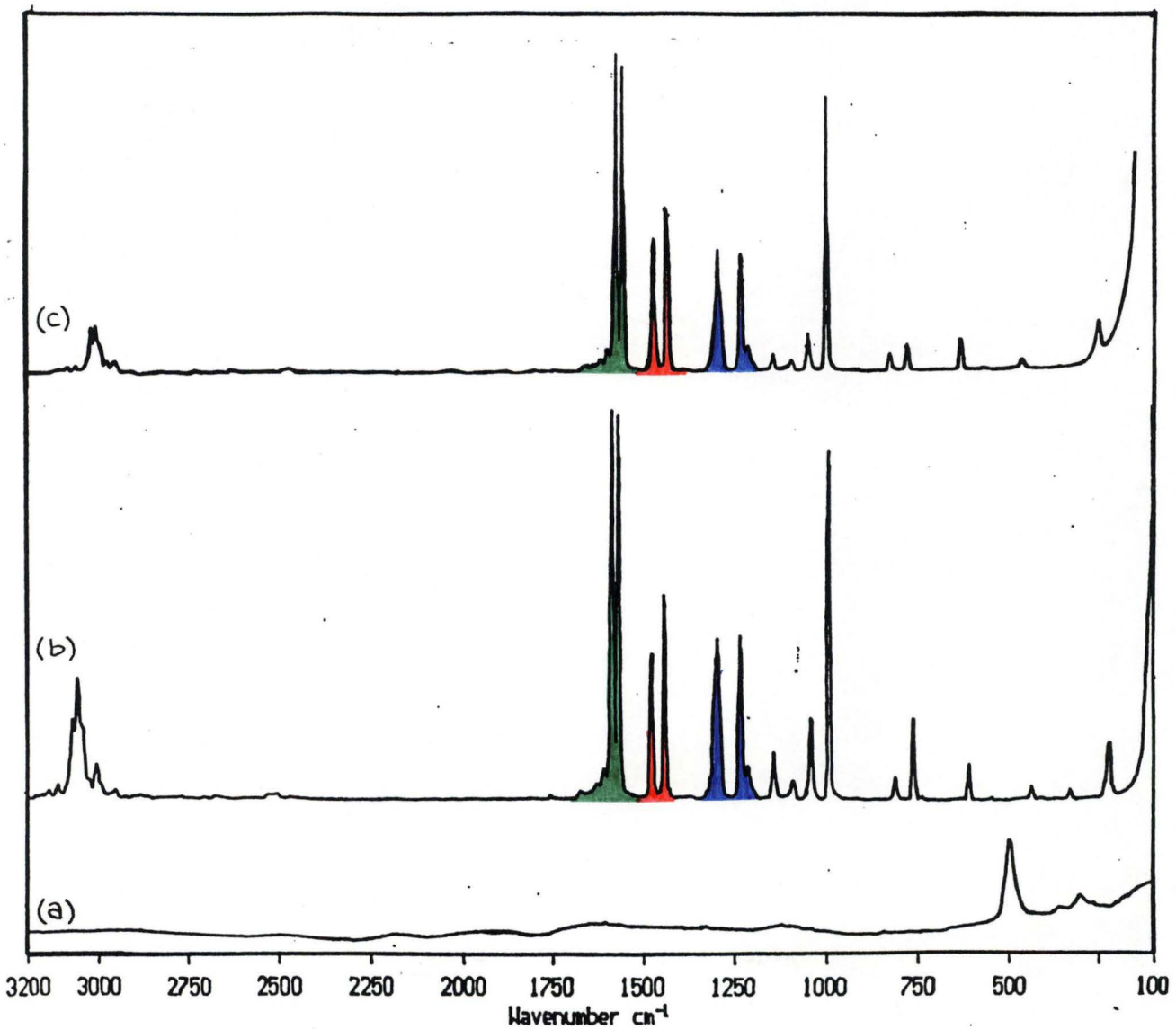

Figure 6.2 Raman spectra of: (a) pure zeolite, (b) 2,2'-bipyridyl used in this study, and (c) 2,2'-bipyridyl {6}

probably results from the complete interaction of the C=N and C=C vibrations thus making assignment of the individual vibrations difficult {7}.

When the 2,2'-bipyridyl is bonded to palladium, its spectrum changes as can be seen in the spectra of Pd(2,2'-bipy)Cl_2 and [Pd(2,2'-bipy)$_2$]$(NO_3)_2$ complexes shown in Figure 6.3., in particular the relative intensities of peaks highlighted in colours. Figure 6.4 shows the Raman spectra of the zeolite-supported complexes obtained via method I, II, and III with similar Pd loading of around 0.6 wt%. As can be seen, there is no indication that free 2,2'-bipyridyl is present unbonded inside the zeolite structure. Similar spectra were identified for the whole series of the zeolite-supported complexes prepared via these methods. Since the penetration of the beam from the raman spectrometer used for this analysis was a few microns, whilst the average particle size of the zeolite was 1 micron as determined by scanning electron microscopy, it is safe to say that the raman spectra give a bulk analysis.

The proportional ratios of Pd : 2,2'-bipy = 1 : 2 for zeolite-supported complexes prepared via methods I and II together with their raman spectra which show no free 2,2'-bipyridyl present inside the zeolite cages, suggest that the Pd and 2,2'-bipyridyl are present inside the zeolite cages as $[Pd(2,2'\text{-bipy})_2]^{2+}$.

It is now necessary to recall the information obtained from the microprobe analyses shown in table 6.1. By taking the difference between the maximum Pd loadings in the zeolite-supported complex prepared via method I and II, the distribution of the$[Pd(2,2'\text{-bipy})_2]^{2+}$ complex present in the supercages can be calculated. With 0.53 wt% difference, there are $5.3x10^{-3}$ g Pd present in 1 g of the impregnated zeolite. Since this mass is negligible compared to the mass of the support, it is safe to say that there are 5.3x10-3 g Pd (= $5.0x10^{-5}$ mole)/g of zeolite. From the empirical formula of the zeolite, its molecular weight is approximated to be 16,544 g/mole. Knowing that 1 mole of zeolite has

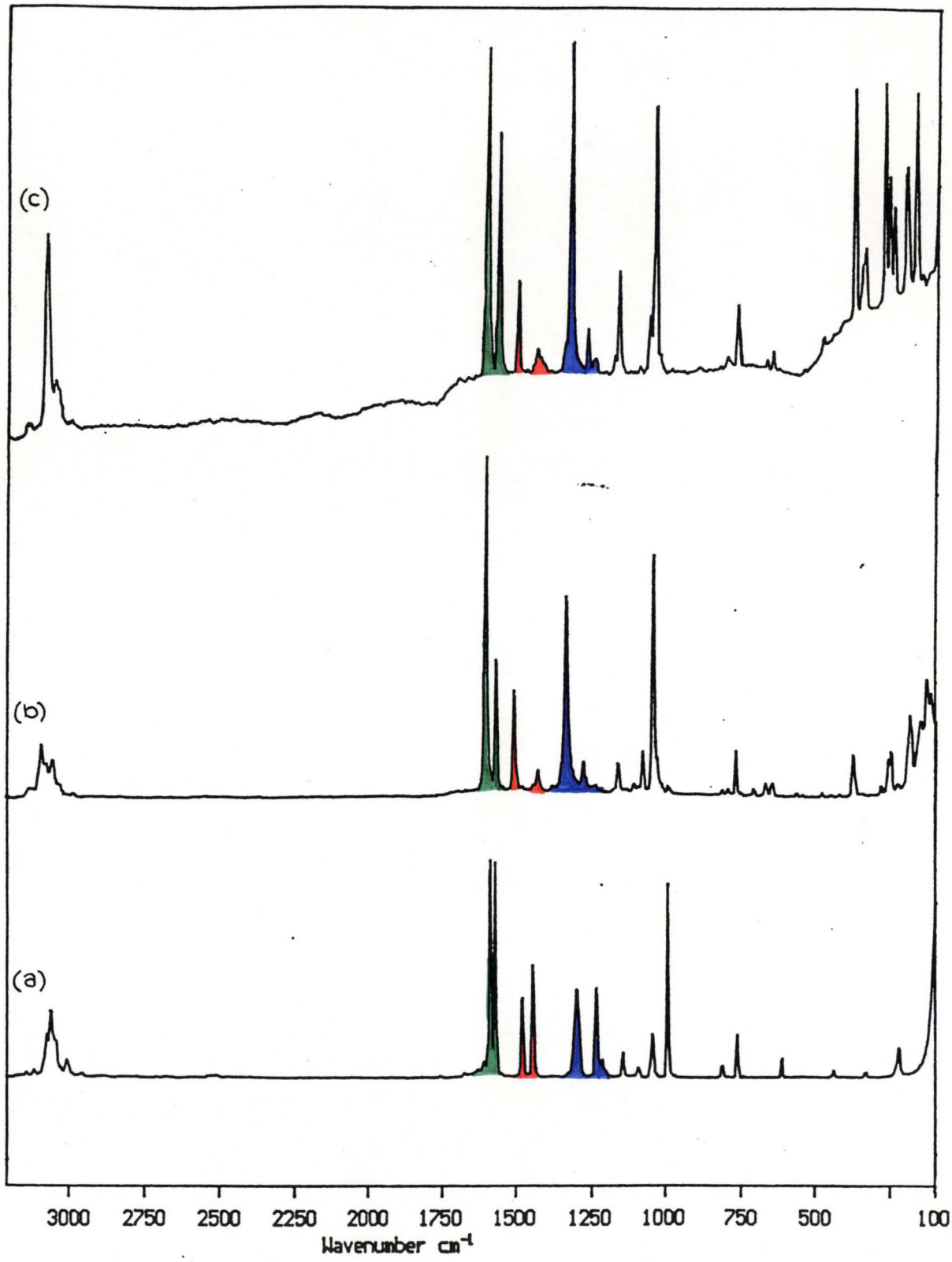

Figure 6.3 Raman spectra of: (a) 2,2'-bipyridyl (b) $[Pd(2,2'\text{-bipy})_2](NO_3)_2$, and (c) $Pd(2,2'\text{-bipy})Cl_2$

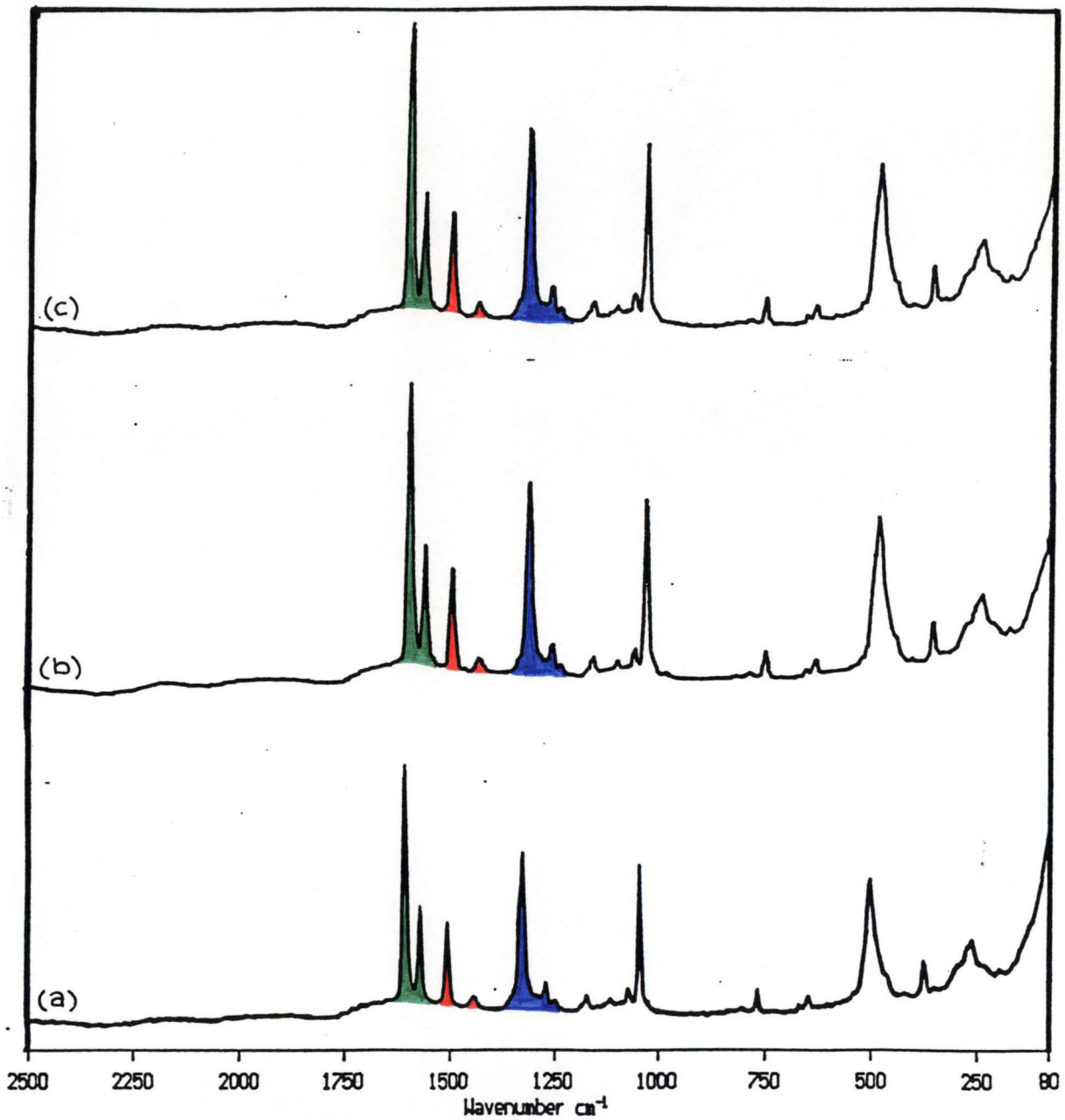

Figure 6.4 Raman spectra of zeolite-supported complexes prepared via method I (a), method II (b), and method III (c)

6.023×10^{23} unit cells, and there is precisely 1 supercage in 1 unit cell, then there are no less than 3.6×10^{19} unit cell/g of zeolite. Assuming an even distribution of complex in the internal structure, then the density of the complex is approximately 0.8 molecule/unit cell. This is a reasonable value when comparing the size of the complex and the dimension of the supercage.

6.5 Conclusion

Attempts to directly ion-exchange $[Pd(2,2'\text{-bipy})_2]^{2+}$ into the NaY zeolite resulted in a maximum palladium loading of 0.62 wt% compared with a maximum loading of 8.97 wt% when $[Pd(NH_3)_4]^{2+}$ was ion-exchanged into the zeolite. However, it was found that conversion of $[Pd(NH_3)_4]^{2+}$ to $[Pd(2,2'\text{-bipy})_2]^{2+}$ for palladium loadings greater than 0.16% could only be partially achieved. A mixture of cationic complexes $[Pd(NH_3)_4]^{2+}$, $[Pd(2,2'\text{-bipy})(NH_3)_2]^{2+}$, and $[Pd(2,2'\text{-bipy})_2]^{2+}$ may be produced by this method of immobilisation.

The theoretical maximum loading of palladium with 16 molecules of palladium complex per unit cell is 10.22 wt%. Efforts to obtain higher loadings of $[Pd(2,2'\text{-bipy})_2]^{2+}$ by *in-situ* synthesis from $Pd(2,2'\text{-bipy})Cl_2$ in the presence of 2,2'-bipyridyl resulted in an increased maximum palladium loading to 1.15 wt%. This indicates that the penetration of $Pd(2,2'\text{-bipy})Cl_2$ is deeper than that of $[Pd(2,2'\text{-bipy})_2]^{2+}$, as can be expected from their relative molecular sizes with respect to the diameter of the aperture of the zeolite.

It is then proposed that the $[Pd(2,2'\text{-bipy})_2]^{2+}$ complex ions could only exchange Na^+ present on the external surface of the zeolite particles and probably several incomplete supercages near the surface, whilst the smaller $Pd(2,2'\text{-bipy})Cl_2$ complex could enter the aperture of the zeolite, penetrate further into the zeolite channels and occupy the supercages in the pore interior.

However, this cationic complex is still too big to get into the sodalite cages and hexagonal prisms of the zeolite. Assuming that the complex is distributed evenly inside the zeolite structure, a density of 0.8 complex molecule/unit cell was achieved by method II, which is a reasonable value when considering the comparative sizes of the complex and the supercage where it is located. It was also observed in method II that the equilibria involved in the second addition of the 2,2'-bipyridyl ligand shift in such a way so addition inside the zeolite structure is favoured.

With method III, $[Pd(NH_3)_4]^{2+}$ complex is small enough to diffuse through the channels and almost completely exchange all Na^+ present both in the internal and external structures of the zeolite. The inability to achieve 100% conversion of $[Pd(NH_3)_4]^{2+}$ to $[Pd(2,2'\text{-bipy})_2]^{2+}$ using method III is probably due to the steric constraints within the smaller zeolite cages. The exact proportion of each complex was not able to be determined, however, the boundary values for supported cationic $[Pd(2,2'\text{-bipy})(NH_3)_2]^{2+}$ and $[Pd(2,2'\text{-bipy})_2]^{2+}$ complexes were approximated.

Raman analyses showed that all 2,2'-bipyridyl detected in the impregnated zeolites were present as complexes. These together with the proportionality of Pd : 2,2'-bipyidyl ratios from microprobe and elemental analyses indicate that the Pd and 2,2'-bipyridyl are both present as $[Pd(2,2'\text{-bipy})_2]^{2+}$ complex.

References

1. Drent, E., *Pure. Appl. Chem.*, (1990) 661-669.
2. Seen, A.J., Cavell, K.J., Mau, A.W-H., and Hodges, A.M., "Nafion Supported Cationic Palladium Complexes as Catalysts", *J. Membrane Sci.*, **87** (1994) 149-157.
3. Carty, A.J. and Chieh, P.C., "Steric Effects in a Distorted Square Planar Bis-(2,2'-bipy) Metal Complex: X-Ray Crystal Structure of Aquobis-(2,2'-bipy)palladium(II) Nitrate", *J.C.S., Chem. Commun.*, (1971) 158-159.
4. DeWilde, W., Peeters, G., and Lunsford, J.H., "Synthesis and Spectroscopic Properties of Tris(2,2'-bipyridine)ruthenium(II) on Zeolite Y", *J. Phys. Chem.*, **84** (1980) 2306-2310.
5. Quayle, W.H., and Lunsford, J.H., "Tris(2,2'-bipyridine)ruthenium(III) in Zeolite Y: Characterisation and Reduction on Exposure to Water", *Inorg. Chem.*, **21** (1982) 97-103.
6. Schrader, B. and Meier, W., "DMS Raman/IR Atlas of Organic Compounds", Verlag Chemie, Germany, vol 1 (1974).
7. Rao, C.N.R., "Chemical Applications of IR Spectroscopy", Academic Pres., London, (1963) 317-335.

Chapter 7

Catalytic Testing of Zeolite-Supported Complexes

CHAPTER 7

Catalytic Testing of Zeolite-Supported Complexes

7.1 Introduction

There have been numerous studies of oligomerisation reactions of a wide range of olefins over various homogeneous catalysts {1, 2}. These studies have taken into account factors such as the type of central metal ions, ligands, and solvents. However, fewer reports are available on the reactions over supported catalysts {3}.

In this chapter, the zeolite-supported $[Pd(2,2'\text{-bipy})_2]^{2+}$ complexes prepared as outlined in Chapter 6 were investigated for dimerisation of ethene. Ethene was used because it is a widely used test olefin whose dimers (butenes) are simple enough to analyse. Unfortunately, since there is a possibility of the presence of a mixture of different palladium complexes with no information about their exact proportions, zeolite-supported complex prepared via method III were not tested.

7.2 Experimental

Dimerisation Procedure:-

The catalytic testing of the zeolite-supported complexes for dimerisation of ethene was carried out in a 250 mL medium pressure autoclave with a water jacket, fitted with a MAGNEDRIVE stirrer. For a typical catalytic test, about 0.25 g of impregnated zeolite, containing 2 - 50 μmole of $[Pd(2,2'\text{-bipy})_2]^{2+}$ catalyst, was added to the reactor followed by 100 mL of methanol as the solvent. A blank reaction was carried out using pure zeolite as the catalyst.

The space above the solvent was made oxygen-free by purging the reactor with nitrogen for 5 minutes before *n*-butane was added as an internal standard. The reactor was then heated to the reaction temperature of 60 °C with water from a hot water bath flowing through the autoclave jacket, after which the reactor was pressurised with ethene to the reaction pressure of 25 bar. Catalytic tests were carried out with stirring at 400 rpm for 4 -5 hrs, during which samples were collected every 15 minutes. A 150 mL stainless steel bottle was used to collect about 1 mL of catalytic solution, and after expansion the sample headspace vapour was analysed by GC. The catalytic solution was analysed by AA spectroscopy for any palladium leached during the test.

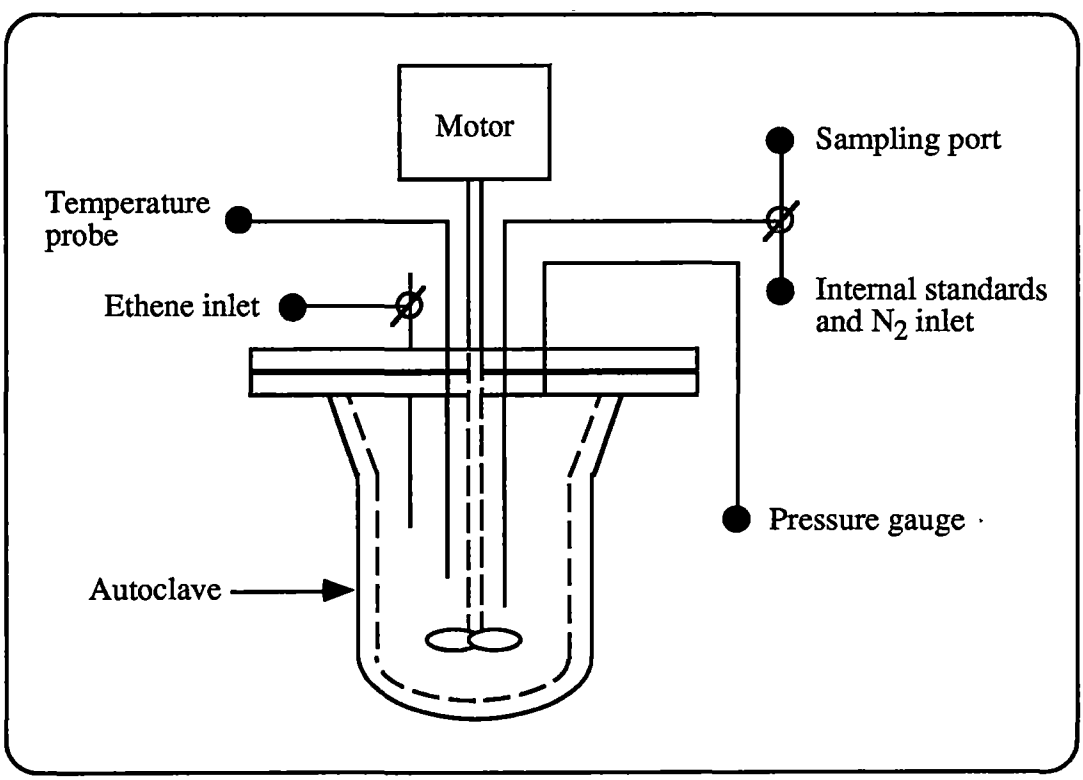

Figure 7.1 Schematic experimental apparatus forcatalytic testing

Determination of relative distribution coefficients for butene isomers:-

A calibration was required to determine the relative distribution of butene isomers between the reactor and the sample bottle headspace. This was done by adding known masses of *n*-butane and butene isomers to the reactor under standard catalytic reaction conditions in the absence of catalyst. Sampling and GC analysis were done as for normal catalytic testing.

Data acquisition and analysis of catalytic samples:-

Gas chromatographic analyses were carried out using a Hewlett Packard 5890 II GC fitted with a SGE 50 QC3/BP1-2.0 column (25 m x 0.33 mm i.d.) with a flame ionisation detector and using N_2 as the carrier gas. Separation of *n*-butane and butenes was achieved by undertaking analyses at 30 °C with N_2 velocity of 12 cm/s. Identification of the butene isomers was made by injecting individual pure isomers. Data handling was facilitated using a DAPA software package (Chromatography System V1.30).

7.3 Results and Discussion

Relative distribution coefficients of butene isomes:-

In order to obtain quantitative data of the amount of butene isomers produced in the reactor during catalytic testing, relative distributions of the isomers between the sample bottle headspace and the reactor had to be established. This was achieved by developing a sampling technique whereby a small aliquot (1mL) of catalytic solution was collected in a 150 mL stainless steel bottle and depressurised by expansion.

A 'reference model system' {4} was employed to determine this relative distribution, which involved solvation of known masses of the *n*-butane and the butene isomers in the methanol, placed in the reactor, and treated in a manner

similar to that used for catalytic testing. The relative distribution coefficients for 1-butene, t-2-butene, and c-2-butene were determined relative to *n*-butane and were found to be 1 : 1 : 1, as it was observed in an earlier work (5}.

Catalysis:-

Dimerisation of ethene was selected as the test reaction because ethene is a widely used olefin for tests whose dimers (butenes) are simple enough to analyse. Also Seen *et al.* {5} recently reported the same reaction over several σ-arylnickel(II) species supported on Nafion®, so that comparison could be made.

More than 95% of the dimerisation products obtained from reactions over homogeneous complex were butenes. A mixture of linear and branched hexenes account for the remaining. Their distribution throughout the duration of the catalysis is near consistent (1-butene : t-2-butene : c-2-butene = 1 : 2 : 2), confirming previous study by Seen *et al.* {5}. Distribution from the same reaction over zeolite-supported complexes was found to be similar, as shown in Figure 7.2. Analysis of the catalytic solutions by AA spectroscopy showed that less than 3% of the supported catalyst was leached from the zeolite during catalytic testing.

Activities of the homogeneous complex, zeolite-supported complexes, and the zeolite itself are rather difficult to compare because of the unconsistency in the unit. Typically, activity is expressed as mole of reactant reacted per mole of catalyst per hour. In this case, however, the activity of the homogeneous and supported complexes were expressed in mol of ethene dimerised/(mole of catalyst present x hour), whilst that of pure zeolite was in mol of ethene dimerised/(g of zeolite x hour). Thus, by having the same mass of zeolite for the reactions over zeolite-supported complexes and pure zeolite, activity of the

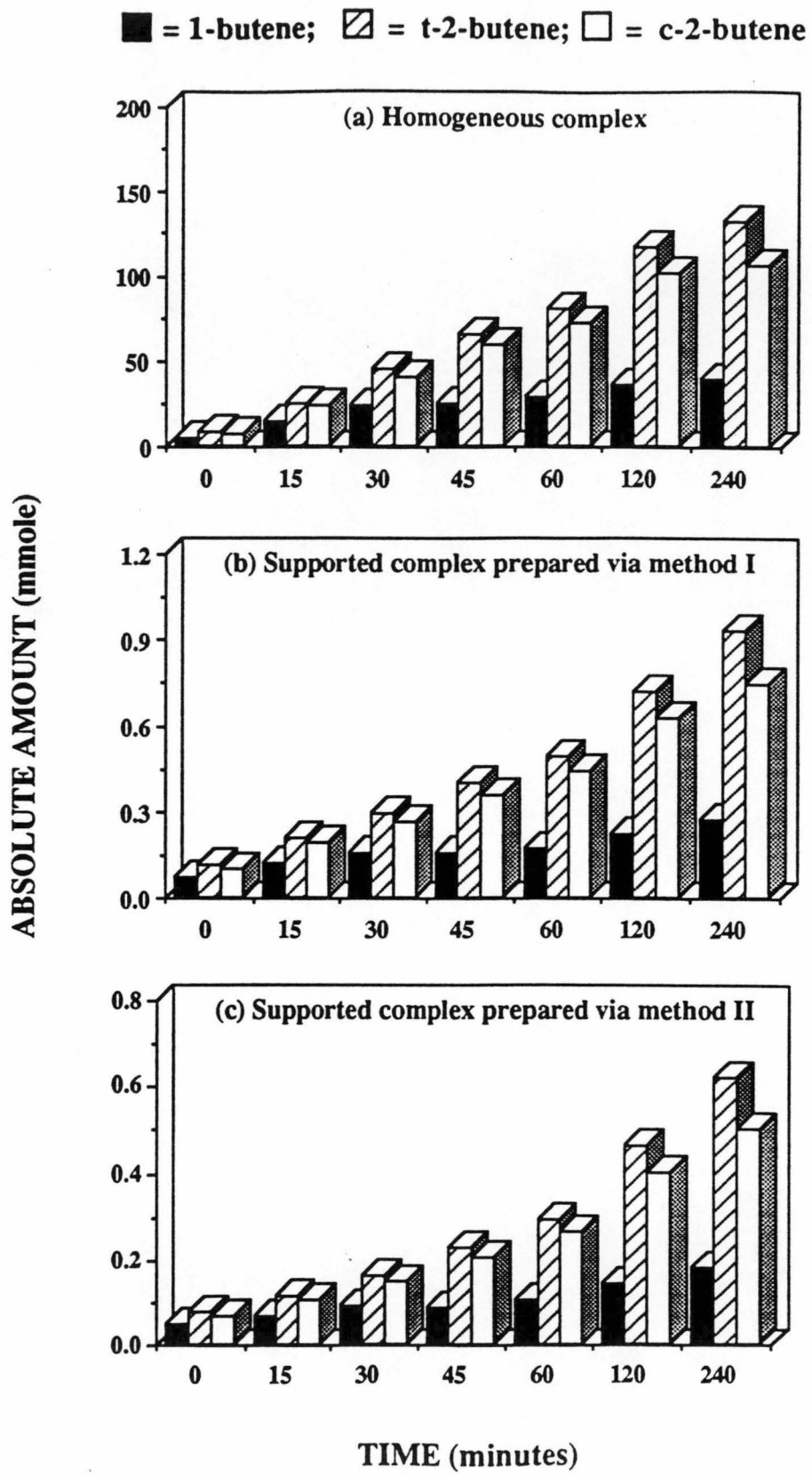

Figure 7.2 Product distribution from dimerisation of ethene over:-
(a) homogeneous $[Pd(2,2'\text{-bipy})_2]^{2+}$ (*ca.* 100 μmole)
(b) zeolite-supported $[Pd(2,2'\text{-bipy})_2]^{2+}$ (*ca.* 3 μmole)
at 60 °C, 25 bar

zeolite-supported complexes was corrected for contribution from the zeolite itself.

The activity of homogeneous $[Pd(2,2\text{-bipy})_2](NO_3)_2$ complex in methanol under the reaction conditions employed was as high as 8000. While those of supported complexes prepared via methods I and II were only 1000 - 1500. There was a slight tendency for the activity to decrease as the loading increased. For comparison, the activity of 8000 for $[Pd(2,2\text{-bipy})_2]^{2+}$ immobilised within Nafion® polymer was reported by Seen *et al.* {5}. The difference is probably due to the influence of the support and reaction conditions studied. These results are given in Table 7.1. The more accessible complexes located on the external surfaces may give rise to the slightly higher activity for the zeolite-supported complex prepared via method I.

Table 7.1 Catalytic activity of pure zeolite, homogeneous and supported catalysts in methanol for dimerisation of ethene at 60 °C, 25 bar

Catalyst	Activity
Homogeneous $[Pd(2,2\text{-bipy})_2](NO_3)_2$	8000
Zeolite supported $[Pd(2,2\text{-bipy})_2]^{2+}$ (method I)	1495 (a)
Zeolite supported $[Pd(2,2\text{-bipy})_2]^{2+}$ (method II)	1130 (a)
$[Pd(2,2\text{-bipy})_2]^{2+}$ supported on Nafion-Na^+	5500 (b)
Pure zeolite	65

Key:
(a) Pd loading of ~0.6 wt%
(b) After Ref. 5.

7.4 Conclusion

The catalytic activity of the zeolite-supported complex $[Pd(2,2\text{-bipy})_2]^{2+}$ for dimerisation of ethene was found to be around 15% of that of the corresponding homogeneous system. This may be due to the influence of anions surrounding the cationic complex. In a homogeneous system, the complex is surrounded by nitrate ions, whilst on the zeolite surface, it interacts with oxygen ions. Because of this interaction, the complex may become less reactive toward dimerisation when compared to its homogeneous state. The location of the complex seems to influence its activity as indicated by the difference in activity of the zeolite-supported complexes prepared via method I and II. Those located on the external surfaces may tend to behave more like a homogeneous system.

Product distributions are similar for both homogeneous and heterogenised catalysts. Even the same reaction over pure zeolite gave similar product distributions. These results indicate that the butenes are too small to be affected by the shape and size selectivity of the zeolite. A mixture of linear and methyl-branched higher olefins may serve as a better feedstock in order to see the selectivity factor imposed by the zeolite. However, isomerisation is feasible to take place when higher olefins are used as the feedstock.

References

1. Bogdanovic, B., "Selectivity Control in Nickel-Catalyzed Olefin Oligomerization", *Advances in Organometallic Chemistry*, **17** (1979) 105-140.
2. Keim, W., Behr, A., and Röper, M., "Alkene and Alkyne Oligomerization, Cooligomerization and Telomerization Reactions", *Comp. Organometallic Chemistry*, **8** (1982) 371.
3. Cai, T., Cao, D., Song, Z., and Li, L., "Catalytic Behaviour of $NiSO_4/\gamma$-Al_2O_3 for Ethene Dimerization", *Appl. Catal. A: General*, **95** (1993) L1-L7.
4. Drozd, J. and Novak, J., *J. Chromatography*, **165** (1979) 141-165.
5. Seen, A.J., Cavell, K.J., Mau, A.W-H., and Hodges, A.M., "Ethene Dimerisation Using a Nafion® Supported σ-arylnickel(II) Species", *J. Molec. Catal.*, **90** (1994) 245-256.

Chapter 8

Conclusions

CHAPTER 8

Conclusions

The main objective of this study was to investigate the use of zeolites in catalysis, in particular as conventional, industrially used cracking catalysts, and more recently as supports for metal complex catalysts widely used for various important reactions in homogeneous catalysis. The first part of this study provides an insight into the influence of each type of zeolites HY and HZSM-5 as well as that introduced by two different isomers of C_8 paraffins (*n*-octane and 2-methylheptane). The second part explores the feasibility of supporting a cationic palladium complex, $[Pd(2,2'\text{-bipy})_2]^{2+}$, onto the surface of NaY zeolite via simple ion-exchange technique. The activity of the supported complexes were tested for dimerisation of ethene.

n-Octane and 2-methylheptane were used in cracking reactions over zeolites HY, HZSM-5, and their combinations. The two hydrocarbons were selected to discern the skeletal effect introduced by the structure of a molecule, while the zeolites were chosen because of their common use in commercial catalytic cracking. The influence of each zeolite on a particular feedstock was able to be isolated by mixing the zeolites in the following ways:-

i. Placing the bed of zeolite HY prior to that of zeolite HZSM-5.

ii. Placing the bed of zeolite HZSM-5 prior to that of zeolite HY.

iii. Mixing the two zeolites thoroughly.

It was found that overall distributions of cracking products by carbon number from reaction of either paraffin on combinations of HY and HZSM-5, and from reaction of a mixture of the paraffins on either zeolite, can be reasonably described by the addition of product distributions on individual catalysts and from individual paraffins, weighted according to the relative amounts present. The observed distributions of paraffins, olefins and aromatics

comprising a product group at any particular carbon number shows more widespread deviations from calculated product ratios. This arises particularly from hydrogen transfer processes which occur on the Y zeolite, leading to more extensive formation of paraffins and aromatics at the expense of olefins. The observed disappearance of ethane and methane, however, suggests that the behaviour of a particular reactant within a complex mixture may not be easily predicted from studies where that reactant is introduced as a single feedstock.

Isomerisation reactions of both olefin and paraffin cracking products are promoted by the presence of HZSM-5. The presence of the HZSM-5 produces higher concentrations of branched olefin isomers. There is also evidence that preferential isomerisation of branched paraffins can occur when high concentrations of product olefins are also present, whereas cracking is favoured at low olefin concentrations. The addition of pentasil results in enrichment of the linear saturates at lower carbon numbers which is due to preferential cracking of linear paraffins over the branched isomers.

It has been known that an important function of HZSM-5 additive during gas oil cracking is to reduce bimolecular hydrogen transfer processes which would otherwise easily occur on the Y zeolite. The competing monomolecular process leading to olefin formation through cracking of the carbenium ion is more favourable on HZSM-5. From this study, it appears that increased proportions of small olefinic products are the direct result of the contribution of feed cracking by the pentasil, rather than an interruption of hydrogen transfer processes which would otherwise occur on the Y zeolite.

This study consistently shows that upon addition of HZSM-5 cracking of either linear or branched paraffins over HY results in a greater proportion of linear paraffin isomers of lower molecular weight, in contrast to reported cracking studies on gas oils. This suggests that selective cracking of linear

paraffin isomers by HZSM-5 may not be the dominant mechanism for octane number enhancement.

The use of zeolite as a catalyst support was investigated by immobilising a cationic palladium complex, $[Pd(2,2'\text{-bipy})_2]^{2+}$, in zeolite NaY. Three ways of immobilisation were employed, by which a model for location and distribution of the supported complex was proposed:-

i. Prepared from $[Pd(2,2'\text{-bipy})_2](NO_3)_2$ complex which was exchanged directly with the zeolite (method I).

ii. Synthesised *in-situ* from $Pd(2,2'\text{-bipy})Cl_2$ complex which was exchanged with the zeolite in the presence of 2,2'-bipyridyl (method II).

iii. Synthesised *in-situ* from $[Pd(NH_3)_4]^{2+}$ which was exchanged with the zeolite. Free 2,2'-bipyridyl was then added to the cation-exchanged zeolite in solution to replace the ammine (method III).

This study shows that cationic complexes could be supported into the structure of zeolites via a simple ion-exchange process. Among the three methods, attempts to directly ion-exchange $[Pd(2,2'\text{-bipy})_2]^{2+}$ into the zeolite resulted in the minimum palladium loading, whilst the maximum loading was obtained when $[Pd(NH_3)_4]^{2+}$ was ion-exchanged into the zeolite. However, it was found that conversion of $[Pd(NH_3)_4]^{2+}$ to $[Pd(2,2'\text{-bipy})_2]^{2+}$ could only be partially achieved. A mixture of cationic complexes may be produced by this method of immobilisation. Synthesising the complex *in-situ* from $Pd(2,2'\text{-bipy})Cl_2$ in the presence of 2,2'-bipyridyl resulted in an increased maximum palladium loading when compared to method I. It was found that the addition of the second 2,2'-bipyridyl tends to occur inside the zeolite structure.

It is then proposed that the $[Pd(2,2'\text{-bipy})_2]^{2+}$ complex ions could only exchange Na^+ present on the external surface of the zeolite particles and several supercages near the surface, whilst the smaller $Pd(2,2'\text{-bipy})Cl_2$ complex could

enter the aperture of the zeolite, penetrate the channels, and occupy most of the supercages in the interior. However, this cationic complex is still too big to enter the sodalite cages and hexagonal prisms of the zeolite. Assuming an even distribution, the supercage is occupied by about 0.8 molecule of the complex. With method III, the $[Pd(NH_3)_4]^{2+}$ complex is small enough to diffuse through the channels and exchange almost all Na^+ present both in the external and internal structures of the zeolite.

The catalytic activity of the zeolite-supported complexes was tested for dimerisation of ethene. The activity of the heterogenised catalyst was found to be around 15% of that of the homogeneous system. This may be partly due to the influence of anions surrounding the cationic complex. Location of the complex was observed to show some contribution. In a homogeneous system, the complex is surrounded by nitrate ions, whilst when immobilised it is 'attached' to oxygen ions on the zeolite surface, hence less susceptible towards the reaction. Product distributions are similar for both homogeneous and heterogenised catalysts. Even a similar pattern of product distribution is obtained from the same reaction over pure zeolite. The shape and size selectivity of the zeolite was not quite observed due to the relatively small size of the ethene and butenes.

Appendix

Publication

APPENDIX

Publication

JOURNAL OF CATALYSIS **140**, 150–167 (1993)

Cracking and Isomerization of Hydrocarbons with Combinations of HY and HZSM-5 Zeolites

Z. ZAINUDDIN, F. N. GUERZONI, AND J. ABBOT

Chemistry Department, University of Tasmania, Hobart, Tasmania, Australia

Received November 15, 1991; revised June 26, 1992

Catalytic reactions of *n*-octane on sequential combinations of HY and HZSM-5, as well as on random mixtures of the zeolites, have been examined. Theoretical product distributions have been calculated for reactions on these catalyst combinations by assuming relative contributions based on the individual product distributions as well as the conversions on the individual components. Effects due to interactions of products of one catalyst with the other in a binary combination can be identified by comparing theoretical and observed product distributions. Predicted values from this approach provide a good approximation when considering the product distributions in terms of total hydrocarbons formed at each carbon number. Significant differences are found between observed and predicted values in the relative proportion of paraffins and olefins at a particular carbon number, and also in the ratios of branched to linear paraffin isomers. Reaction processes attributable for these deviations have been identified as hydrogen transfer processes, particularly on HY, and paraffin isomerization on HZSM-5.

INTRODUCTION

There have been numerous studies of cracking and isomerization reactions of pure hydrocarbons on individual zeolite catalysts (*1–5*). Kinetic phenomena relating conversions of feedstocks to variables such as catalyst to feed ratios and reaction times have been extensively studied. These studies have taken into account factors such as aging characteristics of the catalyst, as active sites are poisoned, and competitive adsorption on the available sites, which may give rise to product inhibition. Product selectivity has also been examined for many systems, providing details of initiation processes at low conversion and also at higher conversions revealing secondary reaction phenomena, where primary products participate in further reactions. Such investigations have been extended to include studies of simple mixtures of hydrocarbons (*6–8*) on individual catalysts, as well as very complex gas oils (*9*) which contain hundreds of individual components.

Although commercial cracking catalysts are composed of a mixture of solid components which can exhibit catalytic activity (*10–12*), there have been few detailed studies which have attempted to relate the resultant effect of the composite catalyst to that of the individual components. For the past two decades cracking catalysts have contained a form of Zeolite Y. More recently there has been interest in addition of a small proportion of a second zeolite component, in particular the pentasil HZSM-5 (*13–22*). There have, however, been very few reported studies of reactions on individual hydrocarbons on binary zeolite mixtures. For example, in a study by Buchanan (*22*), the cracking of C_6–C_{10} normal paraffins and olefins on combinations of zeolites was investigated. It was reported that the pentasil additive plays an active role in the isomerization and cracking reactions of olefin species, while the reactivity toward paraffins is limited.

In the present study we have examined the behaviour of *n*-octane under cracking conditions in the presence of faujasite–pentasil combinations (HZSM-5 to HY ra-

0021-9517/93 $5.00

tios ranged from 0.3 to 1.8) at 400°C. Previous studies on cracking with zeolite combinations have generally focused on the effect of the presence of a second zeolite on the product distribution obtained on a single zeolite. Our aim is to develop a methodology based on adding together product distributions from individual catalysts. This should permit us to identify additional effects in which the products from reaction on one zeolite interact with the other zeolite. The use of *n*-octane as a feedstock is well suited for this purpose, as the cracking distributions obtained are simple enough to be analyzed in detail.

EXPERIMENTAL

The feedstock, *n*-octane (99.7%), was obtained from Aldrich and used without further purification. Impurities in the feedstock were *n*-hexane (0.2%), 2-methylheptane (0.08%), and isopentane (0.02%).

HY zeolite (97.3% exchanged) was prepared from NaY (Linde Lot No. 45912, SK40; Si/Al = 2.4) by repeated exchange with 0.5 *M* ammonium nitrate solution. HZSM-5 (Si/Al = 105) was provided by SNAM Progretti S.P.A. (Milan, Italy). Details of synthesis and characterization of the pentasil have been reported previously (*23*). Catalysts were calcined at 500°C before use, and experiments were performed on catalysts of mesh size 80/100.

All experiments were performed by using an integral, fixed-bed gas-phase plug flow reactor with independently controlled three-zone heater. The experimental apparatus and procedures used were similar to those described in previous studies (*24*). All reactions were carried out at 400°C and 1 atm pressure. Catalysts were mixed with granules of washed sand which served as an inert support matrix within the reactor. Blank experiments at long times on stream showed that thermal conversion of *n*-octane at 400°C was negligible (<0.5%). Liquid products were analyzed using a Hewlett–Packard 5890A gas chromatograph with a 50-m capillary column and flame ionization detector. Gaseous products were also analysed using a Hewlett–Packard gas chromatograph of the same type with a Chrompak capillary column (25 m × 0.32 mm i.d.). Data handling was facilitated using a DAPA software package. Identification of hydrocarbon products was assisted by use of a Hewlett–Packard 5890 gas chromatograph coupled to a 5970 mass selective detector.

RESULTS AND DISCUSSION

Conversion of n-Octane on Individual Zeolites and Catalyst Combinations

In this study we have examined the cracking and isomerization processes which occur during reaction of *n*-octane on the Zeolites HY and HZSM-5 at 400°C both individually and in combinations. At this temperature, the contribution from thermal cracking processes was found to be negligible, confirming the previous studies (*24, 25*). Our approach has been to relate observed effects of particular combinations of these zeolites to the predicted combined contributions from the individual catalysts under the same conditions. In theory, any discrepancy between the observed and the predicted effects of a combination should be explainable in terms of the influence of the presence of the second catalyst on the products from the first, or vice versa.

In this study we have attempted to reach general conclusions regarding combination effects which are independent of process conditions such as time on stream or the level of conversion examined. For catalysts of different types, such as a faujasite and a pentasil, intrinsic activity and decay characteristics can differ very significantly (*26–28*). This is illustrated in Fig. 1 which shows plots of conversion of *n*-octane at 400°C against time on stream for three catalyst to feed ratios for each catalyst. In this work we chose to make comparisons under conditions where the activity of the individual catalyst (as measured by cumulative conversion of *n*-octane) was equivalent. This condition can be taken as points of intersection of curves in Fig. 1, correspond-

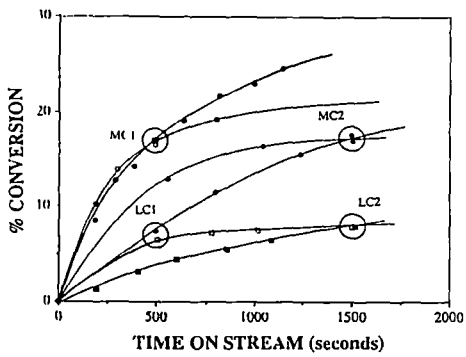

FIG. 1. Effect of time on stream and catalyst to feed ratio for conversion of *n*-octane on HY and HZSM-5 at 400°C. Catalyst to feed ratio: On HY, □ = 0.0101, ◇ = 0.0579, ○ = 0.0900; on HZSM-5: ■ = 0 0101, ◆ = 0 0179, ● = 0.0310.

ing to a specific time on stream. Four such points have been identified in that figure. These have been labeled LC1 and LC2 (corresponding to low conversion at two distinct values of time on stream) and MC1 and MC2 (corresponding to medium conversion levels). Taking conditions at each of these four points in turn, we have compared the behavior of individual catalysts (HY and HZSM-5) with that of various combinations of the zeolites always using the same time on stream, the amount of *n*-octane feedstock, and the amount of catalyst introduced. At low conversions of *n*-octane, it is also valid to state that the individual catalyst to reactant values are approximately equal to those presented to the isolated catalysts. This assumption of course becomes less valid as levels of conversion are increased. We have therefore restricted our study to low and medium conversion (<20%). It should be noted that the results obtained herein are obtained using a fixed bed reactor with integral averaged conversion. This is quite distinct from the industrial case, in which deactivated catalysts convert products and never actually contact the feed.

Three types of combinations of zeolites were selected for study. The first combination consisted of HY followed by HZSM-5 in sequence in the reactor, designated [Y → Z]. The second combination, [Z → Y], used a sequence in the reverse order. The third combination consisted of a random mixture of HY and HZSM-5, designated [RANDOM], and this would correspond to the combination used in most previous investigations using gas–oil mixtures (*13–21*). Table 1 shows the total conversion of *n*-octane corresponding to each of the four points LC1, LC2, MC1, and MC2. In each case, as expected, the conversion of *n*-octane with a catalyst combination is greater than that on an individual zeolite, but the total conversion is always less than the sum of the individual conversions, designated by (Y + Z). The difference observed lies in the fact that for second order reactions as is the case for catalytic cracking, the crackability (defined as conversion/(100-conversion)) is additive and not the conversion (*29*). This may be expected, considering that doubling the catalyst to feed ratios for any given catalyst generally produces less than twice the conversion (*30*). Alternatively, for a sequential mixture of zeolites, it could be inferred that the products from reactions on the first component may cause more rapid aging than the reactant itself. In Table 1, [Y] and [Z] refer to the conversion of *n*-octane on the individual faujasite and pentasil catalysts, respectively, using identical amounts of catalysts and times on stream as for each of the catalyst combinations reported.

Product Distributions on Individual Catalysts

Product distributions from reactions of *n*-octane on HY and HZSM-5 at 400°C at equivalent levels of conversion are shown in Fig. 2. Distributions from cracking of linear paraffins on individual HY and HZSM-5 catalysts have been previously reported (*2, 31*). It is apparent that acyclic olefins and paraffins are the dominant products. The maximum in the distribution of total hydrocarbons was shifted to lower molecular size on HZSM-5 relative to that on HY in each case examined (*2, 31*) as illustrated for LC1 in Fig. 2a. A similar trend was observed con-

TABLE 1

Observed and Calculated Conversions of *n*-Octane on Zeolites at 400°C

Run conditions	Percentage conversion for catalyst configurations							
	[Y]	[Z]	(Y + Z)	[Y → Z]	[Z*][a]	[Z → Y]	[Y*][a]	[RANDOM]
LC1	6.5	7.0	13.5	11.8	5.3	10.2	3.2	13.4
LC2	7.9	8.0	15.9	10.6	2.7	9.7	1.7	11.2
MC1	17.1	17.0	34.1	30.6	13.5	22.4	5.4	33.5
MC2	16.9	18.0	34.9	29.1	12.2	21.6	3.6	32.1

[a] [Z*] and [Y*] give the calculated conversion of *n*-octane on the second component of the [Y → Z] and [Z → Y], respectively.

sidering the distributions of saturated products according to carbon number (Fig. 2b). In particular, it can be seen that at the same levels of *n*-octane conversion, C_1, C_2, and C_3 paraffins are formed in greater abundance on HZSM-5 compared to HY. Figure 2c shows that the abundance of olefinic products on HY is lower than that on HZSM-5. This can be explained in terms of the increased tendency toward hydrogen transfer processes on the faujasite compared to the medium pore pentasil (*19*). This is also revealed by the much higher tendency to produce aromatic products on HY, as illustrated in Fig. 2d.

Figures 3 and 4 show the ratios of branched to linear (B/L) isomers for product C_4–C_6 paraffins and C_4 and C_5 olefins, re-

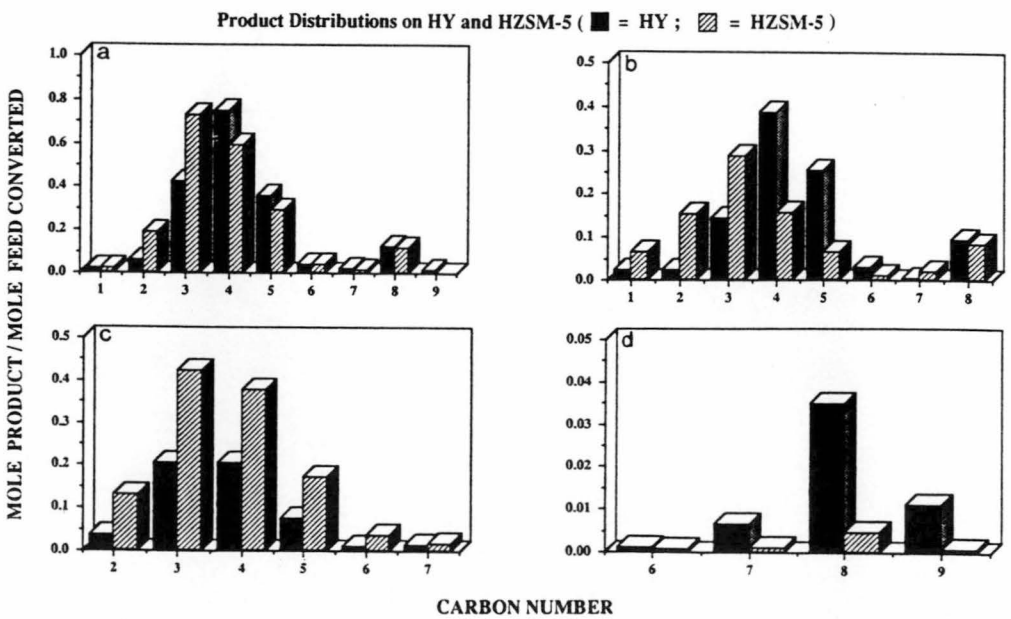

FIG. 2. Product distributions from catalytic reaction of *n*-octane on HY and HZSM-5 at 400°C. (Representative examples from conditions LC1, LC2, MC1, and MC2). (a) Total hydrocarbons (LC1), (b) paraffins (LC2), (c) olefins (MC2), (d) Aromatics (MC1).

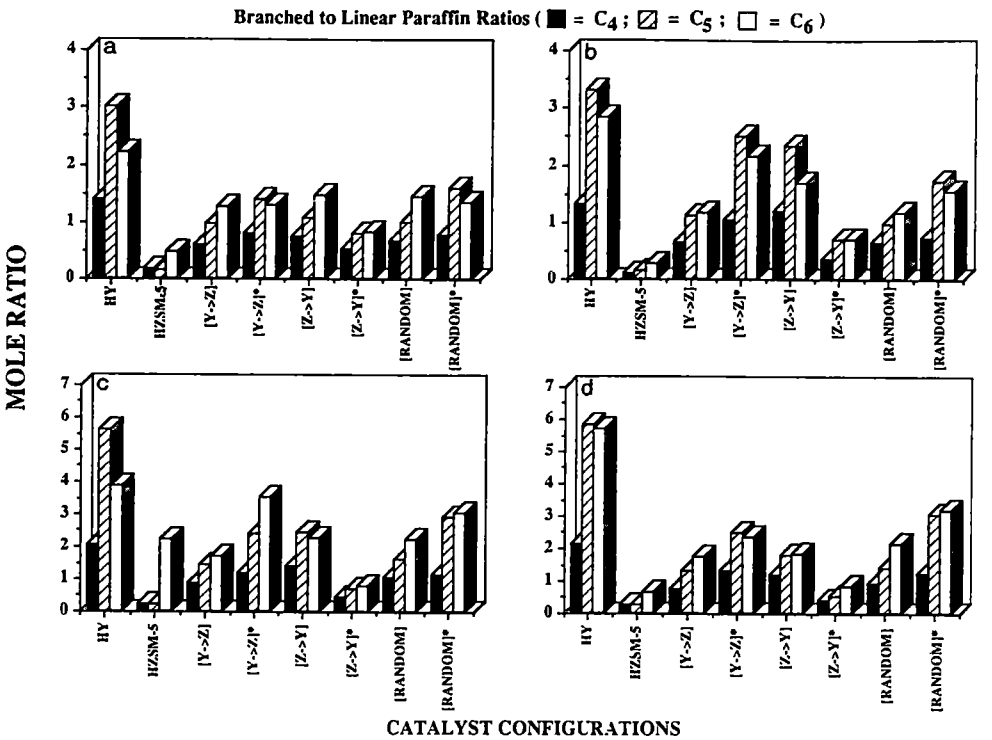

FIG. 3. Ratios of branched to linear paraffins (C_4–C_6) from individual catalysts and catalyst combinations (a) LC1, (b) LC2, (c) MC1, (d) MC2.

spectively. It is apparent that for reaction of *n*-octane on the individual zeolites (Fig. 3) there are significant differences in the branched to linear ratios of paraffin products. Branched paraffins are dominant on HY while the linear isomers are preferentially formed on HZSM-5 (*6*). Figure 4 shows that for C_4 and C_5 olefins the branched to linear ratios show less variation than for the corresponding saturated products, with values generally in the range 1 to 2.5. It can be seen that there is a higher tendency to form branched C_4 olefins on HZSM-5 (B/L ratios 1.38–1.46) compared to HY (B/L ratios 0.92–1.02). A similar trend is also found for the C_5 olefins. Ratios of branched to linear isomers for products formed on combinations of catalysts are also shown in Figs. 3 and 4, and these are discussed in subsequent sections.

Reactions on Sequential HY Followed by HZSM-5

The total conversions of *n*-octane when passed over HY together with HZSM-5 are given in Table 1. In each case (LC1, LC2, MC1, and MC2), knowing the conversion of *n*-octane under the same conditions without the presence of HZSM-5, it is possible to calculate the total conversion of *n*-octane on the pentasil component, designated [Z*] in Table 1. In the first instance, it can be assumed that product distributions from reaction of *n*-octane on HZSM-5 on the combination [Y → Z] are the same as those observed on HZSM-5 alone. Taking into account the calculated conversion of *n*-octane on each zeolite component of the sequence, it is then possible to compute predicted distributions of products for reaction on the catalyst sequence [Y → Z]. These predicted

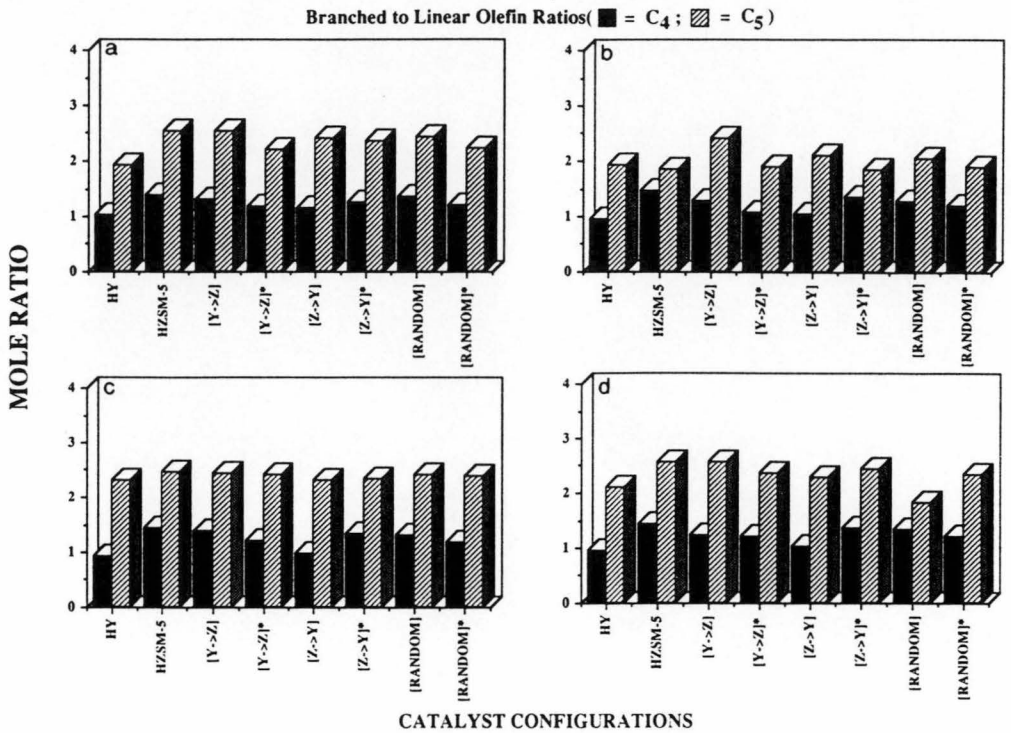

FIG. 4. Ratios of branched to linear olefins (C_4 and C_5) from individual catalysts and catalyst combinations. (a) LC1, (b) LC2, (c) MC1, (d) MC2.

distributions assume that only *n*-octane reacts on the second catalyst component of the sequence (in this case, HZSM-5) and that the catalyst reaction products formed on HY pass through the pentasil unchanged. These predicted product distributions are designated [Y → Z]*. By comparing these predicted distributions with those actually observed, it is possible to infer the extent to which the assumptions made, concerning the interactions on the second zeolite, are correct. Variations between observed and predicted distributions can then be explained in terms of interactions and additional reaction processes.

Figures 5–8 show comparison between observed and predicted distributions (i.e., [Y → Z] and [Y → Z]*) corresponding to each of the four reaction conditions. Separate comparisons have been made for total hydrocarbons (Fig. 5), paraffins (Fig. 6), olefins (Fig. 7), and aromatics (Fig. 8). Inspection of Fig. 5 clearly shows that the observed distributions for total hydrocarbons produced are generally well represented by the predicted values.

Comparison between the observed and the predicted values of C_3, C_4, and C_5 paraffins (Fig. 6) shows that in every case, extensive hydrogen transfer processes, which would lead to significant additional paraffins in this range, do not occur on ZSM-5. This is confirmed by a similar inspection of the results for the corresponding olefins (Fig. 7), which does not reveal extensive depletion of olefins present within the distribution. Further inspection of this figure shows that while C_3 and C_4 olefins are very close to predicted values, there are losses in C_3 olefins, with gains in C_5, C_6, and C_7 olefins, while higher olefins were not detected. These observations can be explained by as-

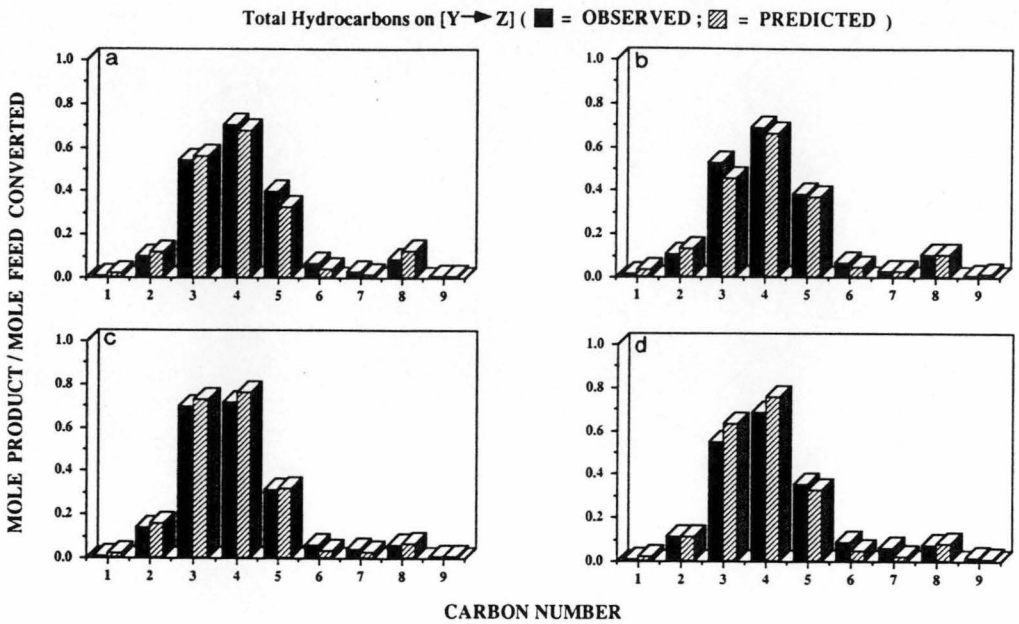

FIG. 5. Total hydrocarbon distributions from catalytic reaction of *n*-octane on the sequential catalyst [Y → Z]. (a) LC1, (b) LC2, (c) MC1, (d) MC2.

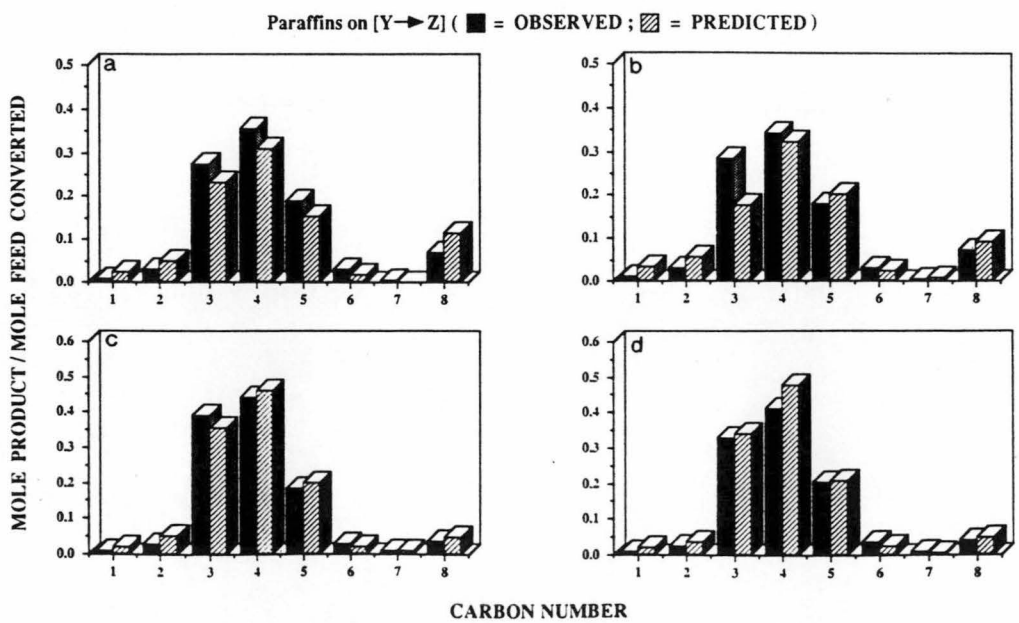

FIG. 6. Paraffin distributions from catalytic reaction of *n*-octane on the sequential catalyst [Y → Z]. (a) LC1, (b) LC2, (c) MC1, (d) MC2.

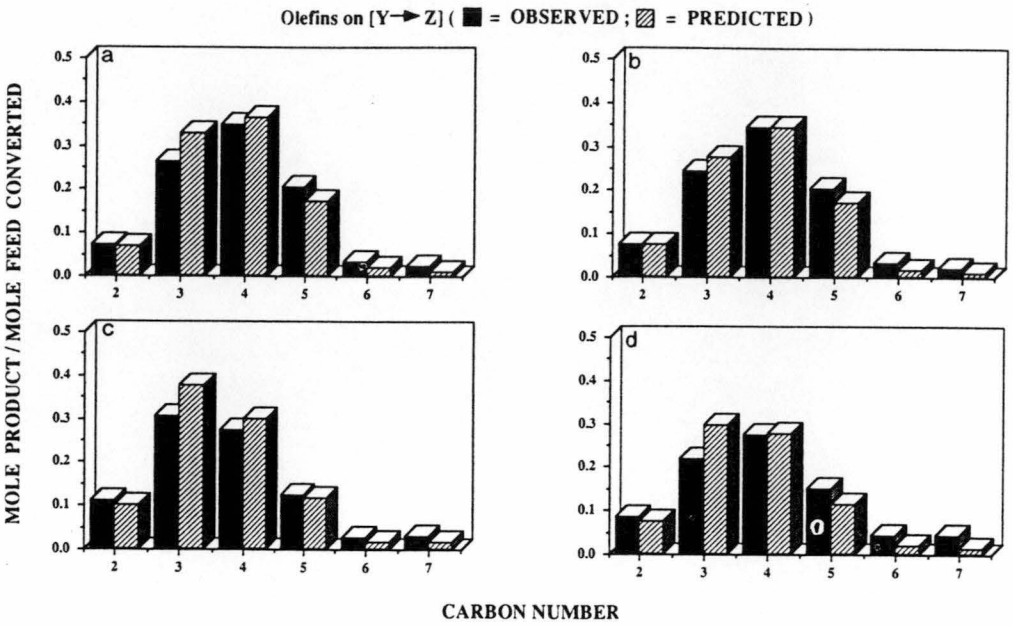

FIG. 7. Olefin distributions from catalytic reaction of *n*-octane on the sequential catalysts [Y → Z]. (a) LC1, (b) LC2, (c) MC1, (d) MC2.

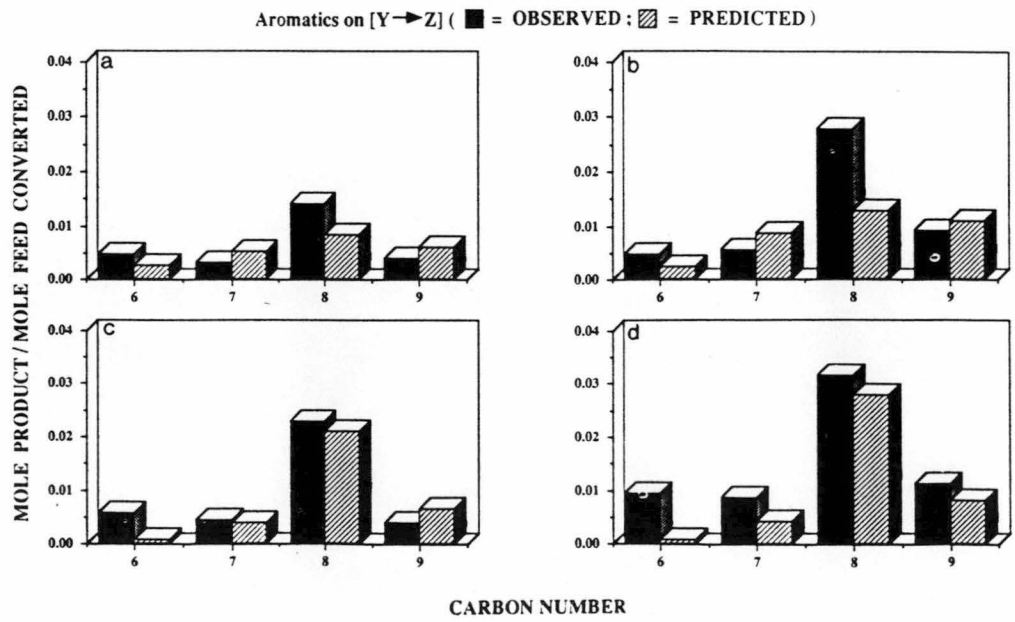

FIG. 8. Aromatic distributions from catalytic reaction of *n*-octane on the sequential catalyst [Y → Z]. (a) LC1, (b) LC2, (c) MC1, (d) MC2.

suming that the olefins produced on ZSM-5 from cracking of *n*-octane, and those entering as products from reactions on HY, can participate in a dimerization-cracking process (*32, 33*), which can result in a redistribution of the olfein species present. These processes eventually result in a net loss in propylene, net gains in C_5, C_6, and C_7 olefins, and little net change in the butenes. Figure 4 shows that the ratios of branched to linear C_4 and C_5 olefins for [Y → Z] are close to predicted values ([Y → Z]*), with the observed ratios consistently slightly larger than those obtained by calculation. This indicates that while the dimerization-cracking processes may alter the distribution of molecular size of olefins present, there is little net influence on isomer distribution at each carbon number. The consistent agreement between observed and predicted values for the proportion of ethylene may suggest that the C_2 olefin does not extensively participate in the dimerization processes, possibly due to instability of the C_2 carbenium ion.

Once formed, a carbenium ion produced from a dimerization processes can crack via β-scission processes, to give smaller olefins, or desorb directly as a C_6 or C_7 olefin. Alternatively, cyclization can lead to formation of additional aromatic species. From Fig. 8, it is evident that, in particular, the amount of benzene produced on this sequential combination is higher than that predicted by simple addition of the distributions. At the same time Fig. 6 shows consistently higher values for production of C_6 and C_7 paraffins than predicted. Possibly some C_6 and C_7 carbenium ions are available for hydrogenation during concurrent formation of aromatics, and these give rise to the saturated products. The depletion in C_8 paraffins as shown in Fig. 6 can be explained in terms of the instability of the corresponding carbenium ion (i.e., it cracks before it can either desorb as an olefin or participate in hydrogen transfer to produce a C_8 paraffin).

Figure 3 shows that the ratios of branched to linear C_6 paraffins for the combination [Y → Z] are lower than those predicted on the basis of simple addition of distributions, [Y → Z]*. However, if it is assumed that additional C_6 paraffins formed on HZSM-5 (Fig. 6) by hydrogen transfer are predominantly linear, the observed branched to linear ratios can be rationalized. The observed and predicted values of these ratios are given in Table 2. Adjusted values represent the predicted values that have been recalculated to meet the observed values, based on the assumption that any additional paraffins are formed through hydrogen transfer process, and any loss of paraffins can be attributed to selective cracking of branched saturated isomers.

The total amounts of C_3, C_4, and C_5 paraffins do not markedly differ from the predicted values, which assumes products emerging from reaction on the Y zeolite are unchanged on HZSM-5. The absence of extensive hydrogen transfer processes, which could give rise to additional paraffin formation from olefins produced on Y has already been noted. The lack of additional small cracking fragments (C_1 and C_2) also suggests that these paraffins do not undergo significant cracking on passing through the pentasil (Fig. 6). It is therefore interesting to note that, in contrast to the corresponding olefins, the ratios of branched to linear paraffins for C_4 and C_5 are significantly lower than predicted in each case by comparing values obtained for [Y → Z] and [Y → Z]* in Fig. 3.

In contrast to the C_6 paraffin isomers previously discussed, the required adjustment in the branched to linear isomer ratio in favor of linear C_4 and C_5 saturated products to coincide with the observed distributions cannot be explained merely in terms of hydrogen transfer with selective production of linear paraffins. In the cases where additional paraffins are observed, (Fig. 6, LC1 and LC2) the amounts are insufficient to account for the observed branched to linear ratio, as illustrated in Table 2. In the other cases (MC1 and MC2), there is in fact an apparent reduction in the amounts of C_4 and

TABLE 2

Ratios of Branched to Linear Paraffins from the Catalytic Reaction of *n*-Octane on the Sequential Catalysts [Y → Z] at 400°C

Run conditions	C_6			C_5			C_4		
	Observed	Predicted	Adjusted	Observed	Predicted	Adjusted	Observed	Predicted	Adjusted
LC1	1.26	1 28	0.55[a]	0.98	1.38	0.90[a]	0 59	0 79	0.62[a]
LC2	1.17	2 15	1.21[a]	1.12	2.50	2.13[b]	0 64	1.05	0.92[a]
MC1	1.19	3.53	1.18[a]	1.44	2.39	2.13[b]	0.89	1.17	1.08[b]
MC2	1.72	2.34	0.82[a]	1.30	2.47	2.35[b]	0.75	1 29	0.96[b]

[a] Calculation assumes excess paraffins formed by selective hydrogen transfer to give linear paraffins.
[b] Calculation assumes loss of paraffins through selective cracking of branched isomers.

C_5 paraffins formed. Neither can the observed branched to linear ratios for C_4 and C_5 paraffins after contact with HZSM-5 be explained easily by selective cracking of the branched saturated isomers. Cracking reactions of small branched paraffins such as isobutane and isopentane on HZSM-5 (*34–36*) give high selectivity toward formation of C_1 and C_2 fragments, whereas Fig. 6 shows that additional amounts of these products are not observed.

It appears that in order to explain the observed branched to linear ratios for C_4 and C_5 paraffins, isomerization of the branched paraffins must occur on HZSM-5. However, previous studies of reactions of individual branched paraffins on HZSM-5 show that the predominant reaction process is cracking rather than isomerization, as shown in Table 3. For example, reaction of isobutane (*34, 36*) on HZSM-5 at 400°C shows a selectivity for formation of *n*-butane of less than 20%. In our study, reaction of 2-methylpentane at 400°C shows a selectivity of 0.4% for production of *n*-hexane. These results suggest that isomerization rather than cracking becomes the preferred reaction mode when the feed contains a high proportion of olefins. The isomerization of branched paraffins on HZSM-5 represents the first significant difference between predicted and observed behavior.

Other reported investigations, particularly with isobutane, have shown that a significant selectivity for paraffin isomerization to produce *n*-butane is observed for reactions on Y zeolites in some cases (*37*). High selectivities toward isomerization have been observed using solid superacid catalysts (*38, 39*), in particular for catalysts re-

TABLE 3

Selectivities of Cracking and Isomerization of Branched Paraffins on HZSM-5

Feed	Temperature (°C)	Selectivity			Reference
		Cracking	Total isomerization	Isomerization to linear isomer	
Isobutane	400	1.0	0	0	(*34*)
Isobutane	500	0.95	0.5	0.5	(*34*)
Isobutane	400	0 83	0.17	0.17	(*36*)
2-Methylpentane	500	0.967	0.025	0	(*28*)
3-Methylpentane	500	0.922	0.066	0	(*28*)
2-Methylpentane	400	0.960	0.040	0.004	This study

ported to have an appropriate balance in the amounts of strong Brønsted and Lewis acid sites. It is possible that the change in selectivity in favor of isomerization of branched paraffins for the system under present consideration may be associated with formation of Lewis sites due to adsorption of product olefins at Brønsted sites in HZSM-5. Lewis acid sites alone do not appear to be active in most hydrocarbon transformations (*40–43*). However, coupling of Lewis sites and Brønsted sites can apparently result in significant changes in both acidity (*41*) and activity.

The second significant difference between observed and predicted distributions for the sequence [Y → Z] relates to the amounts of methane and ethane formed (Fig. 6). In each case, it is apparent that there is significantly less of these C_1 and C_2 fragments observed than would be predicted by addition of individual distributions. Again, it can be inferred that reactions of *n*-octane on HZSM-5 are perturbed when the feedstock contains a significant proportion of olefins. The observed reductions in methane and ethane are consistent with the proposal (*44*) that the cracking pathway via direct protonation of the paraffin becomes less significant in the presence of olefins, in favor of a bimolecular cracking mechanism. This reasoning can explain the reduction in the proportion of ethane formed (Fig. 6). For methane, however, the absolute amounts present after the product mixtures emerge from reactions on the sequence [Y → Z] is less than that entering the HZSM-5 stage of the sequence (Fig. 9). This implies not only that there is a reduction in cracking processes via protonation yielding methane, but that now there is also evidence for reaction of methane itself on this catalyst to form other products. This is unexpected, as methane is generally regarded as a stable product of cracking.

It has been shown that although higher paraffins ($>C_3$) can undergo reaction over HZSM-5, methane and ethane are themselves unreactive when passed through the catalyst as a pure feedstock (*45*). The present results show, however, that it is possible for methane to be converted into other products when passed over a zeolite catalyst in the presence of other hydrocarbons. Recent studies (*46–48*) have shown that methane and ethylene can undergo coupling reactions to produce higher hydrocarbons on solid superacid catalysts, and it is possible that our observed losses in methane and ethane are due to coupling reactions involving unsaturated species. Alternatively, it is possible that methane may be involved in a reversible reaction in which interaction with an adsorbed carbenium ion at a Brønsted site produces a pentacoordinated carbonium ion, as proposed by Kanai *et al.* (*49*).

The results presented for the sequential catalyst [Y → Z] corresponding to the four conditions show that the general conclusions are independent of time on stream and conversion levels. This was also found to be the case for the combinations discussed in subsequent sections. However, due to space limitations, results presented in the following sections are representative.

Reaction on Sequential HZSM-5 Followed by HY

Examples of observed product distributions for reaction of *n*-octane on the zeolite sequence [Z → Y] are presented in Figs. 10 and 11. As for the previous catalyst sequence, predicted distributions are also presented ([Y → Z]*), using conversions in Table 1 and the appropriate distributions of products on individual zeolites as illustrated in Fig. 2. As for the [Y → Z] sequence, the predicted distributions of total hydrocarbons according to carbon number also provide reasonable approximations to the observed values, as shown in Fig. 10. Again, it is possible to focus on differences in the various observed and predicted product distributions, particularly those for paraffins, olefins, and aromatics, to describe any possible additional reactions and interactions as products formed on HZSM-5 pass over the Y zeolite.

A feature which is apparent from inspec-

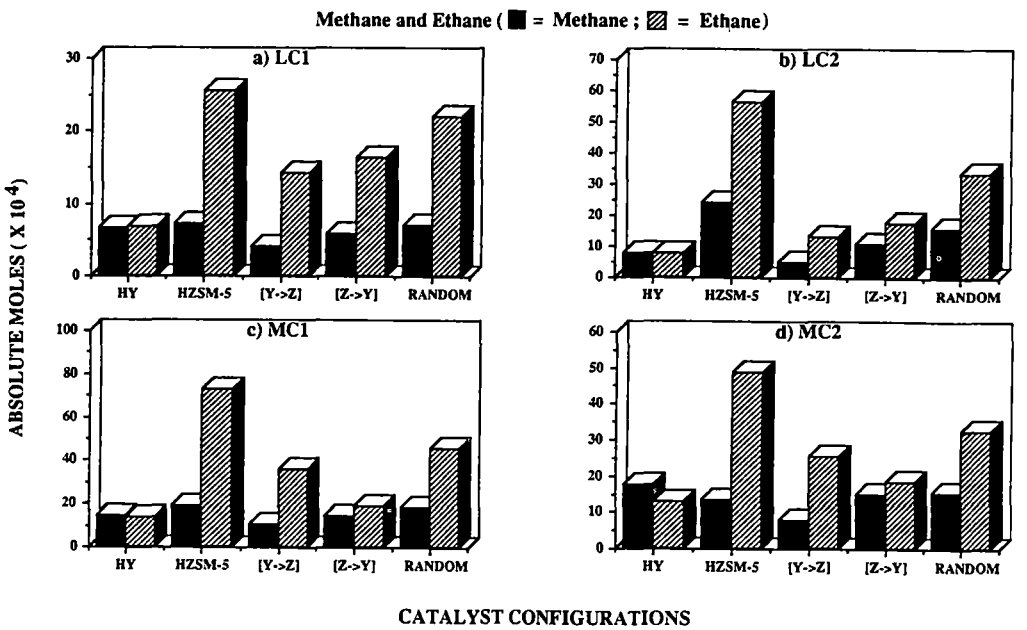

FIG. 9. Molar amounts of methane and ethane produced from catalytic reaction of *n*-octane at 400°C. (a) LC1, (b) LC2, (c) MC1, (d) MC2.

tion of these distributions is that the amounts of C_3–C_6 paraffins are generally in excess of the predicted values, as illustrated in Fig. 10b. In contrast, the observed amounts of olefins in this range are significantly less than those predicted (Fig. 10c). This is indicative of significant additional hydrogen transfer processes occurring on the Y zeolite, particularly involving product olefins formed on the HZSM-5. For this catalyst configuration, the extent of these processes is, in fact, sufficient to explain the observed branched to linear ratios for paraffins in the range C_4–C_6, as shown in Fig. 3, by comparing the results obtained on the sequences [Z → Y] and [Z → Y]*. The predicted ratios are lower than those actually observed on the assumption that products formed on the ZSM-5 pass through the Y zeolite unchanged. Table 4 shows the limiting adjusted values of these ratios, assuming that all additional C_4, C_5, and C_6 paraffins formed on HY through hydrogen transfer to olefins result in formation of the corresponding branched saturated isomers. In all cases, the adjusted values are already higher than the corresponding observed value, so that it is not necessary here to invoke a paraffin isomerization process on the faujasite, as proposed for reaction on the pentasil for the [Y → Z] sequence previously discussed.

Figure 11 shows that there is significant additional formation of aromatics using the [Z → Y] sequence, shown here for LC1 and MC2, comparing calculated values for simple addition of product distributions. This can be rationalized in terms of reactions of olefinic species formed on the HZSM-5 in the first stage of the sequence, through cyclization and hydrogen transfer processes on HY to produce aromatic species as well as the saturated products already discussed. Figure 4 shows that the observed branched to linear ratios for C_5 olefins are very close to the predicted values, while the observed ratios for the C_4 olefins are generally somewhat lower than those predicted. This may

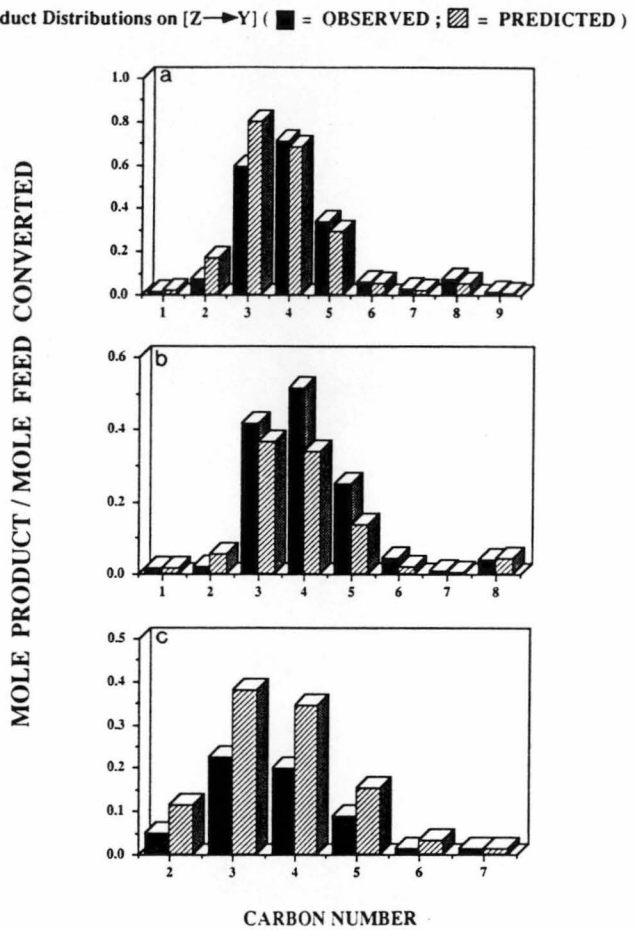

FIG. 10. Product distributions from catalytic reaction of *n*-octane on the sequential catalyst [Z → Y] at MC2; (a) Total hydrocarbons, (b) paraffins, (c) olefins.

be explained by assuming that the hydrogen transfer process occurring on the faujasite was selectively directed toward the branched C_4 olefins yielding branched isomers of the corresponding paraffins. This assumption was fairly well justified by the excess C_4 paraffins observed compared to predicted values (Fig. 10b) and the larger observed ratios of branched to linear isomers of C_4, C_5, and C_6 paraffins (Fig. 3).

As noted previously for reaction on the sequence [Y → Z], reaction of *n*-octane on the sequence [Z → Y] also shows an interesting result for formation of methane and ethane (Fig. 10b). There is consistently less of the C_1 and C_2 paraffin fragments observed then predicted by calculation. Figure 9 shows that, as for methane on the catalyst sequence [Y → Z] catalyst, these reductions are not simply due to reduced C_1 and C_2 paraffin formation on the second catalyst of the sequence, but an actual reduction in the amounts finally emerging due to reactions on the Y zeolite. Again, it seems that methane and ethane undergo reaction with other hydrocarbons when the mixture comes into contact with the second catalyst component. Therefore it can be concluded that it

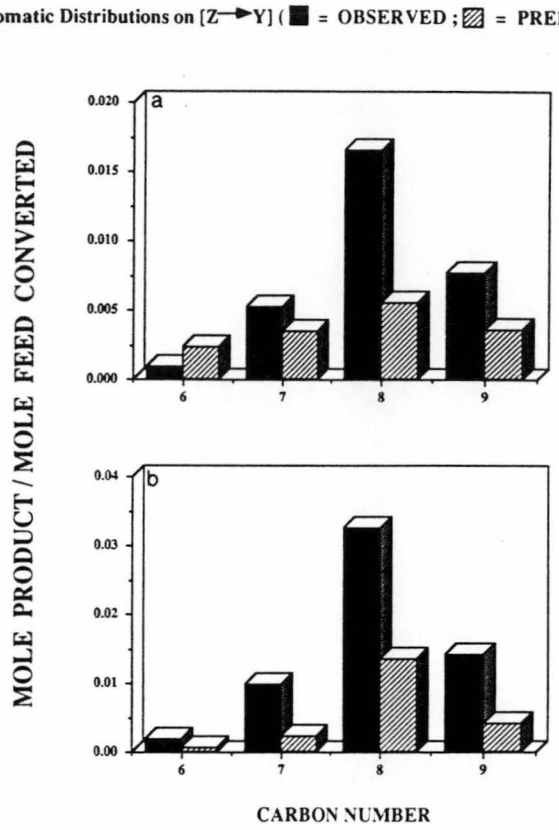

FIG. 11. Aromatic distributions from catalytic reaction of *n*-octane on the sequential catalyst [Z → Y]; (a) olefins (LC1), (b) aromatics (MC2).

is not the specific type of zeolite that is responsible for this observed phenomenon, but rather the influence of other hydrocarbons present in the mixture.

Reactions on Random Mixtures of HY and HZSM-5

The random mixtures of HY and HZSM-5 used corresponded to amounts of HY and HZSM-5 which produced equal conversions of *n*-octane under the same conditions. The total conversions of *n*-octane observed for reaction on these random mixtures of catalysts are given in Table 1. It was found that a simple averaging of distributions for total products on the individual catalysts according to carbon number again provides a very reasonable representation of the observed distribution (Fig. 12a). This shows that, as for the sequential combinations previously considered, the overall distribution of total hydrocarbon products by carbon number is well represented by the sum of the individual contributions on the isolated catalysts. It might be thought that a random mixture of particles of HY and HZSM-5 could be regarded as a large number of repeated [Y → Z] and [Z → Y] sequences. If that were the case, then we might expect the overall effect to result in a summation of the influences already discussed in the simple binary sequences.

Figure 12b shows that the observed amounts of paraffins in the range of C_3–C_6

TABLE 4

Ratios of Branched to Linear Paraffins from the Catalytic Reaction of *n*-Octane on the Sequential Catalysts [Z → Y] at 400°C

Run conditions	Branched to linear ratios								
	C_6			C_5			C_4		
	Observed	Predicted	Adjusted	Observed	Predicted	Adjusted	Observed	Predicted	Adjusted
LC1	1.46	0.83	2.24	1.07	0.79	1.59	0.74	0.51	1.09
LC2	1.69	0.69	2.59	2.33	0.69	2.85	1.20	0.35	1.58
MC1	2.44	0.78	3.05	2.42	0.69	3.45	1.41	0.44	2.16
MC2	1.83	0.82	3.22	1.78	0.54	1.82	1.17	0.41	1.14

are in excess of predicted values. This can again be correlated with reduced amounts of olefins (Fig. 12c) and increased amounts of aromatics (Fig. 12d). This appears to show that HZSM-5 does not suppress the hydrogen transfer process occurring on HY (*19*). Rather, the excess formation of small olefins observed by addition of HZSM-5 to a Y cracking catalyst is for the direct contribution of olefin products from reaction on the pentasil. An indication of the related tendency to undergo hydrogen transfer is provided by paraffin to olefin ratios at similar conversion levels. Ratios are presented in Table 5 corresponding to C_4, C_5, and C_6 for the three binary catalyst systems. It is

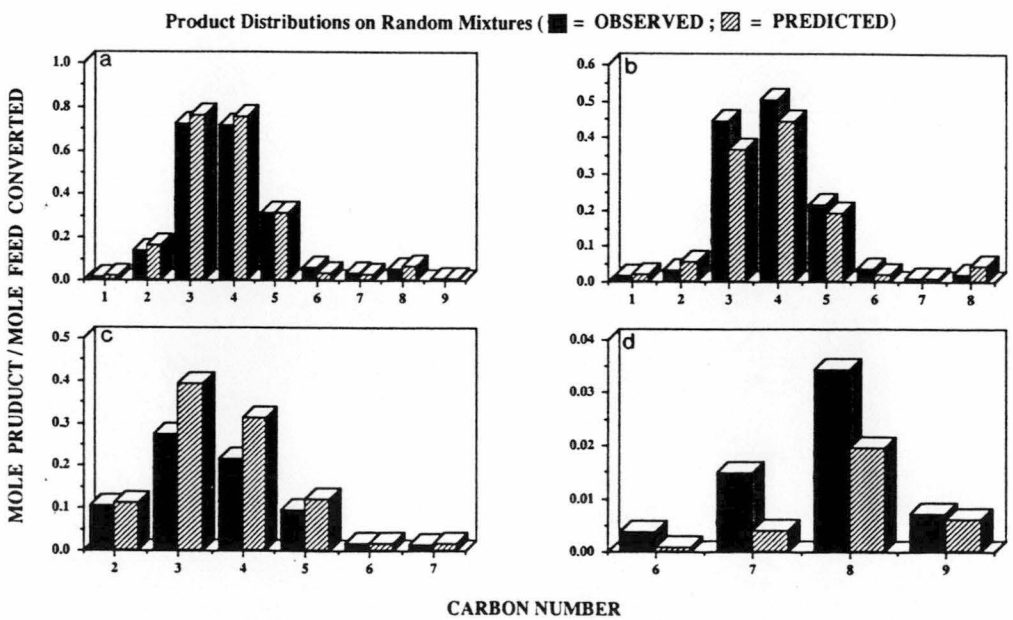

FIG. 12. Product distributions from catalytic reaction of *n*-octane on the random mixture of HY and HZSM-5 at MC1; (a) total hydrocarbons (b) paraffins, (c) olefins (d) aromatics.

TABLE 5

Paraffin to Olefin Ratios from Catalytic Reaction of *n*-Octane on Combinations of HY and HZSM-5, at 400°C

Run conditions: Catalyst configurations	Paraffin to olefin ratio					
	LC1			MC1		
	C_4	C_5	C_6	C_4	C_5	C_6
[Y → Z]	1.02	0.91	0.89	1.60	1.48	0.93
[RANDOM]	1.14	1.08	1.39	2.33	2.30	1.96
[Z → Y]	1.18	1.21	1.9	3.03	4.00	4.76

apparent that values are highest for the [Z → Y] sequence, lowest for the [Y → Z] combination, and intermediate for [RANDOM] mixtures.

For the random mixtures, the ratios of branched to linear olefins (Fig. 4) are close to predicted values given by [RANDOM]*. A comparison of these ratios for all systems studied shows that the variations in observed values are not large, with somewhat higher values for the [Y → Z] sequence than for either [Z → Y] or [RANDOM]. Figure 3 shows much more overall variation in branched to linear ratios for saturated products, depending on the particular catalyst or catalyst combination. The observed branched to linear ratios for paraffins on the mixture [RANDOM] are consistently smaller than the predicted values [RANDOM]* as given in Table 6.

Figure 12b shows that the proportions of methane and ethane produced on a random mixture of HY and HZSM-5 are less than those predicted. Figure 9 shows that the actual amounts of these products lie between those detected from reaction on the individual catalysts. In contrast to the sequential combinations, the amount of methane formed is not reduced below that formed on HY itself.

The results reported herein are in conflict with those of Buchanan (*22*), who suggests that the cracking of *n*-octane on ZSM-5 alone is negligible. We find significant reaction of the linear feedstock, in accord with previous studies (*42*). Such differences can be attributed to the use of different reaction conditions. The conclusions with regards to the pentasil additive acting to enhance isomerization processes, particularly for olefinic

TABLE 6

Ratios of Branched to Linear Paraffins from the Catalytic Reaction of *n*-Octane on the Random Mixture of HY and HZSM-5 [RANDOM] at 400°C

Run conditions	Branched to linear ratios								
	C_4			C_5			C_6		
	Observed	Predicted	Adjusted	Observed	Predicted	Adjusted	Observed	Predicted	Adjusted
LC1	0.68	0 78	0 47[a]	0.99	1 59	1.34[a]	1.43	1 35	2.28[c]
LC2	0.65	0.72	0 34[b]	0.96	1 72	0.67[b]	1.18	1.55	1.04[b]
MC1	1.06	1 13	0.88[a]	1 61	2.91	1 93[a]	2 22	2.91	0.63[a]
MC2	0.93	1.20	1 14[b]	1.40	3 04	1.97[a]	2.11	3 18	0 67[a]

[a] Calculation assumes excess paraffins formed by selective hydrogen transfer to give linear paraffins.
[b] Calculation assumes loss of paraffins through selective cracking of branched isomers.
[c] Calculation assumes excess paraffins formed by selective hydrogen transfer to give branched paraffins.

species, are however in accordance with those made by Buchanan (*22*).

CONCLUSION

Overall distributions of cracking products by carbon number from reaction of a linear paraffin on combinations of HY and HZSM-5 can be reasonably described by the addition of product distributions on individual catalysts, weighted according to the relative amounts present. The observed distributions of paraffins, olefins, and aromatics composing a product group at any particular carbon number show more widespread deviations from calculated product ratios. This arises particularly from hydrogen transfer processes which occur on the faujasite, leading to more extensive formation of paraffins and aromatics at the expense of olefins.

Isomerization reactions of both olefin and paraffin cracking products are promoted by the presence of HZSM-5. The presence of the pentasil produces higher concentrations of branched olefin isomers. There is also evidence that preferential isomerization of branched paraffins can occur when high concentrations of product olefins are also present, whereas cracking is favored at low olefin concentrations.

The latter observation demonstrates that the behavior of a particular reactant within a complex mixture may not be easily predictable from studies where that reactant is introduced as a pure feedstock. This also applies to the observed disappearance of ethane and methane when contacted with a fresh zeolite sample as a minor component of a complex hydrocarbon mixture.

ACKNOWLEDGMENTS

Financial support was provided by the Australian Research Council, an APRA (to F.N.G.), and through the Indonesian Institute of Sciences (to Z.Z.).

REFERENCES

1. Lombardo, E. A., Pierantozzi, R., and Hall, W. K., *J. Catal.* **110,** 171 (1981).
2. Corma, A., Monton, J. B., and Orchilles, A. V., *Appl. Catal.* **16,** 59 (1985).
3. Nace, D. M., *Ind. Eng. Chem. Prod. Res. Dev.* **8,** 24 (1969).
4. Haag, W. O., Lago, R. M., and Weisz, P. B., *Faraday Discuss. Chem. Soc.* **72,** 317 (1982).
5. Abbot, J., *J. Catal.* **126,** 628 (1990).
6. Abbot, J., and Wojciechowski, B. W., *Ind. Eng. Chem. Prod. Res. Dev.* **24,** 501 (1985).
7. Kobolakis, I., and Wojciechowski, B. W., *Can. J. Chem. Eng.* **63,** 269 (1985).
8. Chen, N. Y., and Garwood, W. E., *J. Catal.* **52,** 453 (1978).
9. John, T. M., and Wojciechowski, B. W., *J. Catal.* **37,** 240 (1975).
10. Scherzer, J., *Appl. Catal.* **75,** 1 (1991).
11. Venuto, P. B., and Habib, E. T., *Catal. Rev. Sci. Eng.* **18**(1), 1 (1991).
12. Otterstedt, J. E., Yan-Ming, Z., and Sterte, J., *Appl. Catal.* **38,** 143 (1988).
13. Rajagopalan, K., and Young, G. W., *ACS Symp. Ser.* **375,** 34 (1988).
14. Biswas, J., and Maxwell, I. E., *Appl. Catal.* **58,** 1 (1990).
15. Elia, M. F., Iglesias, E., Martinez, A., and Perez Pascual, M. A., *Appl. Catal.* **73,** 195 (1991).
16. Donnelly, S. P., Mizrahi, S., Sparrell, P. T., Huss, A., Jr., Schipper, P. H., and Herbst, J. A., *Prepr.-Am. Chem. Soc., Div. Pet. Chem.* **32**(3), 621 (1987).
17. Anderson, C. D., Dwyer, F. G., Koch, G., and Niiranen, P., Proceedings, Ninth Iberoamerican Symposium on Catalysis, Lisbon, 1984.
18. Pappal, D. A., and Schipper, P. H., *Prepr.-Am. Chem. Soc., Div. Pet. Chem.* **35**(4), 678 (1990).
19. Miller, S. J., and Hsieh, C. R., *Prepr.-Am. Chem. Soc., Div. Pet. Chem.,* **3**(4), 685 (1990).
20. Maddon, R. J., *J. Catal.* **129,** 275 (1991).
21. Anders, G., Burkhardt, I., Illgen, U., Schulz, I. W., and Scheve, J., *Appl. Catal.* **62,** 271 (1991).
22. Buchanan, J. S., *Appl. Catal.* **74,** 83 (1991).
23. Cornaro, U., and Wojciechowski, B. W., *J. Catal.* **120,** 182 (1989).
24. Abbot, J., and Wojciechowski, B. W., *J. Catal.* **107,** 451 (1987).
25. Abbot, J., and Wojciechowski, B. W., *Can J. Chem. Eng.* **66,** 825 (1988).
26. Abbot, J., and Wojciechowski, B. W., *J. Catal.* **115,** 521 (1989).
27. Magnoux, P., Cartraud, P., Mignard, S. and Guisnet, M . *J. Catal.* **106,** 242 (1987).
28. Abbot, J., *Appl. Catal.* **57,** 105 (1990).
29. Mott, R. W., *Oil Gas J.,* Jan 26, 73 (1987).
30. Abbot, J., and Wojciechowski, B. W., *J. Catal.* **104,** 80 (1987).
31. Abbot, J., and Wojciechowski, B. W., *Appl. Catal.* **47,** 33 (1989).
32. Abbot, J., and Wojciechowski, B. W., *Can. J. Chem. Eng.* **63,** 278 (1988).

33. Abbot, J., and Wojciechowski, B. W., *Can. J. Chem. Eng.* **63,** 451 (1988).
34. Lombardo, E. A., and Hall, W. K., *J. Catal.* **112,** 565 (1988).
35. Hall, W. K., Lombardo, E. A., and Englehardt, J., *J. Catal.* **115,** 611 (1989).
36. Shigeishi, R., Garfoth, A., Harris, I., and Dwyer, J., *J. Catal.* **130,** 423 (1991).
37. McVicker, G. B., Kramer, G. M., and Riemiak, J. J., *J. Catal.* **83,** 286 (1983).
38. Fuentes, G. A., Boegel, J. V., and Gates, B. C., *J. Catal.* **78,** 436 (1982).
39. Dooley, K. M., and Gates, B. G., *J. Catal.* **96,** 347 (1985).
40. Bourdillon, G., Gueguen, C., and Guisnet, M., *Appl. Catal.* **61,** 123 (1990).
41. Mirodatos, C., and Barthomeuf, D., *J. Chem. Soc. Chem. Commun.* **39,** (1981).
42. Abbot, J., *J. Catal.* **123,** 383 (1990).
43. Abbot, J., *J. Catal.* **126,** 628 (1990).
44. Haag, W. O., and Dessau, R. M., *in* Proceedings, 8th International Congress on Catalysis, Berlin, 1984, Vol. II, p. 305. Dechema, Frankfurt-au-Main, 1984.
45. Dass, D. V., and Odell, A. L., *J. Catal.* **113,** 259 (1988).
46. Scurrell, M. S., *Appl. Catal.* **32,** 1 (1988).
47. Scurrell, M. S., *Appl. Catal.* **41,** 89 (1988).
48. Scurrell, M. S., and Cooks, M., *Stud. Surf. Sci. Catal.* **36,** 433 (1988).
49. Kanai, J., Martens, J. A., and Jacobs, P. A., *J. Catal.* **133,** 527 (1992).